

**IDENTIFICATION OF NEO-TECTONIC ZONES
AND THEIR EFFECT IN THE DEVELOPMENT
OF GULLIES WITHIN ORLU AND ENVIRONS,
SOUTHEASTERN NIGERIA**

BY

ONWUBUARIRI, CHUKWUEBUKA NNAMDI (B.Tech. Physics, FUTO)

PGS/M.Sc./20104774528

DEPARTMENT OF GEOLOGY

**A THESIS SUBMITTED TO THE SCHOOL OF
POSTGRADUATE STUDIES, FEDERAL UNIVERSITY OF
TECHNOLOGY, OWERRI**

**IN PARTIAL FULFILLMENT OF THE REQUIREMENTS
FOR THE AWARD OF MASTER OF SCIENCE IN
GEOPHYSICS (M.Sc. GEOPHYSICS)**

NOVEMBER, 2015

DECLARATION

I, Onwubuariri, Chukwuebuka Nnamdi, hereby declare that this work titled, “Identification of Neo-Tectonic Zones and Their Effect in the Development of Gullies within Orlu and Environs, Southeastern Nigeria” was carried out by me and submitted to the School of Post-Graduate Studies, Federal University of Technology, Owerri. I declare that apart from references made to other people’s work which have duly been acknowledged, this work is the product of my own research and has neither in whole nor in part been presented for other awards elsewhere.

.....

.....

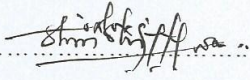
Onwubuariri, Chukwuebuka Nnamdi

Date

Reg. No: 20104774528

CERTIFICATION

I certify that this work "Identification of Neo-Tectonic Zones and Their Effect in the Development of Gullies within Orlu and Environs, Southeastern Nigeria" was carried out by Onwubuariri, Chukwuebuka Nnamdi (20104774528) in partial fulfillment for the award of degree of M.Sc. in Geophysics in the department Geology of Federal University of Technology, Owerri.

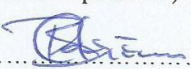

.....
Dr. A.I. Opara
Date
21/09/2015

(Principal Supervisor)

.....
Prof. Nath. Onu
Date
21/09/2015

(Co-Supervisor)

.....
Dr. C.Z. Akaolisa
Date
29/3/16

(Head of Department)

.....
Prof. Bede Anusionwu
Date
21/04/2016

(Dean, School of Physical Sciences)
.....
Date

Engr. Prof. K.B. Oyoh
Date
(Dean of Postgraduate School)


.....

Prof. K. M. Onuoha
Date
(External Examiner)

DEDICATION

This work is dedicated to God, my parents and all who contributed to make this work a reality.

ACKNOWLEDGEMENT

I sincerely appreciate all who impacted on me academically and morally during my post graduates(M.Sc.) studies. This include league of lecturers amongst whom are Dr. Alex Opara (My supervisor), Prof. Nath Onu (Co-Supervisor), Prof. A. Selemo, Dr. C. Z. Akaolisa, Dr. J. Nwagbara (late), Prof K.K. Ibe and many others, non-academic staff inclusive.

The contribution of my colleagues – Agoha Chidiebere, Osaki Lawson Jack, OkoroEze Martins and Ohaeri, Chidozie will not be over emphasized as all played vital role in my academic pursuit.

My wonderful parents Mr Charles and Mrs Pauline Onwubuariri, Uncle, Engr. Charles Onyedimma, and my siblings are highly appreciated for their support, morally, financially and otherwise to ensure I achieve this fit.

TABLE OF CONTENT

Cover Page.....	i
Declaration.....	ii
Certification.....	iii
Dedication.....	iv
Acknowledgement.....	v
Table of Contents.....	vi
List of Tables.....	x
List of figures.....	xi
List of plates.....	xv
Abstract.....	xvi
Chapter One: Introduction	
1.1 Background of study.....	1
1.2 Statement of the problem.....	4
1.3 Justification.....	6
1.4 Aim.....	7
1.5 Objectives.....	7
1.6 Location, physiography and geology of the study area.....	7
1.6.1 Location, climate, physiography and drainage of the study area.....	7
1.6.2 Geological background.....	8
Chapter Two: Literature Review	
2.1 Review of related literature.....	13
2.2. Theoretical framework	15
2.2.1Erosion by water.....	15
2.2.2 Ecological effects of sheet and rill erosion.....	18

2.2.3 Erosion by wind.....	19
2.3 Gully erosion and control.....	20
2.3.1 Factors affecting gully formation	20
2.4 Development and classification of gullies.....	24
2.4.1 Development of gullies.....	24
2.4.2 Classification of gullies.....	26
2.4.3 Criteria for the selection of gully control measures.....	28
2.5. The electrical resistivity method.....	29
2.5.1 Vertical electrical sounding (VES).....	30
2.5.2 Azimuthal resistivity survey.....	32
2.5.2.1 Mathematical theory of electrical anisotropy.....	35
2.6 Geotechnical Methods of Soil Analysis.....	37
2.6.1 California Bearing Ratio (CBR).....	38
2.6.2 Soil consistency	38
2.6.2.1 Rupture resistance (moist and dry consistency)	39
2.6.2.2 Stickiness (wet consistency).....	39
2.6.2.3 Plasticity (wet consistency)	39
2.6.3 Atterberg limits.....	40
2.6.3.1. Liquid limits.....	40
2.6.3.2 Plasticity limits.....	40
2.6.3.3 Shrinkage limits	40
2.6.3.4 Plasticity index	41
2.7 Remote sensing method.....	41

2.7.1 Brief Review of Normalized Difference Vegetation Index (NDVI).....	41
2.7.2 Lineament Interpretation.....	42
2.7.3 Drainage Analysis.....	42
2.7.4 Azimuth Frequency (Rose) Diagram.....	43

Chapter Three: Materials and Methods

3.1 Method of study.....	44
3.2 Desk study.....	44
3.2.1 Desk study materials.....	44
3.3 Field study.....	45
3.3.1 Field equipment.....	46
3.3.2 Software Used.....	46
3.4 Gully characterization.....	47
3.4.1 Site Locations.....	47
3.5 Surface Geologic Mapping.....	48
3.6 Geotechnical Studies.....	48
3.6.1 Sample collection.....	48
3.7 Geophysical Studies.....	49
3.7.1 Vertical electric sounding (VES).....	49
3.7.2 Azimuthal Resistivity Sounding (ARS).....	50
3.8 Landsat imagery/acquisition.....	51

Chapter Four: Result Presentation, Interpretation and Discussion

4.1 Result presentation and interpretation	53
4.1.1 Landsat imagery	53

4.1.2 Azimuthal resistivity sounding result.....	63
4.1.3 Vertical electrical sounding.....	71
4.1.3.1 Iso-Resistivity value tables.....	71
4.1.3.2 Layer Resistivity, Depth, and Thickness values.....	76
4.1.3.3 Geoelectric sections.....	80
4.1.3.4 Geotechnical analysis result presentation.....	80
4.2 Discussion of results.....	102
Chapter Five: Summary, Conclusion and Recommendation	
5.1 Summary and Conclusion.....	108
5.2 Recommendations	110
References.....	112
Appendices.....	120

LIST OF TABLES

Table 1.0: Stratigraphic Succession table.....	9
Table 3.0: Site locations with their easting and Northing.....	47
Table 4.0: Azimuthal Resistivity sounding value table at Ogberuru.....	63
Table 4.1: Azimuthal Resistivity Sounding Value Table at Umueshi.....	64
Table 4.2: Azimuthal Resistivity Sounding Value Table at Umuomeji, Urualla.....	65
Table 4.3: Azimuthal Resistivity Sounding Value Table at Dimagu.....	66
Table 4.4: Azimuthal Resistivity Sounding Value Table at Ihioma.....	67
Table 4.5: Azimuthal Resistivity Sounding Value Table at Njaba.....	68
Table 4.6: Azimuthal Resistivity Sounding Value Table at Okwudor.....	69
Table 4.7: Azimuthal Resistivity Sounding Value Table at Umuhuokabia.....	70
Table 4.8a: Iso-Resistivity value for AB/2 from 5 – 65.....	71
Table 4.8b: Iso-Resistivity value for AB/2 from 70 – 135.....	72
Table 4.8c: Iso-Resistivity value for AB/2 from 135 – 195.....	74
Table 4.8d: Iso-Resistivity value for AB/2 from 200 – 250.....	74
Table 4.9: Table for Layer Resistivity, Depth of Layers and Thickness of Layers.....	76
Table 4.10: Sample statistics table for Afor-Ukwu gully Sample 1.....	81
Table 4.11: Sample statistics table for Afor-Ukwu gully Sample 2.....	85
Table 4.12: Sample statistics table for Ihioma Gully Head.....	88
Table 4.13: Sample statistics table for Middle of Ihioma Gully.....	92
Table 4.14: Sample statistics table for Njaba gully Sample 1.....	96
Table 4.15: Sample statistics table of Njaba gully Sample 2.....	99
Table 4.16: Table of Grain Size Distribution, OMC, MDD, CBR, LL, PL and PI.....	107

LIST OF FIGURES

Fig. 1.0: Map showing gullies within the South Eastern Zone.....	3
Fig. 1.1: Geology map of Orlu and environs.....	10
Fig. 1.2: Location map of Orlu and Environs.....	11
Fig. 1.3: Topographical map of Orlu and Environs.....	12
Fig. 2.0: Schlumberger Array.....	30
Fig. 2.1: Sample of a sounding curve.....	31
Fig. 2.2: Wenner configuration.....	34
Fig 3.0: Schlumberger array.....	49
Fig. 3.1: Field array of Azimuthal Resistivity Sounding.....	50
Fig. 4.0: Digital Elevation Model (DEM) Map.....	53
Fig.4.1: Topographical map of Orlu and Environs of the study area.....	55
Fig. 4.2: Lineament on Drainage Map of the study area.....	55
Fig. 4.3: Lineament on Edge Enhanced Band 5 Map of the study area.....	56
Fig. 4.4: Lineament Density Map of the study area.....	57
Fig. 4.5: Normalized Difference Vegetation Index (NDVI) Map of the study area.....	58
Fig. 4.6: Colour Composite RGB 752 Map of the study area.....	59
Fig. 4.7: Colour Composite RGB 751 Map of the study area.....	59
Fig. 4.8: Colour Composite RGB 357 Map of the study area.....	60
Fig. 4.9: Unsupervised Classification Map of the study area.....	61
Fig. 4.10: Azimuth Frequency map of the study area (Rose Diagram).....	62
Fig 4.11: Ogberuru Azimuthal Sounding plots.....	63
Fig 4.12: Umueshi Azimuthal Sounding plots.....	64

Fig 4.13: Umuomeji Urualla Azimuthal Sounding plots.....	65
Fig 4.14: Dimagu Azimuthal Sounding plots.....	66
Fig 4.15: Ihioma Azimuthal Sounding plots.....	67
Fig 4.16: Njaba Azimuthal Sounding plots.....	68
Fig 4.17: Okwudor Azimuthal Sounding plots.....	69
Fig 4.18: Umuhuokabia Azimuthal Sounding plots.....	70
Fig. 4.19: Iso-Resistivity contour at the value $AB/2 = 5$	71
Fig. 4.20: 3D model with vector map of Iso-Resistivity at the value $AB/2 = 5$	72
Fig. 4.21: Wired 3D model Iso-Resistivity at the value $AB/2 = 5$	72
Fig. 4.22: Iso-Resistivity contour at the value $AB/2 = 125$	73
Fig. 4.23: 3D model with vector map of Iso-Resistivity at the value $AB/2 = 125$	73
Fig. 4.24: Wired 3D model Iso-Resistivity at the value $AB/2 = 125$	73
Fig. 4.25: Iso-Resistivity contour at the value $AB/2 = 250$	74
Fig. 4.26: 3D model with vector map of Iso-Resistivity at the value $AB/2 = 250$	75
Fig. 4.27: Wired 3D model Iso-Resistivity at the value $AB/2 = 250$	75
Fig. 4.28: The elevation contour of the study area.....	76
Fig 4.29:3D Model of the elevation of the study area.....	77
Fig 4.30:Wired 3D Model of the elevation of the study area.....	77
Fig 4.31:The Resistivity contour of the entire first (1 st) – top most- layers.....	77
Fig 4.32:The Resistivity contour of the entire second (2 nd) layers – i.e. 2 nd from the top most layer.....	78
Fig 4.33:The Resistivity contour of the entire third (3 rd) layers – i.e. 3 rd from the top most layer.....	78
Fig 4.34:The Resistivity contour of the entire fourth (4 th) layers – i.e. 4 th from the top most layer.....	78
Fig 4.35:The Resistivity contour of the entire fifth (5 th) layers – i.e. 5 th from the top most layer.....	79

Fig 4.36: The Resistivity contour of the entire fifth (6th) layers – i.e. 6th from the top most layer.....	79
Fig 4.37: Geo-electric sections and profiling of the study locations.....	80
Fig. 4.38: Grain Size class of weight distribution chart for Afor-Ukwu gully sample 1.....	81
Fig. 4.39: Pyramidal chart of Afor-Ukwu Gully sample 1 grain size distribution.....	82
Fig. 4.40: Afor-Ukwu Gully Sample 1 grain size class of weight graph in phi.....	82
Fig. 4.41: Afor-Ukwu Gully Sample 1 Grain Size Cumulative mass Retained graph in phi...83	
Fig. 4.42: Afor-Ukwu Gully Sample 1 class of weight graph in microns.....	83
Fig. 4.43: Afor-Ukwu Gully Sample 1 cumulative mass retained graph in microns.....	84
Fig. 4.44: Grain Size class of weight distribution chart for Afor-Ukwu gully sample 2.....	85
Fig. 4.45: Pyramidal chart of Afor-Ukwu Gully sample 2 grain size distribution.....	86
Fig. 4.46: Afor-Ukwu Gully Sample 2 Grain Distribution class of weight graph in phi.....	86
Fig. 4.47: Afor-Ukwu Gully Sample 2 Grain Size Cumulative mass Retained graph in phi..87	
Fig. 4.48: Afor-Ukwu Gully Sample 2 class of weight graph in microns.....	87
Fig. 4.49: Afor-Ukwu Gully Sample 1 cumulative mass retained graph in microns.....	88
Fig. 4.50: Grain Size class of weight distribution chart for Ihioma Gully Head.....	89
Fig. 4.51: Pyramidal chart of Ihioma Gully Head grain size distribution.....	89
Fig. 4.52: Ihioma Gully Head Grain Size Distribution class of weight graph in phi.....	90
Fig. 4.53: Ihioma Gully Head Grain Size Cumulative mass Retained graph in phi.....	91
Fig. 4.54: Ihioma Gully Head class of weight graph in microns.....	91
Fig. 4.55: Ihioma Gully Head cumulative mass retained graph in microns.....	92
Fig. 4.56: Grain Size class of weight distribution chart for Middle of Ihioma Gully.....	93
Fig. 4.57: Pyramidal chart of Middle of Ihioma Gully grain size distribution.....	93

Fig. 4.58: Middle of Ihioma Gully Grain Size Distribution class of weight graph in phi.....	94
Fig. 4.59: Middle of Ihioma Gully Grain Size Cumulative mass Retained graph in phi.....	94
Fig. 4.60: Middle of Ihioma Gully class of weight graph in microns.....	95
Fig. 4.61: Middle of Ihioma Gully cumulative mass retained graph in microns.....	95
Fig. 4.62: Grain Size class of weight distribution chart of Njaba Gully sample 1.....	96
Fig. 4.63: Pyramidal chart of Njaba Gully sample 1 grain size distribution.....	97
Fig. 4.64: Njaba Gully Sample 1 Grain Size Distribution class of weight graph in phi.....	97
Fig. 4.65: Njaba Gully Sample 1 Grain Size Cumulative mass Retained graph in phi.....	98
Fig. 4.66: Njaba Gully Sample 1 class of weight graph in microns.....	98
Fig. 4.67: Njaba Gully Sample 1 cumulative mass retained graph in microns.....	99
Fig. 4.68: Grain Size class of weight distribution chart for Njaba gully sample 2.....	100
Fig. 4.69: Pyramidal chart of Njaba Gully sample 2 grain size distribution.....	100
Fig. 4.70: Njaba Gully Sample 2 Grain Size Cumulative mass Retained graph in phi.....	101
Fig. 4.71: Njaba Gully Sample 2 class of weight graph in microns.....	101
Fig. 4.72: Njaba Gully Sample 2 cumulative mass retained graph in microns.....	102

LIST OF PLATES

Plate 1: Destroyed building at Umueshi in Ideato North L.G.A. of Imo State.....	5
Plate 2: Destroyed farmland at Ogberuru in Orlu L.G.A. of Imo State.....	5
Plate 3: Destroyed road at Ogberuru in Orlu	6
Plate 4: U Shape gullies at Ogberuru in Orlu L.G.A of Imo state.....	27
Plate 5: V-Shape erosion at Umuomeji Urualla in Ideato North L.G.A of Imo State.....	27

ABSTRACT

A detailed geoscientific study was carried out within Ordu and environs with the objective of evaluating the influence of tectonic and neo-tectonic features on gully development and propagation in the study area. Field geological mapping was carried out to characterize the gullies and to estimate the strikes and directional attributes of the gullies. Similarly, GIS interpreted Landsat-ETM imageries were used to map lineaments, evaluate their trends and to infer their possible tectonic significance in the study area. Azimuthal resistivity sounding was carried out at various locations within the study area to determine the direction of electrical anisotropy as well as the coefficient of anisotropy. They were rotated in four azimuths at angles of 0° , 45° , 90° and 135° corresponding to the N-S, NE-SW, E-W and NW-SE directions. Similarly, vertical electrical sounding (VES) was also carried out using a maximum current electrode separation of 400m. Finally, a detailed geotechnical analysis of the soils within the locations of the gully sites was carried out to evaluate the properties of the soils within the study area. Results of the geotechnical analysis revealed that the soils in the study area are predominantly moderately sorted sand, poly-modal, symmetrical and leptokurtic. The Optimum Moisture Content ranges from 8.8% to 11%, while the Maximum Dry Density ranges from 1.91% to 1.99%. Atterberg test results revealed Liquid Limits ranging between 22.8% and 35%, Plasticity Limit of between 13.7% and 25%, and Plasticity Index varying between 6% and 10.6%. Results of Vertical Electrical Sounding (VES) carried out in the study area revealed that the resistivity of the first layer varies from $65.168\Omega\text{m}$ to $5,970\Omega\text{m}$ with an average of $1,155.209\Omega\text{m}$ with thickness values of 0.6106m to 4.8m respectively. Geological field mapping of the study area revealed that the gullies in the study area trend approximately in the NW-SE and NE-SW directions with the NE-SW direction being preponderant. Similarly, Rose diagrams generated from the strikes and lengths of lineaments interpreted from Landsat-ETM⁺ images revealed two structural trends of NW-SE and NE-SW with the NW-SE being dominant. Results of the azimuth frequency diagrams generated from the anisotropic resistivity soundings revealed uni-modal to poly-modal pattern with the dominant trend directions observed to be in the NW-SE and NE-SW directions. The correlation of the trends of the gullies with the lineament trends from landsat and the direction of electrical anisotropy suggests that gully origin and propagation in the study area may be structurally or tectonically controlled.

KEYWORDS:

Neo-Tectonism, landsat-ETM , Erosion, Azimuth, Lineaments, Resistivity, Atterberg.

CHAPTER ONE

INTRODUCTION

1.1 Background of Study

Erosion is a natural process involving the removal of soil and rock materials from the Earth's surface by agents of denudation, such as wind and water flow, and then transported and deposited in other locations. Environmental degradation by such exogenic processes has become a major concern, especially now that human activities have increased the rate of erosion occurrence by more than 40 times, globally. Desertification, decrease in agricultural productivity due to land degradation, sedimentation of waterways, and ecological collapse due to loss of the nutrient rich upper soil layers forms some of the major impacts of excessive erosion evident in our environment today, with water and wind erosion being the two primary causes of land degradation. The effects of these two combined together are responsible for 84% of degraded acreage, making excessive erosion one of the most significant global environmental problems(Blanco et al., 2010).

Erosion gullies in southeastern Nigeria have been variously attributed to high rainfall intensity, wind action, slope instability, poor engineering and agricultural processes by earlier scholars(Onu, et al. 2012). While human activities and programs tend to accelerate erosion processes, it seems that some endogenic geological factors make some parts of southeastern Nigeria more erosion prone than other areas(Igbokwe, M.U., et al).

Gullies in Orlu and environs within the Southeastern Nigeria have peculiar and very interesting origin and characteristics. Their genesis was spontaneous. A major failure suddenly occurred around the area a few years ago along a linear zone following a heavy rainfall. Slumping and land sliding followed. This incident which has degraded the landform

in the vicinity and caused great panic in the neighborhood has attracted the attention of geologists/earth scientists and various levels of government in Nigeria. There is a speculation that this sudden failure cannot be a chance occurrence. There must have been a pre-existing condition hitherto undetected which acted as a trigger for the spontaneous event that opened up the gully. The first suspicion is the existence of a major fracture in the area whose extent may not be readily known(Onu N.N., et al., 2012).

Figure 1 is a map of southeastern Nigeria showing the occurrence of gullies in the area. It can be readily observed that all the gullies within the southeastern region lie along a straight line predominantly in the NW-SE direction, suggesting a structural weakness along this direction, which may be as a result of early tectonism. The opening of the South Atlantic Ocean on a “Triple R” junction initiated tectonism in the Southern Nigeria. One of the failed arms of this rift junction, known as an “aulacogen”, developed to become the Benue Trough (Wright, 1966; Nyong, 1995). The development of the Benue Trough provided the main structural control and framework for subsequent geologic evolution of Southeastern Nigeria. Three major tectonic cycles could be identified in Southeastern Nigeria (Murat, 1972), the first major tectonic phase (Aptian-early Santonian) directly followed, and was related to, the initial rifting of the Southern Nigeria continental margin and the opening of the Benue Trough.

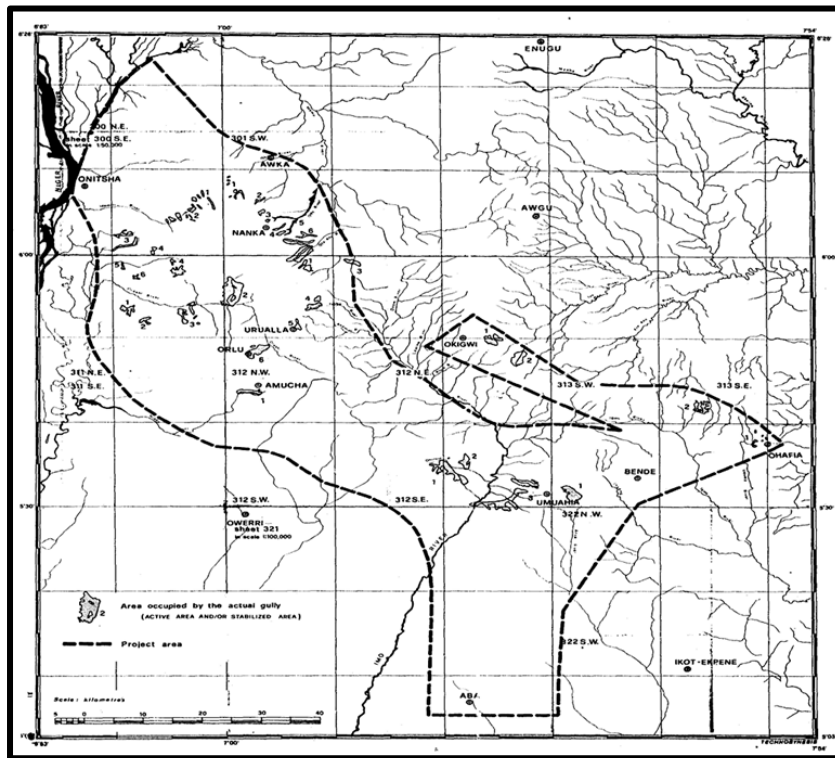


Fig. 1.0. Map showing gullies within the South Eastern Zone

This phase produced two principal sets of faults, trending NE-SW and NW-SE. The NE-SW set of faults bound the Benue Trough, while the NW-SE sets defined the Calabar Flank. The second tectonic phase (Turonian -Santonian) was characterized by compressional movements resulting in the folding of the Abakaliki Anticlinorium and the complementary Afikpo Syncline. The third phase (Late Campanian - Middle Eocene) involved rapid subsidence and uplift in alternation, with subsequent progradation of the Niger delta.

Thus, the sedimentary basin of Southern Nigeria originated in early cretaceous time as an X-shaped depression oriented NE-SW and NW-SE and defined by a set of mega-tectonic elements, among which is the Benin Flank to the northwest, the Benue Trough to the north and the Calabar Flank to the east (Agagu, 1979). Short and Stauble (1967) stated that the depression formed in the Basement complex of the African shield. The architecture and the rather straight course of long reaches of the Niger and Benue Rivers have led to the speculation that the depression is fault controlled. The depression is genetically related to the Benue Valley; a trough which originated as a drift structure (Cratchley and Jones, 1965).

Structural movements in the Benue Trough began in the Coniacian time and accumulated in the Santonian. Three major depositional and tectonic cycles have been identified by Short and Stauble (1967). The first cycle (Albian - Santonian) was confined in the southern end of the Benue Trough. The second (Campanian-Eocene) filled the Anambra Basin and Afikpo syncline, and the third cycle paved the way for the development of the modern Niger Delta (Mamah and Ekine, 1989). Each cycle was terminated by folding and uplift. There have been continued basement movements, sedimentation and minor faulting along earlier lines of weakness. The Ogwashi/Asaba and Benin Formations represent the Miocene to Recent sediments of the depositional cycle of the Benue Trough, and these gave rise to the modern Niger Delta. The lithostratigraphy of the Benin and Ogwashi/Asaba Formations has been documented by various scholars (Reyment, 1967, Short and Stauble 1967, Kogbe 1976 and Asseez, 1979). The sediments of the Benin Formation are lenticular, unconsolidated, friable and sandy. Clays and sandy clays occur occasionally at deeper levels. The Ogwashi/Asaba Formation is predominantly sandy. The sands alternate with lignite seams and few beds of clay (Reyment, 1965).

1.2 Statement of the Problem

Gully erosion is has become the most prominent landscape feature in the Orlu area and environs in southeastern Nigeria. Most communities in the area have tales of woes as a result of ever increasing occurrence of the mayhems and dangers posed by the presence of gullies, which have reduced socio-economic, agricultural and other activities to the minimal in these areas.

Plates 1, 2 and 3 are pictures showing the effect of gullies in these areas.



Plate 1. Destroyed building at Umueshi in Ideato North L.G.A of Imo State.



Plate 2. Destroyed farm land at Ogberuru in Orlu L.G.A of Imo State.



Plate 3. Destroyed road at Ogberuru, in Orlu.

1.3 Justification

The study area – Orlu and environs was selected for this research as a result of serious environmental challenges caused by gully erosions within the area and the rate at which this menace eats up the top soil within the area. This menace poses serious problem to agricultural activities, causes damage to buildings and roads as seen above, thereby making life difficult and unbearable for the inhabitants of the area.

Hence, it becomes necessary to carry out a detailed study of the area using advanced geophysical tools such as Remote Sensing (Landsat Imagery) and Resistivity Method (VES and ARS) in order to have a clear picture of the structural architecture of the subsurface on a

regional scale as well as identify the trends of the mapped lineaments and to evaluate the soil type, texture and strength using Geotechnical methods.

1.4 Aim

The aim of this study is to carry out an integrated geophysical study of the area (Orlu and environs) to infer the effects of tectonism and neo-tectonism to gully erosion initiation and development.

1.5 Objectives

The main objective of this work is as stated below

1. To carry out an azimuthal resistivity sounding to determine the direction or directions of structural weakness.
2. To determine the coefficient of anisotropy and root mean square values
3. Landsat data were acquired to generate Rose diagram, lineament map and lineament density map
4. Geotechnical analyses were carried out to determine the soil type, their textural characteristics and compaction.
5. Geological mapping of the gully erosions were carried out to determine the trends of the gullies and the soil units exposed by the gullies.
6. Finally to integrate all the above listed objectives to determine the action cause of these gullies.

1.6 Location, physiography and Geology of the Area of Study

1.6.1 Location, Climate, Physiography and Drainage of the study area

The study area (Orlu and environs) is located in the Southeastern region of Nigeria. It lies between latitude 5°52'N and 5°44'N, longitude 7°00'E and 7°08'E. The study area (Orlu and Environs) is located between the lower River Niger and the upper and middle Imo River, with

Njaba River being a pronounce River in the area. Its Climate State is humid, semi-hot equatorial type. The area experiences heavy rainfall, with an average annual rainfall of 2000 - 2400 mm/yr particularly during the rainy seasons (April – October). The superficial rainfall distribution is bimodal, with peaks in July and September and a two weeks break in August. The rainy season begins in March and lasts till October or early November. Rainfall is often at its maximum at night and during the early morning hours. The higher annual rainfall depths and rainfall days encourages large volumes of runoff. However, variations occur in rainfall amount from year to year, usually between 1,990mm and 2,200mm. Relative humidity oscillates between 75% and 90% in the Dry and Rainy seasons. Temperatures are similar all over the study area, with January to March being the hottest months, and having a mean annual temperature above 20°C.

1.6.2 Geological Background

The study area is dominated by three different geologic units viz: Benin, Ogwashi-Asaba and Ameki Formations. The figure below shows that the Benin Formation is the youngest Formation outcropping in the study area. The name Benin Formation was reinstated by Reyment (1965) for the formation known as “Coastal Plain Sands” (Avbovbo, 1978). It consists mainly of yellow and white sands, sandstone and gravel with clays occurring in lenses (Reyment, 1965). The sands and sandstones are coarse to fine partly unconsolidated (Avbovbo, 1978). The sediments represent upper deltaic plain deposits. The environment of deposition is partly marine, partly deltaic, partly estuarine, partly lagoonal and fluviolacustrine (Reyment, 1965). The Benin Formation is composed mainly of high resistant fresh water-bearing continental sands and gravels with clay and shale intercalations (Onyeagocha, 1980). The formation which dips South-westwards starts as a thin edge layer at its contact with the Ogwashi-Asaba Formation in the northern part of the area and thickens southwards to about 100m in Owerri area (Reyment, 1965). The sandy unit

which constitutes about 95% of the rock in the area is composed of over 96% of quartz (Onyeagocha, 1980). The Ogwashi-Asaba Formation underlies the Benin Formation and occupies the Northern part of the area. It was referred to as Lignite series (Onyeagocha, 1980). It consists of alternated unconsolidated sandstones with sandy clays and lignite seams. The Ameki Formation underlies the Ogwashi-Asaba Formation, consisting of deltaic sands and shallow marine clastics. Two main lithological divisions have been recognized: a lower with fine to coarse sandstones with intercalation of calcareous shale and thin shelly limestone, limestone modules; and an upper with coarse cross bedded sandstones bands of fine grey-green sandstone and sandy clay (Whiteman, 1982).

The stratigraphic succession of the area is summarized in Table 1 below.

Table 1: Stratigraphic Succession table

AGE	FORMATION	LITHOLOGY
Miocene – Recent	Benin	Medium to coarse grained, poorly consolidated with clay lenses and stringers
Oligocene – Miocene	Ogwashi-Asaba	Unconsolidated sand with lignite seams at Various layers.
Eocene	Ameki	Grey clayey sandstone and sandy clay stone

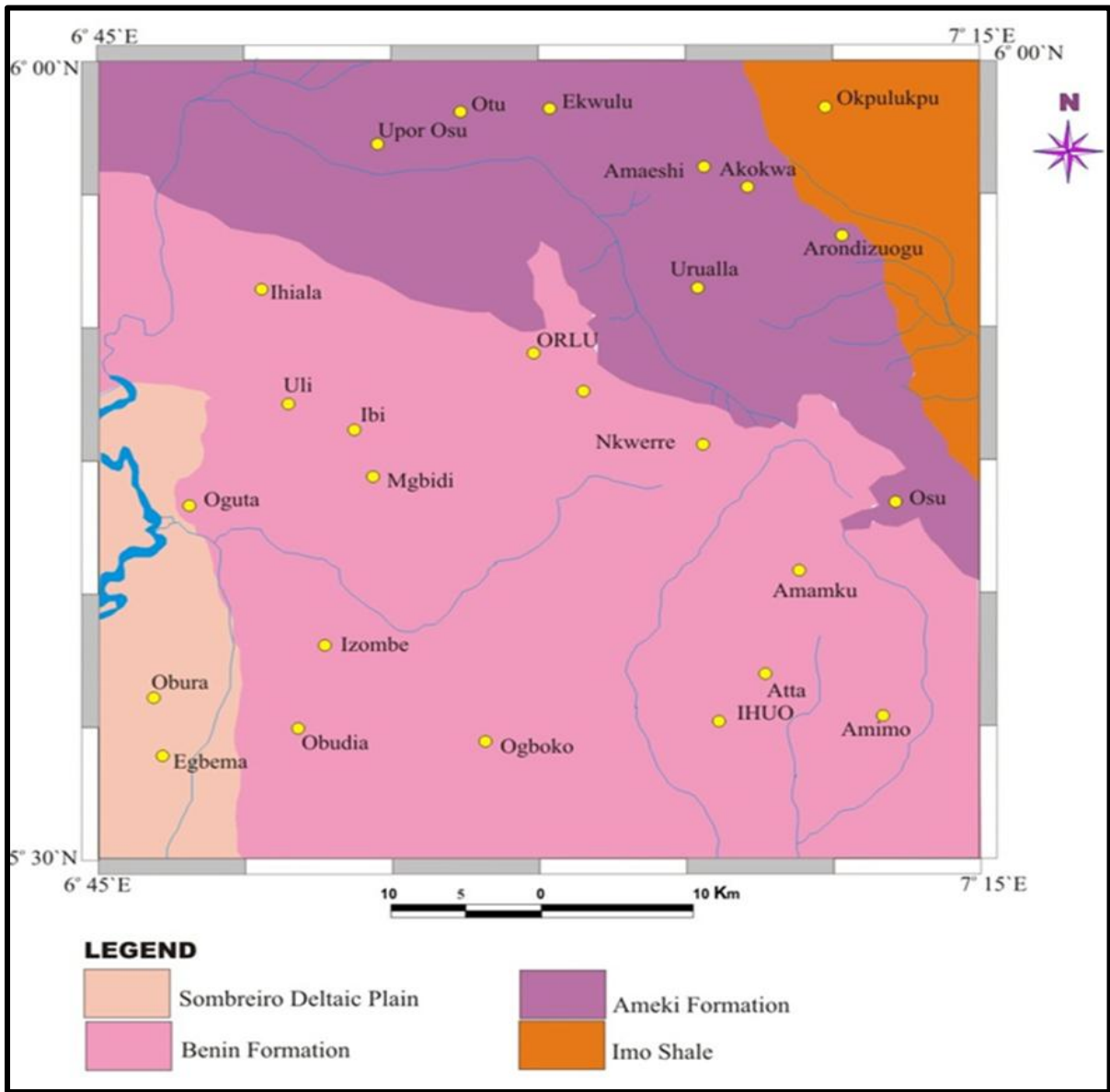


Fig. 1.1 Geology map of Orlu and environs

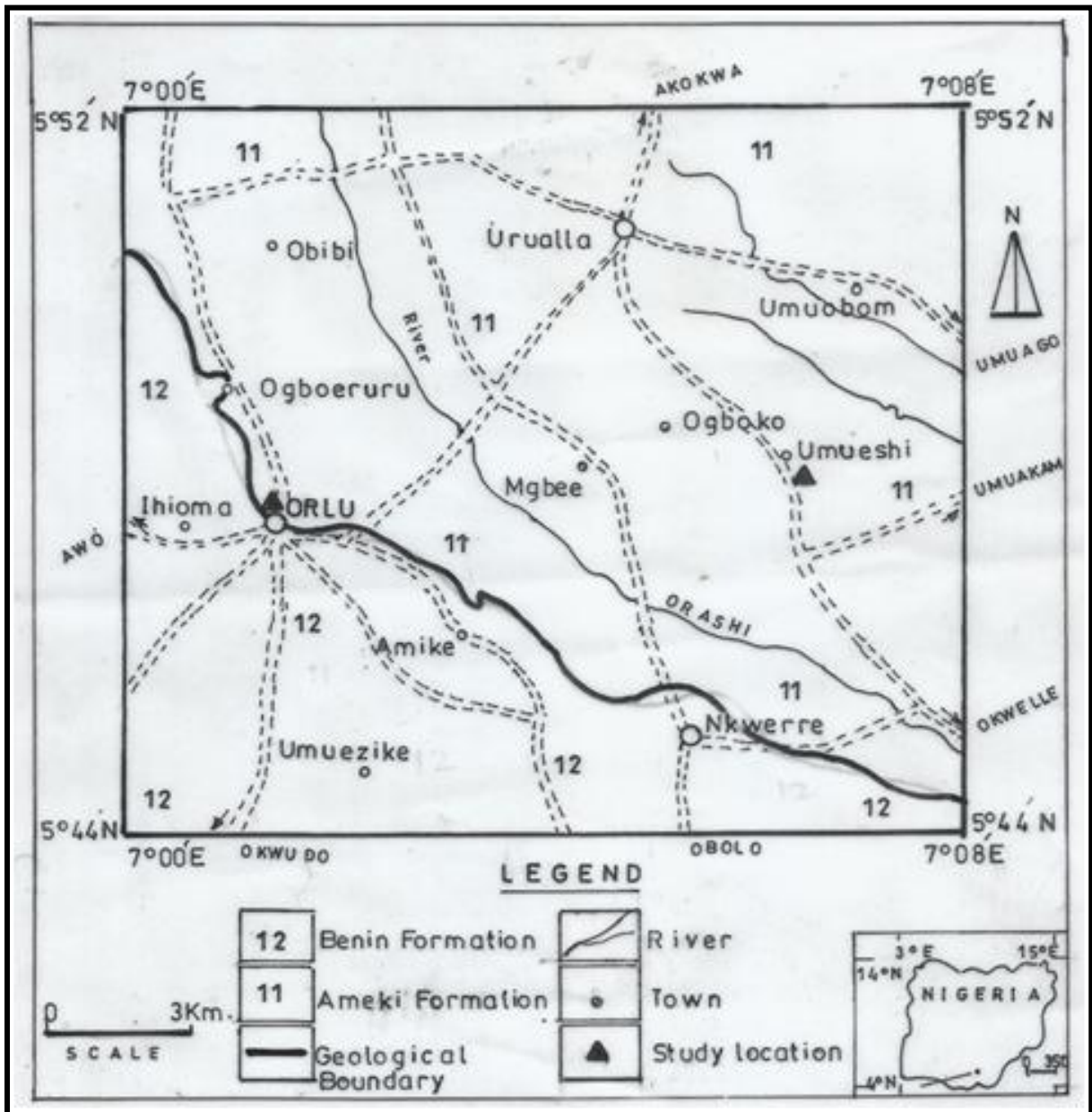


Fig. 1.2 Location map of Orlu and Environs

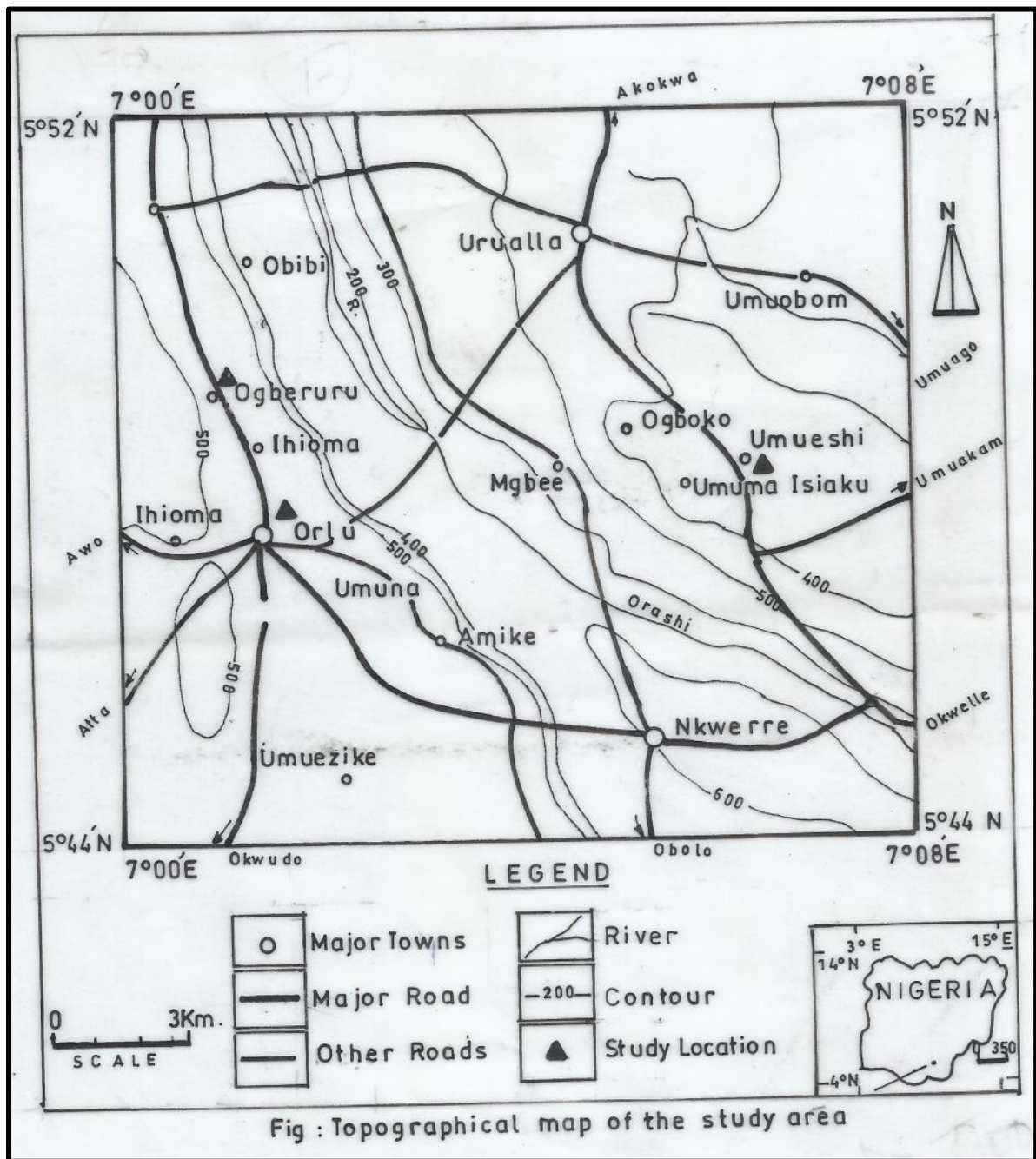


Fig : Topographical map of the study area

Fig. 1.3 Topographical map of Orlu and Environs

CHAPTER TWO

LITERATURE REVIEW

2.1 Review of related literature

Erosion is one of the major environmental disasters which many scholars from different fields have researched on. A lot of research has been done on it, particularly in the southeastern part of Nigeria. The aim for these numerous researches is to effectively evaluate the causes, problems and solutions to erosion. Some of these early researchers include, Grove (1951), Carter (1958), Nwajide and Hoque (1979), Babalola (1988), Fubara (1988), Ofomata (1988), Ogbukagu (1976), and Nwankwo et al (1988). They made useful discussions and inferences of the problem and solution of soil erosion in southeastern Nigeria. Grove (1951) recognized two main types of gully on the scarp slopes of the Udi plateau and the Awka - Orlu uplands:

1. Spring gullies, where permeable sands and sandstones rest on less permeable deposits and
2. Slope gullies, which originate as channels (for example, sunken footpaths) in bottom-of-slope locations.

Spring gullies are enlarged by sapping, caving and landslips and slope gullies by potholing; both types are further enlarged by waterfall action at the rim and undercutting of the sides promotes earth falls and landslips. Intensive rainfall clears the debris from the gully bottom and the more continuous rains saturate the bank materials and cause the slumping of larger blocks. Grove (1951) noted a possible connection between gully erosion and the increased runoff, associated with the clearing of woodland and road building. Nearly forty years later, the FAO (1990) concluded that most of the gully erosions in southeastern Nigeria were caused by badly designed roads and the clearance of vegetation from building sites. It was noted that some gullies originate as narrow rills with a down-slope

orientation, which undergo progressive widening and deepening, with successive rainfall events (Hudec et al., 2006).

These features tend to occur on bare soil surfaces, created by human and animal foot traffic and wheeled traffic in off-road locations and also by the grading of soil along the sides of roads. A special case is provided by lateritic deposits, in which narrow, relatively deep gullies are eroded downwards to the more friable materials beneath the lateritic layer, leading to caverning in the more easily eroded material and collapse. Ogbukagu (1988), in his report on the influence of geology on soil erosion concluded that areas, underlain by sedimentary terrain are more susceptible to erosion than those underlain by either igneous or metamorphic terrain. Niger Techno (1974), in her report on the prefeasibility study of soil erosion in the central states of Nigeria, described the weathered layer within the Benin formation as made up of slightly silty sands, poorly permeable surface with no vegetative cover thus preventing absorption of all high rainfall, causing the water to gather into high concentrated flows, leading to incisions of the surface film. The cohesionless sands are therefore easily eroded with the help of slope degradation via the concentration of the water. Ofomata (1988) in his report on soil characteristics in the rain forest zone of the southeastern Nigeria was of the view that rainfall is one of the important factors of erosion in the area. He is also of the notion that the impact of rainfall (raindrop energy) on overland runoff generate turbulence that increase the load carrying potential of the runoff, thereby causing soil particle movement, which occurs only when the tractive force exceeds the shear resistance of the soil ($F > 1$).

Fubara (1988) reported on the menace of flood and erosion, and environmental disaster combat plan and asserted that the ultimate causes of accelerated erosion is the human interference in the natural ecosystem, such as indiscriminate removal of vegetation,

improper land usage, construction works and other activities which exposes the land to other destructive natural agents.

Babalola (1988), concluded in his report on soil properties affecting infiltration, runoff and erodibility attributed the low percentage of fines in sediments coupled with high porosity, relatively high permeability and low initial water content to causes of erosion. Jeje (1988), worked on soil erosion characteristics, processes and extent in the lowland rainforest area of southeastern Nigeria. He reported that when a surface is exposed, high intensity storms affect near surface and mechanical eluviations will be generated, this will lead to the pore spaces blockage development of the outer coast, decrease in soil permeability and reduction infiltrating on runoff. Pointing out that surface water flow or runoff begins, when the infiltration capacity is exceeded. Nwankwo et al (1988) based on their work along Amucha - Okwudor gully site concluded that the area has high porosity ranging from 30% to 40% with an average void ratio of 0.6.

They also estimated the average growth rate of the gully to about 25m/yr.

2.2. Theoretical framework

Soil erosion is one form of soil degradation along with soil compaction, low organic matter, loss of soil structure, poor internal drainage, salinization, and soil acidity problems. These other forms of soil degradation, serious in themselves, usually contribute to accelerated soil erosion. Soil erosion is a naturally occurring process on all land.

The major agents of soil erosion are water and wind, each contributing a significant amount of soil loss. Soil erosion may be a slow process that continues relatively unnoticed, or it may occur at an alarming rate causing serious loss of topsoil. The loss of soil from farmland may be reflected in reduced crop production potential, lower surface water quality and damaged drainage networks.

2.2.1 Erosion by Water

The rate and magnitude of soil erosion by water is controlled by the following factors:

1. Rainfall Intensity and Runoff:

Both rainfall and runoff factors must be considered in assessing a water erosion problem. The impact of raindrops on the soil surface can break down soil aggregates and disperse the aggregate material. Lighter aggregate materials such as very fine sand, silt, clay and organic matter can be easily removed by the raindrop splash and runoff water; greater raindrop energy or runoff amounts might be required to move the larger sand and gravel particles.

Soil movement by rainfall (raindrop splash) is usually greatest and most noticeable during short duration, high-intensity thunderstorms. Although the erosion caused by long-lasting and less intense storms is not as spectacular or noticeable as that produced during thunderstorms, the amount of soil loss can be significant, especially when compounded over time. Runoff can occur whenever there is excess water on a slope that cannot be absorbed into the soil or trapped on the surface. The amount of runoff can be increased if infiltration is reduced due to soil compaction, crusting or freezing. Runoff from the agricultural land may be greatest during spring months when the soils are usually saturated, snow is melting and vegetative cover is minimal.

2. Soil Erodibility

Soil erodibility is an estimate of the ability of soils to resist erosion, based on the physical characteristics of each soil. Generally, soils with faster infiltration rates, higher levels of organic matter and improved soil structure have a greater resistance to erosion. Sand, sandy loam and loam textured soils tend to be less erodible than silt, very fine sand, and certain clay textured soils.

Tillage and cropping practices which lower soil organic matter levels, cause poor soil structure, and result of compacted soil contributes to increase in soil erodibility. Decreased infiltration and increased runoff can be a result of compacted subsurface soil layers. A

decrease in infiltration can also be caused by a formation of a soil crust, which tends to "seal" the surface. On some sites, a soil crust might decrease the amount of soil loss from sheet or rain splash erosion, however, a corresponding increase in the amount of runoff water can contribute to greater rill erosion problems. Past erosion has an effect on a soils' erodibility for a number of reasons. Many exposed subsurface soils on eroded sites tend to be more erodible than the original soils were, because of their poorer structure and lower organic matter. The lower nutrient levels often associated with subsoils contribute to lower crop yields and generally poorer crop cover, which in turn provides less crop protection for the soil.

3. Slope Gradient and Length

Naturally, the steeper the slope of a field, the more the earth is been eroded by water. Soil erosion by water also increases as the slope length increases due to the greater accumulation of runoff. Consolidation of small fields into larger ones often results in longer slope lengths with increased erosion potential, due to increased velocity of water which permits a greater degree of scouring (carrying capacity for sediment).

4. Vegetation

Soil erosion potential is increased if the soil has no or very little vegetative cover of plants and/or crop residues. Plant and residue cover protects the soil from raindrop impact and splash, tends to slow down the movement of surface runoff and allows excess surface water to infiltrate.

The erosion-reducing effectiveness of plant and/or residue covers depends on the type, extent and quantity of cover. Vegetation and residue combinations that completely cover the soil, and which intercept all falling raindrops at and close to the surface and the most efficient in controlling soil (e.g. forests, permanent grasses). Partially incorporated residues and residual roots are also important as these provide channels that allow surface water to move into the soil. The effectiveness of any crop, management system or protective cover also depends on how much protection is available at various periods during the year, relative to the amount of

erosive rainfall that falls during these periods. In this respect, crops which provide food, protective cover for a major portion of the year can reduce erosion much more than can crops which leave the soil bare for a longer period of time (e.g. row crops) and particularly during periods of high erosive rainfall (spring and summer).

Soil erosion potential is affected by tillage operations, depending on the depth, direction and timing of plowing, the type of tillage equipment and the number of passes. Generally, the less the disturbance of vegetation or residue cover at or near the surface, the more effective the tillage practice is in reducing erosion.

5. Conservation Measures

Certain conservation measures can reduce soil erosion by both water and wind. Tillage and cropping practices, as well as land management practices, directly affect the overall soil erosion problem and solutions on a farm. When crop rotations or changing tillage practices are not enough to control erosion on a field, a combination of approaches or more extreme measures might be necessary. For example, contour ploughing, strip cropping, or terracing may be considered.

2.2.2 Ecological Effects of Sheet and Rill Erosion

Sheet erosion is soil movement from raindrop splash resulting in the breakdown of soil surface structure and surface runoff; it occurs rather uniformly over the slope and may go unnoticed until most of the productive topsoil has been lost. Rill erosion results when surface runoff concentrates forming small yet well-defined channels. These channels are called rills when they are small enough to not interfere with field machinery operations. The same eroded channels are known as gullies when they become a nuisance factor in normal tillage.

Surface runoff, causing gull formation or the enlarging of existing gullies, is usually the result of improper outlet design for local surface and subsurface drainage systems. The soil

instability of fully banks, usually associated with seepage of ground water, leads to sloughing and slumping (caving-in) of bank slopes. Such failures usually occur during spring months when the soil water conditions are most conducive to the problem.

Gully formations can be difficult to control if remedial measures are not designed and properly constructed. Control measures have to consider the cause of the increased flow of water across the landscape, and a multitude of conservation measures come into play. Operations with farm machinery adjacent to gullies can be quite hazardous when cropping or attempting to reclaim lost land.

2.2.3 Erosion by Wind

The rate and magnitude of soil erosion by wind is controlled by the following factors:

1. Erodibility of Soil: Very fine particles can be suspended by the wind and then transported great distances. Fine and medium size particles can be lifted and deposited, while coarse particles can be blown along the surface (commonly known as the saltation effect). The abrasion that results can reduce soil particle size and further increase the soil erodibility.

2. Soil Surface Roughness: Soil surfaces that are not rough or ridged offer little resistance to the wind. However, over time, ridges can be filled in and the roughness broken down by abrasion to produce a smoother surface susceptible to the wind. Excess tillage can contribute to soil structure breakdown and increased erosion.

3. Climate: The speed and duration of the wind have a direct relationship to the extent of soil erosion. Soil moisture levels can be very low at the surface of excessively drained soils or during periods of drought, thus releasing the particles for transport by wind. This effect also occurs in freeze drying of the surface during winter months.

4. Unsheltered Distance: The lack of windbreaks (trees, shrubs, residue, etc.) allows the wind to put soil particles into motion for greater distances thus increasing the abrasion and soil erosion. Knolls are usually exposed and suffer the most.

5. Vegetative Cover: The lack of permanent vegetation cover in certain locations has resulted in extensive erosion by wind. Loose, dry, bare soil is the most susceptible; however, crops that produce low levels of residue also may not provide enough resistance. As well, crops that produce a lot of residue also may not protect the soil in severe cases. The most effective vegetative cover for protection should include an adequate network of living windbreaks combined with good tillage, residue management, and crop selection.

2.3 Gully Erosion and Control

Generally, gullies are formed by an increase in surface run-off. Therefore, minimizing surface run-off is essential in gully control. Water sheds deteriorate because of man's misuse of the land, short intensive rainstorms, prolonged rains of moderate intensity, and rapid snow melts. These precipitation factors also turn into high run-off which causes flooding and forms gullies.

In gully control, the following three methods must be applied according to the order given:

- (1) Improvement of gully catchments to reduce and regulate the run-off rates (peak flows);
- (2) Diversion of surface water above the gully area;
- (3) Stabilization of gullies by structural measures and accompanying re-vegetation.

When the first and/ or second methods are applied in some regions of countries with temperate climates, small or incipient gullies may be stabilized without having to use the third method. On the other hand, in tropical and subtropical countries which have heavy rains (monsoons, typhoons, tropical cyclones, etc.) all three methods must be carried out for successful gully control.

2.3.1 Factors Affecting Gully Formation

The factors affecting gully formation can be categorized into two groups, man-made factors, and physical factors.

- 1. Man-Made Factors:** While erosion is a natural process, human activities have increased soil erosion rate by 10 – 40 times as it should occur naturally (Goudie, Andrew 2000).

Man-made factors affecting gully formation are as explained below.

A. Improper land use: In developing countries, rapidly-increasing populations usually migrates upland to occupy forests or rangeland. Most migrants cut trees, burn litter and grasses, and cultivate hillsides without using conservation measures. After a few years, the productivity of the soil is lost because of sheet, rill and gully erosion, and the land is abandoned. This kind of cultivation, (slash and burn or shifting cultivation) is repeated by farmers on other hillsides until the land loses its productivity there as well. Thus, the whole of an area may be completely destroyed by gullying as the gully heads advance to the upper ends of the watershed.

B. Forest and grass fires: Many forest fires are caused by the uncontrolled burning used in shifting cultivation. These fires can easily spread into the forest and destroy the under growth and litter. Grass fires are usually ignited by farmers near the end of the dry season in order to obtain young shoots for their livestock or new land for cultivation. On slopes, the soil that is exposed after forest and grass fires is usually, gullied during the first rainy season.

C. Mining: Underground (block cave) mining is another factor that can cause gullying. Initially, cracks in the ground and soil creep (a kind of gravity erosion) are observed in the mining areas. Then, during rainy seasons, gullies are formed. Gullying in open-pit mining areas is also a big problem in many countries.

D. Road construction: If road cuts and fill slopes are not revegetated during or immediately following road construction, gullies may form on both sides of the road. Inadequate drainage systems for roads (small number of culverts, insufficient capacity of road ditches, etc.) area

major cause of gullying. Widening operations along roadsides do not often follow road construction but, where widening is practiced, the operation usually causes landslide erosion and then gullying during the first rainy season.

2. Physical Factors: As mentioned before, gullies are formed by increased surface run-off which acts as a cutting agent. The main physical factors affecting the rate and amount of surface run-off are precipitation, topography, soil properties and vegetative cover.

A. Precipitation

i. Monthly distribution of rainfall: The duration of wet and dry seasons cannot be deduced from total annual rainfall. The monthly distribution of rainfall is more significant than total annual rainfall because of its effects on the growth of vegetation, as well as the fact that it gives some indications about rainfall intensity.

In humid regions with uniform distribution of rainfall, surface erosion, including gully formation, may not be a serious problem because vegetation grows throughout the year.

However, in areas that do not have uniform rainfall, the vegetation (especially grass) dries up during the prolonged dry season (3 to 5 months or more). If the land is not properly used, or if forest or grass fires occur during the dry period, it cannot sufficiently hold rainwater and so the increased surface run-off in the rainy season produces large scale landslides and gullies.

ii. Rainfall intensity and run-off: There is a relationship between rainfall intensity, rate of run-off, density of vegetative cover, and the size of catchment area. This relationship is generally expressed in equations. The Rational Formula which is used in engineering designs for gully and torrent control is a good way to demonstrate this relationship.

If the amount of rainfall is more than the holding capacity of the soil, there will be an increase in surface run-off, followed by surface erosion and gullying. In some tropical and subtropical countries, after the soil is completely saturated, almost all of the rainfall turns into

run-off during the wettest months, which include the monsoon season, tropical cyclones and especially typhoons. It rains intensively for two or three days without stopping during each typhoon period and the increased run-off causes landslides, huge gullies and devastating floods.

In continental and temperate regions, prolonged rain of moderate intensity (duration several days), or short, intensive rain storms lasting from 15 to 90 minutes (maximum rainfall intensity about 3mm/minute), cause landslides, gullies and floods because of the increased run-off in the watersheds. Torrential floods, which generally occur after the short, intensive rain storms, destroy agricultural lands, residential areas, roads, irrigation ditches and canals at the base of the valley below a deteriorated watershed. Rainfall intensity and run-off rates (peak flows) are expressed in milliliters per hour or minute and cubic meters per second, respectively. In designing engineering measures such as check dams or diversions in gully and torrent control, the rate of run-off is more important than the amount of run-off.

iii. Rapid snowmelts: Rapid snowmelts turn into high run-off. This increased surface run-off acts as a cutting agent and produces gullies. Like prolonged rains of moderate intensity and short intensive rain storms, rapid snowmelts cause destructive floods.

B. Topography: The size and shape of a drainage area, as well as the length and gradient of its slopes have an effect on the run-off rate and amount of surface water. Therefore, all topographic characteristics should be studied in detail before gully control work begins.

C. Soil properties: The following seven soil classes are based on soil texture: sand, loamy sand, sandy loam, loam, silt loam, clay loam and clay. The infiltration rate increases from clay to sand (for loamy sand 2.5 - 5 cm/hour), but resistance against erosion decreases.

D. Vegetative cover: The role of vegetative cover is to intercept rainfall, to keep the soil covered with litter, to maintain soil structure and pore space, and to create openings and

cavities by root penetration. This is best achieved by an undisturbed multistory forest cover. Under special conditions, however, a well-protected, dense grass cover may also provide the necessary protection.

In general, it is management and protection rather than the type of the vegetative cover which determines its effectiveness in gully control. Any vegetation which is well-adapted to local conditions and which shows vigorous growth may be used. In some cases, these may be broadleaf species, in others conifers, tall grasses, etc. In critical areas, it may be necessary to exclude any use of the protecting vegetation.

2.4 Development and Classification of Gullies

2.4.1 Development of gullies

Sheet erosion, which is a uniform removal of soil in thin layers from sloping land, occurs where the velocity of surface run-off is about 0.3 to 0.6 meters per second. More commonly, however, the direct impact of raindrops on soil particles causes their detachment and gradual downhill movement-splash erosion. Sheet erosion is barely detectable in the short term because it is a gradual process. However, over a long period, the consequent exposure of roots and subsoil can be easily observed. Rill erosion is the removal of soil by surface flow that either form small, shallow channels or streamlets - neither is deeper than 30cm. Because of its higher surface-flow velocities, rill erosion has a greater capacity than sheet erosion to remove and transport soil. Still, because they are small, rills can easily be eliminated by normal tilling or ploughing. Gullies are formed where many rills join and gain more than 30cm depth. The rate of gully erosion depends on the run-off, producing characteristics of the watershed: the drainage area; soil characteristics; the alignment, size and shape of the gully; and the gradient of the gully channel. Gullies are very destructive and cannot be eliminated by tilling or ploughing because of their depth. A gully develops in three distinct stages; Waterfall erosion, Channel erosion along the gully bed and landslide erosion on gully banks.

Correct gully control measures must be determined according to these development stages.

1. Waterfall erosion: Waterfall erosion can also be broken down into three steps:

A. First Stage: First, sheet erosion develops into rills; the rills gain depth and reach the B-horizon of the soil.

B. Second Stage: The gully reaches the C-horizon and the weak parent material is removed. A gully head often develops where running water plunges from the upstream segment to the bottom of the gully.

C. Third stage: The falling water from the gully head starts carving a hollow at the bottom of the gully by direct action as well as by splashing. When the excavation has become too deep, the steep gully-head wall collapses. This process is repeated again and again, so that the gully head progresses backwards to the upper end of the watershed. This process is called gully-head advancement.

As the gully head advances backward and crosses lateral drainage ways caused by waterfall erosion, new gully branches develop. Branching of the gully may continue until a gully network or multiple-gully systems cover the entire watershed.

2. Channel erosion along gully beds: Channel erosion along a gully bed is a scouring away of the soil from the bottom and sides of the gully by flowing water. The length of the gully channel increases as waterfall erosion causes the gully head to advance backward. At the same time, the gully becomes deeper and wider because of channel erosion. In some cases, a main gully channel may become as long as one kilometer.

3. Land-slide erosion on gully banks: Channel erosion along gully beds is the main cause of landslides on gully banks. During the rainy season, when the soil becomes saturated, and the gully banks are undermined and scoured by channel erosion, big soil blocks start sliding down the banks and are washed away through the gully channel. Land-slide erosion on gully

banks also occurs in regions with temperatures that alternate between freezing and thawing. When the temperature drops below zero (Celsius), wet gully banks freeze. After the temperature rises above zero, the banks thaw, the soil loosens, and the loose gully banks easily slide during the first rainy season. After landslides have occurred on all gully banks, a considerable number of new branch gullies may begin along the disturbed banks. During the third stage of gully development, gullies become deeper and longer as well as wider.

The three stages of gully development (waterfall erosion, channel erosion along the gully bed, and landslides on gully banks) will continue unless the gully is stabilized by structural control measures and re-vegetation.

2.4.2 Classification of Gullies

Gullies are classified under several systems based on their different characteristics.

1. Gully classification base on shape: This system classifies gullies according to the shape of their cross-sections.

a. U-Shaped gullies: These are formed where both the topsoil and subsoil have the same resistance against erosion. Because the subsoil is eroded as easily as the topsoil nearly vertical walls are developed on each side of the gully.

b. V-Shaped gullies: These develop where the subsoil has more resistance than topsoil against erosion. This is the most common gully form.

c. Trapezoidal gullies: These can be formed where the gully bottom is made of more resistant material than the topsoil



Plate 4. U Shape gullies at Ogberuru in Orlu L.G.A of Imo state



Plate 5. V-Shape erosion at Umuomeji Urualla in Ideato North L.G.A of Imo State

2. Gully classification based on continuation

(a) Continuous gullies consist of many branch gullies. A continuous gully has a main gully channel and many mature or immature branch gullies as seen in Ogberuru in Orlu. A gully network (gully system) is made up of many continuous gullies. A multiple-gully system may be composed of several gully networks.

(b) Discontinuous gullies may develop on hillsides after landslides. They are also called independent gullies. At the beginning of its development, a discontinuous gully does not have a distinct junction with the main gully or stream channel. Flowing water in a discontinuous gully spreads over a nearly flat area. After sometime, it reaches the main gully channel or stream. Independent gullies may be scattered between the branches of a continuous gully, or they may occupy a whole area without there being any continuous gullies.

2.4.3 Criteria for the Selection of Gully Control Measures

1. Size of gully and its relationship to a torrent: In deteriorated mountain watersheds, each continuous gully in a gully network usually has a distinct catchment and a main gully channel, but it may or may not have a fan. The main gully channel of each continuous gully is about one kilometer long and its catchment area is not usually more than 0.2 square kilometer (20 hectares). In general, there is not any vegetative cover in a gully system. A torrent catchment usually comprises several gully systems; forest and rangelands destroyed or in good condition; hillside farming areas; low croplands; and urban areas (villages, towns). Therefore, the catchment area of a torrent may spread over more than 1000 hectares and be 2 kilometers long. In order to control a torrent and avoid upstream floods, it is essential to stabilize all the gullies throughout the entire catchment area.

2. Continuous gully as a basic treatment unit: Gully control is one of the most important restoration methods used in watershed management, and timing is an essential element. The

field work in all structural and vegetative control measures selected should be completed during the dry and early rainy season. This is the most important aspect of gully control - especially in tropical and subtropical countries. Otherwise, the incomplete structural work can easily be destroyed during the first rainy season. In addition, vegetative measures such as the planting of tree seedlings and shrub and grass cuttings cannot begin until structural work is complete. Each continuous gully in a gully system should be regarded as a basic treatment unit, and all the control measures in that unit should be finished before the rainy season.

3. Selection of gully control measures: For a continuous gully, the main criteria for selecting structural control measures are based on the size of the gully catchment area, the gradient and the length of the gully channel. The various portions of the main gully channel and branch gullies are stabilized by brush fills; earth plugs; and brushwood, log, and loose-stone check dams. The lower parts are treated with loose-stone or boulder check dams. At a stable point in the lowest section of the main gully channel, for example, on a rock outcrop, a gabion check dam or cement masonry check dam should be constructed. If there is not a stable point, a counter-dam (gabion or cement masonry) must be constructed in front of the first check dam. The points where the other check dams will be constructed are determined according to the compensation gradient of the gully channel and the effective height of the check dams.

2.5. The Electrical Resistivity Method

As resistivity is a fundamental electrical property of rock materials closely related to their lithology, the determination of the subsurface distribution of resistivity from measurements on the surface yields useful information on the structure or composition of buried formations. Therefore, Vertical Electrical Sounding (VES) was used for this purpose. VES furnishes information about the vertical succession of different conductive zones and their individual thickness and resistivities. For homogeneous and horizontally stratified earth, VES results

represent only resistivity variation across the layers up to the maximum depth of probe. Practically, as the spacing between the current electrodes is increased about a centre, the total volume of earth included in the measurement also increases both vertically and horizontally (Telford, et al 1990).

2.5.1 Vertical Electrical Sounding(VES)

Vertical electric sounding (VES) employs collinear arrays designed to output a 1-D vertical apparent resistivity versus depth model of the subsurface at a specific observation point. In this method a series of potential differences were acquired at successively greater electrode spacing while maintaining a fixed central reference point. The induced current passes through progressively deeper layers at greater electrode spacing. The potential difference measurements are directly proportional to the changes in the deeper subsurface. Apparent resistivity values calculated from measured potential differences can be interpreted in terms of overburden thickness, water table depth, and the depths and thicknesses of subsurface strata. The two most common arrays used for VES are the **Wiener array** and the **Schlumberger array**. Typical vertical electrical sounding design using Schlumberger array is shown in figure below.

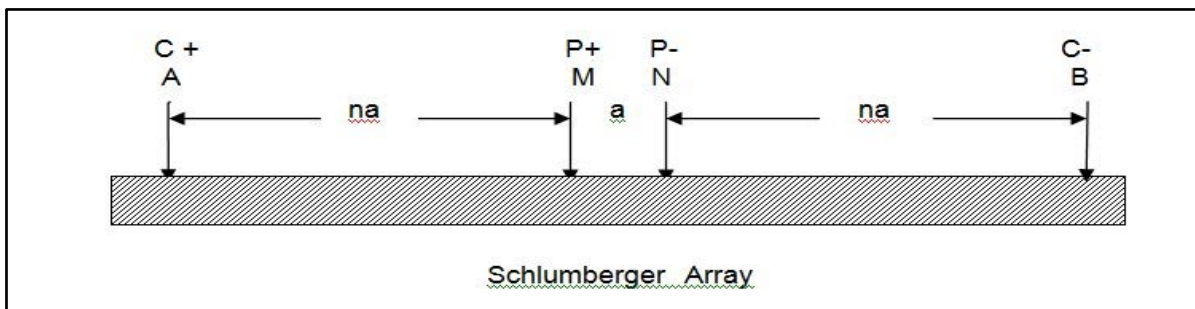


Fig. 2.0. Schlumberger Array

The electrodes are in a straight line and like the Wenner array, the outer electrodes are the current electrodes and the inner electrodes are the potential electrodes. The potential

electrodes, usually designated **M** and **N**, should never be separated by more than one-fifth the separation between the current electrodes. The current electrodes are usually labelled **A** and **B**. Apparent resistivity is given by the following formula where π is 3.14, **AB** is the distance between the current electrodes, **MN** is the distance between the potential electrodes and **R** is the resistance read on the MiniRes. MN can also be designated **a** and the distance between a current electrode and the nearest potential electrode designated as **na**. $R_a = \pi R (AB) (AB)/4(MN) = \pi R a n (n+1) \dots\dots\dots 1$

As the current electrodes are expanded farther, the potential difference between the fixed potential electrodes becomes smaller and smaller. Finally the signal to noise ratio becomes noticeably small. Then the potential electrodes are expanded and an observation is made with the current electrodes at the same spacing. Theoretically, the apparent resistivities should be the same. However, they will always differ by at least a small amount. This may be due to lateral inhomogeneities in the earth or to a localized irregularity near one of the potential electrodes. The survey is resumed with the several more observation made with the current electrodes being placed at greater and greater separation. For a single sounding there may be three, four or even five separations used for the potential electrodes. This, in turn, generates three, four or five segments of sounding curve, each with at least a small offset from the adjacent segments.

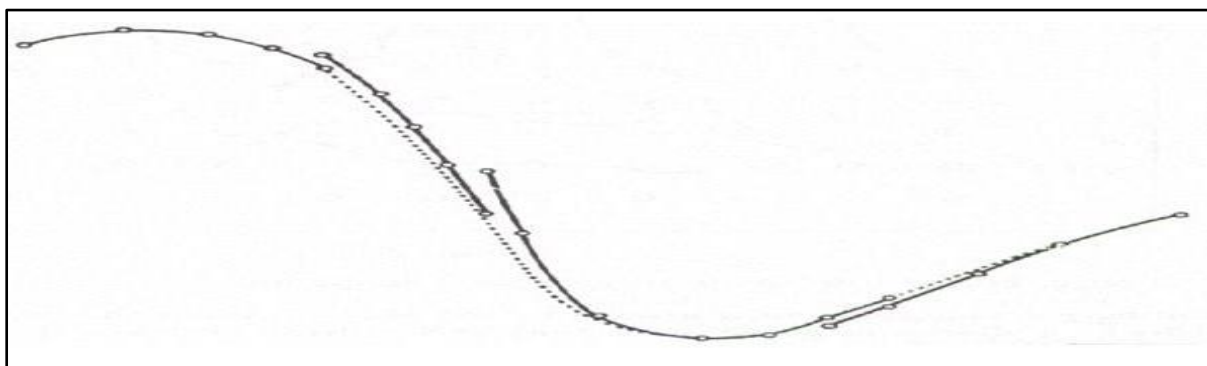


Fig. 2.1: Sample of a sounding curve

The Schlumberger array has an advantage over the Wenner array. The potential electrodes are moved less often and therefore there is less fieldwork in collecting the data for a sounding. Despite this timesaving, there are great advantages to the Wenner sounding technique. First, the Wenner array gives the highest signal-to-noise ratio. Second, if there is an inhomogeneity in the vicinity of the inner (potential) electrodes, a whole segment of the apparent resistivity curve will have an erroneous offset. With the Wenner method, there would be only one data point having an erroneous offset. If there are numerous surficial inhomogeneities, the Wenner method would show the interpreter this important feature of the survey and the smoothed curve fitted through the Wenner data will reflect a truer value for the subsurface.

2.5.2 Azimuthal Resistivity Survey

Azimuthal resistivity surveys increasingly are being used by hydrogeologists in the identification and characterization of fractured rocks. In these investigations, electrical resistivity is measured as a function of azimuth about a fixed central point. In most recent published examples, any observed change in apparent resistivity with azimuth is interpreted as being indicative of fracture anisotropy. However, interpretation of rotational sounding data is actually more complicated, as azimuthal variations in apparent resistivity are also produced by the presence of dipping stratigraphy and other lateral changes in formation resistivity. Such effects are generally overlooked because the field techniques normally employed is incapable of detecting them. Consequently, it is quite probable that the results of many published surveys have been wrongly interpreted. An alternative field procedure and interpretation methodology has been developed to differentiate anisotropy, dipping layers and lateral effects. This approach makes use of the offset Wenner technique and examines the different responses of the individual Wenner resistances above different geological structures. Analysis of data obtained using the azimuthal offset Wenner technique from sites in Britain and Ireland have successfully identified subsurface structures and determined the anisotropy

where it is present. The identification and characterization of fractures is important in rocks with low primary (matrix) porosity because the bulk porosity and permeability are determined mainly by the intensity, orientation, connectivity, aperture, and infill of fracture systems (Skjernaas and Jørgensen, 1994). Conductivity of fracture systems can be ranged over several orders of magnitude. The flow regimes and chemical processes associated with fracture networks are complex and, hence, have considerable implications as regards waste disposal, groundwater protection, and contaminant transport (Taylor and Fleming, 1988). Understanding the production and propagation of fracture sets is important in geotechnical studies. For example, differential subsidence across landfills can fracture the cover materials, releasing landfill gases and providing surface water infiltration pathways which could result in the creation of leachate. Constant monitoring of fracture development in such situations would highlight areas requiring structural remediation and provide qualitative assessment of the production of leachate. Accepted methods of fracture mapping and characterization cover a broad range of investigation scales. On the large scale, fracture-trace analysis involves the location of fractures from observation of linear features (tonal variation in soils, alignment of vegetation patterns, straight stream segments or valleys, aligned surface depressions, gaps in ridges, etc.) on aerial or satellite photographs (Fetter, 1994). On a smaller scale, extensive pump, packer, or tracer tests may be necessary to determine the magnitude and azimuthal variation of permeability. This is especially true in areas of little or no rock exposure, although correct interpretations of fracture orientation, continuity, and connectivity are not easy to extract even in situations where the formation is well exposed. In addition, hydraulic testing can be very expensive, slow, and laborious.

Azimuthal resistivity surveying has been adopted (Leonard - Mayer, 1984; Taylor and Fleming, 1988; Ritzi and Andolsek, 1992; Skjernaas and Jørgensen, 1994; Hagrey, 1994) as a technique for determining the principal directions of electrical anisotropy and, hence, hydraulic conductivity using the analogy between Ohm's law and Darcy's law. Typically,

any observed change in apparent resistivity with azimuth is interpreted as indicative of anisotropy (generally fracture anisotropy). However, azimuthal variations in apparent resistivity may also be produced by

- (1) The presence of a dipping interface,
- (2) Gradational lateral change in resistivity
- (3) Or combination of 1 and 2.

Most published examples of azimuthal surveying have overlooked this possible ambiguity and, consequently, it is likely that the observed response has been misinterpreted on many occasions. In this work, I reviewed some of the pitfalls of the azimuthal resistivity technique and suggested a practical method for eliminating serious sources of interpretational ambiguity.

Azimuthal resistivity survey was used (Skjerna and Jorgensen, 1994 and Busby, 2000), as a technique for mapping and characterizing electrical anisotropies in terms of the nature, direction, and coefficient of electrical anisotropy; and was adopted in this study. Azimuthal electrical surveys were carried out using the ABEM Terameter SAS 4000B, with the Offset Wenner electrode configuration.

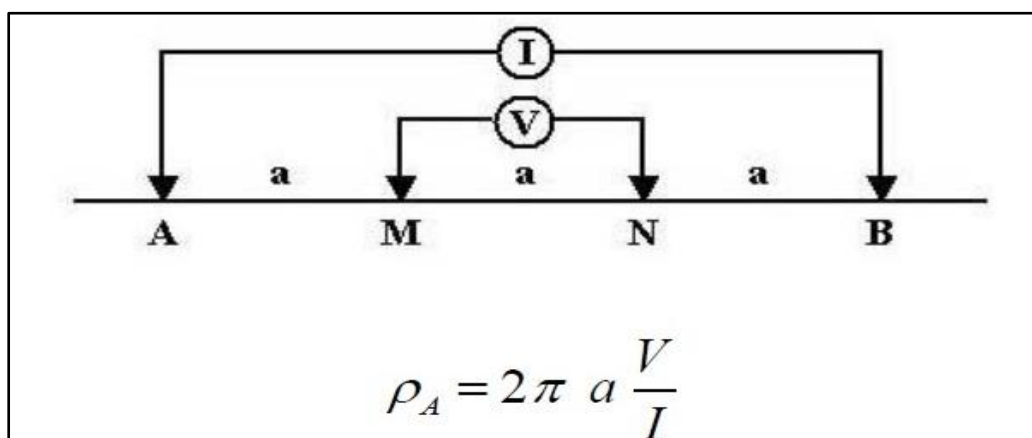


Fig. 2.2: Wenner configuration.

Electrode expansions of 10, 20 to a maximum of 60m were adopted. Measurements were made by rotating the array about a center point at 45° increments in four Azimuthal directions. The resistance R (Ω) data obtained from the measurements were converted to equivalent apparent resistivity ρ_a (Ωm) values for subsequent data analysis.

2.5.2.1 Mathematical Theory of Electrical Anisotropy

Anisotropy is considered in two scales: micro and macro. **Micro-anisotropy** relates to variations of resistivity with direction within a given layer or lithology (Sauck and Zabik, 1992) and is a common feature in water-laid sedimentary deposits e.g. fluvial, clastic lake, deltaic and glacial outwash deposits (Kruseman and De Ridder, 1994). It is generally formed through the alignment of elongate minerals and the creation of micro fabrics. **Macro-anisotropy** is generally attributed to alternating layers or beds of rock. A homogeneous isotropic unit containing water, air, or rock-filled fractures is also considered to exhibit macro-anisotropy. In most hard rocks, fractures occur in sets with more or less well-defined preferred orientations (Skjerna and Jørgensen, 1994). Horizontal fractures contribute equally to the horizontal permeability independent of direction; however, the contribution from vertical or steep fracture sets varies with azimuth, creating an anisotropic distribution of hydraulic conductivity. The distribution of potential due to a point source in a homogeneous anisotropic medium is found by transforming Laplace's equation for a homogeneous isotropic medium into Laplace's equation for a homogeneous anisotropic medium by a simple coordinate system stretch (Keller and Frischknecht, 1966; Bhattacharya and Patra, 1968). For stratified, or fractured, rock types which typically only exhibit two dimensional anisotropies, just two variables are used in the transformation:

1. **The longitudinal resistivity (ρ_L):** Which occurs parallel to the plane of stratification or fracturing, and

2. The transverse resistivity (ρT): This measure normal to the plane of stratification.

Using ρL and ρT , two more parameters diagnostic of an anisotropic medium are defined:

(a) The coefficient of anisotropy, λ : $\lambda = \sqrt{(\rho T / \rho L)}$

(b) The RMS resistivity, ρM : $\rho M = \sqrt{(\rho L \rho T)}$

For homogeneous isotropic media, λ is equal to 1. For a homogeneous anisotropic media, λ generally ranges between 1 and 2 because ρT is greater than ρL (Keller and Frischknecht, 1966).

A solution of Laplace's equation for a generalized two-dimensional anisotropic system is given by

$$V = \frac{I \rho M}{2\pi r \sqrt{[1 + (\lambda^2 - 1) \sin 2\phi \sin 2\alpha]}} \dots\dots\dots (2)$$

Equation 2 describes the potential V at any point M on the surface, a distance r from a point source of current I and in the direction which makes an angle ϕ with the strike direction (Bhattacharya and Patra, 1968). The resultant equipotential surfaces are ellipsoids of revolution. However, the orientation of these and the subsequent distribution of potential on the surface of the earth are, nevertheless, intrinsically related to the type of anisotropy present. For instance, in the case of horizontal fractures, $\alpha = 0$, and equation (2) reduces to

$$V = \frac{I \rho M}{2\pi r} \text{ Hence, } \rho \alpha = \rho M = \lambda \rho L \dots\dots\dots (3)$$

Thus, above horizontal fractures or flat-lying beds, the measured apparent resistivity ρ_a is larger than the true longitudinal resistivity by the ratio λ (Keller and Frischknecht, 1966). The apparent resistivity is numerically equal to the rms resistivity of the formation ρM . Consequently, surface azimuthal resistivity surveys cannot detect horizontal anisotropy at the

micro or macro scale because the resulting equi-potentials manifest as circles of different radii about the central point. In the case of vertical beds ($\alpha = \pi/2$), the array orientation is more important. For example, when $\phi = 0$, equation (2) reduces again to equation (3). But when $\phi = \pi = 2$, $V = \frac{I\rho M}{2\pi r} = \frac{I\rho L}{2\pi r}$ Hence $\rho_a = \rho_L = \frac{\rho M}{\square}$ (4)

When an azimuthal resistivity survey is executed in an area of vertical fracture or bedding, the measured apparent resistivity will be equal to the mean resistivity of the formation when the array is orientated parallel with the strike direction (equation 3). When the array is perpendicular to strike, the apparent resistivity is equal to the longitudinal resistivity (equation 4), not the transverse resistivity as one might expect. Hence, the apparent transverse resistivity ρ_{aT} is less than the apparent longitudinal resistivity ρ_{aL} , as opposed to the relationship between the true resistivities where $\rho_T > \rho_L$. Consequently, in the case of vertical anisotropy, the equipotentials at the surface will be similar ellipses elongated parallel to the stratification (Kunetz, 1966), in accordance with the paradox of anisotropy (Keller and Frischknecht, 1966), and the ratio of the two principal axes will be λ . In the intermediate case of dipping anisotropy, the equipotential curves will still be ellipses but the elongation will be less (Kunetz, 1966) and, consequently, the anisotropy will not be fully characterized.

2.6 Geotechnical Methods of Soil Analysis

Geotechnical method is one of the methods employed in this study to investigate gully within Orlu and environs. In this method, soil samples were collected in eight (8) different erosion locations within the study area. These locations include Umueshi, Ogberuru, Afor – Ukwu, Ihioma and Okwudor gully sites. These samples were subjected to series of laboratory test to be able to determine majorly amongst others:

1. The California Bearing Ratio of the Area
2. The Soil Consistency

- (i) Rupture Resistance –Moist and Dry Consistency
- (ii) Stickiness – Wet Consistency
- (iii) Plasticity- Wet Consistency

3. Atterberg Limits

- (i) Liquid Limits
- (ii) Plasticity Limits
- (iii) Shrinkage Limits
- (iv) Plasticity Index.

2.6.1 California Bearing Ratio (CBR)

The California bearing ratio (CBR) is a penetration test for evaluation of the mechanical strength of road subgrades and base courses which was designed by California State Highway Department (U.S.A.) for evaluating the bearing capacity of sub grade soil for design of flexible pavement. This test is carried out on natural or compacted soils in water soaked or un-soaked conditions and the results so obtained are compared with the curves of standard test to have an idea of the soil strength of the sub grade soil. This is the ratio of force per unit area required to penetrate into a soil mass with a circular plunger of 50mm diameter at the rate of 1.25mm / min. The Higher the CBR of any soil the more resistive it is to erosion and the more comfortable it is for construction on such soil.

2.6.2 Soil Consistency

Soil consistence provides a means of describing the degree and kind of cohesion and adhesion between the soil particles as related to the resistance of the soil to deform or rupture. Since the consistence varies with moisture content, the consistence can be described as dry consistence, moist consistence, and wet consistence. Consistence evaluation includes rupture resistance and stickiness. Soil consistency is defined as the relative ease with which a soil can

be deformed use the terms of soft, firm, or hard. Consistency largely depends on soil minerals and the water content.

2.6.2.1 Rupture Resistance (Moist and Dry Consistency)

The rupture resistance is a field measure of the ability of the soil to withstand an applied stress or pressure as applied using the thumb and forefinger.

2.6.2.2 Stickiness (Wet Consistency)

The capacity of soil to adhere to other objects and is estimated at moisture content that displays maximum adherence between thumb and fore finger. Cohesion is the attraction of one water molecule to another resulting from hydrogen bonding (water-water bond) while Adhesion is similar to cohesion except with adhesion involves the attraction of a water molecule to a non-water molecule (water-solid bond). There are four classes of Stickiness

i. Non Sticky – There is little or no soil adheres to fingers after release of pressure

ii. Slightly Sticky – Soil adheres to both fingers after release of pressure with little stretching on separation of fingers

iii. Moderately Sticky – Soil adheres to both fingers after release of pressure with some stretching on separation of fingers

iv. Very Sticky - Soil adheres firmly to both fingers after release of pressure with stretches greatly on separation of fingers

2.6.2.3 Plasticity (Wet Consistency)

This is the degree to which puddled or reworked soil can be permanently deformed without rupturing. Water Content Significantly affects properties of Silty and Clayey soils (unlike sand and gravel). Plasticity property describes the response of a soil to change in moisture

content. Note that soil strength decreases as water content increases, it swell-up when water content increases, fine-grained soils at very high water content possess properties similar to liquids, as the water content is reduced, the volume of the soil decreases and the soils become plastic and if the water content is further reduced, the soil becomes semi-solid when the volume does not change.

2.6.3 Atterberg Limits

This is the limits of water content used to define soil behavior.

2.6.3.1. Liquid Limits: Liquid Limit (LL) is defined as the moisture content at which soil begins to behave as a liquid material and begins to flow. Liquid limit of a fine-grained soil gives the moisture content at which the shear strength of the soil is approximately 2.5kN/m^2 . The lowest water content in soil at which soil behaves like liquid normally is below one hundred (100).

2.6.3.2 Plasticity Limits: Plastic Limit (PL) is defined as the moisture content at which soil begins to behave as a plastic material. The lowest water content in soil at which soil behaves like a plastic material normally is below forty (40).

2.6.3.3 Shrinkage Limits: Shrinkage Limit (SL) is defined as the moisture content at which no further volume change occurs with further reduction in moisture content. This represents the amount of water required to fully saturate the soil one hundred percent (100%). It is the water content at which soils does not decrease their volume anymore as they continue dry to out. – As seen in producing bricks, blocks and ceramics.

2.6.3.4 Plasticity Index: Plasticity Index is the difference between the liquid limit and plastic limit of a soil (PI = LL –PL).

2.7 Remote Sensing Method

In this particular approach, landsat data were obtained from the national space research and development center agency (NSRDA). Using this acquired landsat data by NSRDA, normalized vegetation difference index (NDVI), the lineaments, the drainage patterns and the Rose diagram of the study area was considered tenateously to see how it relates and interpret the erosion menace within the study areas.

2.7.1 Brief Review of Normalized Difference Vegetation Index (NDVI)

The Normalized Difference Vegetation Index (NDVI) is a numerical indicator that uses the visible and near-infrared bands of the electromagnetic spectrum, and is adopted to analyze remote sensing measurements and assess whether the target being observed contains live green vegetation or not. NDVI has found a wide application in vegetative studies as it has been used to estimate crop yields, pasture performance, and rangeland carrying capacities among others. It is often directly related to other ground parameters such as percent of ground cover, photosynthetic activity of the plant, surface water, leaf area index and the amount of biomass. Since we know the behavior of plants across the electromagnetic spectrum, we can derive NDVI information by focusing on the satellite bands that are most sensitive to vegetation information (near-infrared and red). The bigger the difference therefore between the near-infrared and the red reflectance, the more vegetation there has to be. The NDVI algorithm subtracts the red reflectance values from the near-infrared and divides it by the sum of near-infrared and red bands.

$$NDVI = \frac{NIR-RED}{NIR+RED} \dots\dots\dots 5$$

NIR = Near Infrared, RED = Red Reflectance

This formulation allows us to cope with the fact that two identical patches of vegetation could have different values if one were, for example in bright sunshine, and another under a cloudy sky. The bright pixels would all have larger values, and therefore a larger absolute difference between the bands. This is avoided by dividing by the sum of the reflectance.

Theoretically, NDVI values are represented as a ratio ranging in value from -1 to 1 but in practice extreme negative values represent water, values around zero represent bare soil and values over 6 represent dense green vegetation.

2.7.2 Lineament Interpretation

One common application of lineaments interpreted from satellite images is to reveal dominant azimuth sets whose orientations give an idea of the regional fracture pattern of an area (McElfresh et al., 2002, Casas et al., 2000, Koike et al., 1998). A lineament is defined geomorphologically as a “mappable, simple or composite linear surface feature, whose parts are aligned in a rectilinear or slightly curvilinear relationship and which differs distinctly from the patterns of adjacent features and presumably reflects a subsurface phenomenon” (O’Leary et al., 1976). Linear surface features may include valleys, ridges, boundaries of elevated areas, rivers, coast lines, boundary lines of rock formations, and fracture zones (Hobbs, 1904). The identification of lineaments is conditioned by the outcrop situation of the study area: The presence of dense vegetation, alluvial deposits, recent volcanic ashes and human landscape transformation may prevent the identification of lineaments.

2.7.3 Drainage Analysis

Drainage analysis generally provides clues to structural features and lithology (Howard, 1967). The underlying concept is that rivers necessarily flow from high to low elevations parallel to the maximum regional slope (regional topographic gradient). Several basic drainage patterns have been defined: dendritic, parallel, trellis, rectangular, radial/centrifugal, annular and contorted (Deffontaines and Chorowicz, 1991, Howard, 1967). All deviations

from a dendritic pattern or flow direction oblique to the regional topographic gradient (“misfit drainage”, Deffontaines et al., 1992), are considered as drainage anomalies related either to structural or lithological discontinuities (e.g. Deffontaines et al., 1997, Pubellier et al., 1994). In this work, drainage analysis has been used to support the ideas of distinct lineament sets interpreted from satellite images. Drainage analysis of an area generally starts with the individualization of areas of sub-homogeneous drainage pattern (“subareas”). This individualization can be done on the basis of a regional analysis of the drainage pattern, stream flow direction, and drainage texture. Resulting subareas correspond more or less to the regional lithological units and bioclimatic zones (Deroin and Deffontaines, 1995, Howard, 1967). After individualization, detailed analysis of drainage anomalies brings out the perturbations that cannot be identified on a regional scale. Such regional perturbations consist of rectilinear or curved anomaly alignments.

2.7.4 Azimuth frequency (Rose) Diagram

Rose diagram is a circular histogram plot which displays directional data and the frequency of each class. Rose diagrams are commonly used in sedimentary geology to display paleocurrents data or the orientation of particles or flow. In structural geology rose diagrams are used to plot the orientation of joints and dykes. Wind directions and frequencies can also be plotted on rose diagrams.

CHAPTER THREE

MATERIALS AND METHODS

3.1 Method of Study

The methods of study employed in this investigation include: desk studies, field work, Landsat imagery and laboratory investigations. The desk study was carried out before the field work. All relevant literatures, imagery and archival records of the study area were studied and analyzed.

The field work was initiated with a reconnaissance survey of the area. Observation of the geographical features, exposed sand units along gullies, streams, valleys, erosional surfaces and outcrops were made and features noted. Vertical Electrical and Azimuthal soundings were carried out at the chosen sites of study with the coordinates of the site being recorded using geographic position system (GPS). Landsat imagery of the study area were also provided to ascertain the lineaments and lineament cross points within the areas of study. Geotechnical measurement of insitu soil materials were carried out to ascertain their engineering properties.

3.2 Desk Study

This study simply involves the process of assembling specific and relevant information for the initiation of the project from previous works by other authors in the same study area, which serve as a reference point in the execution of this project.

3.2.1 Desk Study Materials

1. Academic publications, journals, research journals and project works related to this topic.
2. Topographic Map of the study area (Scale, 1:100,000 and 1:250,000)

3. Geologic Map of the study area
4. Existing land use/land covers maps and socio – economic data
5. Existing forest classification
6. Gully erosion maps of the study area
7. High resolution satellite imagery of the area

3.3 Field Study

The field study reconnaissance survey of the selected gully erosion sites on October 28, 2013 supervised by Dr. Opara A. The reconnaissance survey involved a multiple stops at the individual gully sites, observations, visual analysis of outcrops were visually analyzed and lateral measurements done at intervals of 10 m (except gully with less than 20 m length) using measuring tape and leveling staff, for length, width and depths, respectively. Mean gully depths measured at gully shoulders were obtained at the beginning, middle and end of cross-sections.

The Global Positioning System (GPS) was used to measure the coordinates from which averaged area for each catchment was computed. The catchment of each gully was delineated in the field based on the slope gradient and the gully pattern.

For each gully, the measured cross sectional areas were calculated. Azimuthal resistivity sounding were carried out at each site for anisotropic type determination and soil samples were collected respectively from Njaba river, Orlu/Ihiala road, Okwelle/Urualla road, Afor ukwu - Afor nta road, Owerri/Orlu road, Umunguma Ihioma community, Ikpa/Ihioma road, Umuazzala Ogberuru community, Umueshi community, Okwudor and Isiakenesi gully erosion sites for the analysis of physical properties such as sediment loss, bulk density, moisture content, soil texture, Soil consistency (Rupture Resistance –Moist and

Dry Consistency, Stickiness –Wet Consistency, Plasticity- Wet Consistency), Atterberg Limits (Liquid Limit, LL, Plastic Limit, PL) and Plasticity Index, PI.

3.3.1 Field Equipment

1. Location map for direction
2. GPS for taking coordinates and for measuring the longitude, latitude, directional azimuth and altitude of the study areas.
3. ABEM SAS Terameter for VES and azimuthal resistivity determination
4. Compass for direction and measurement of strike and dip
5. Measuring tapes for linear measurements
6. Hand Auger and spade for collection of unweathered samples
7. Field note and writing materials for taking records
8. A topographic map of the study area was used for the geological mapping.
9. Tape for measuring the spacing distance of electrode and length of gully

3.3.2 Software Used

1. Surfer 12
2. Strata 4
3. Grapher 10
4. SAS 4000
5. Ilwis 3.0 Academic
6. ArcGIS 9.3

7. Didger 3.0

3.4 Gully Characterization

The gullies at the sites were characterized in terms of the following basic features of gully erosion, which includes the length, width, side slopes and gully floor.

3.4.1 Site Locations

Table 3.0. Site locations with their easting and Northing

LOCATIONS	NAME	LONGITUDE	LATITUDE	ELEVATION	GULLY ORIENTATION
LOCATION 1	NJABA RIVER	7.193056	5.774167	115m	NE-SW Dominant
LOCATION 2	ORLU/IHALA RD	7.060278	5.878056	102m	NE-SW Dominant
LOCATION 3	OKWELLE/URUALLA RD	7.312500	5.886667	152m	NE-SW Dominant
LOCATION 4	AFOR UKWU - AFOR NTA	7.360556	5.861944	155m	NE-SW Dominant
LOCATION 5	OKWELLE/URUALLA RD 2	7.322222	5.810833	137m	NE-SW Dominant
LOCATION 6	OWERRI/ORLU RD	7.253889	5.761111	107m	NE-SW Dominant
LOCATION 7	UMUNGUMA IHIOMA	7.263889	5.927222	110m	NE-SW Dominant
LOCATION 8	IKPA/IHIOMA	7.142778	5.960000	94m	NE-SW Dominant
LOCATION 9	UMUAZZALA OGBERURU	7.028722	5.830389	195m	NE-SW Dominant
LOCATION 10	UMUESHI 1	7.110472	5.829000	260m	NE-SW Dominant
LOCATION 11	UMUESHI 2	7.109669	5.830806	273m	NE-SW Dominant
LOCATION 12	OGBERURU 2	7.015389	5.832028	121m	NE-SW Dominant

Three methods were adopted to integrate electrical resistivity measurements with geotechnical studies in the evaluation of soil structure and anisotropic type with a view to determine soil structural features that may have the potential to initiate and enhance the process of gully erosion in the study area. Firstly, a detailed geological mapping of the study area was carried out followed a direct current resistivity survey using the vertical electrical sounding method and Azimuthal resistivity survey was carried out for the purpose of characterizing electrical anisotropies in terms of the nature, direction, and coefficient of electrical anisotropy .

3.5 Surface Geologic Mapping

The geologic mapping of the study area was carried out using geologic and topographic maps. Physical investigations were also carried out to observe the surface exposure of outcrops (if any), geomorphological activities such as weathering, erosion processes and as well to, acquire the geological information of the area in order to describe the rock succession. This was done because geologic mapping is a veritable tool for evaluation of hydrological and hydrogeological parameters.

3.6 Geotechnical Studies

3.6.1 Sample Collection

Geotechnical measurement of in-situ soil materials were carried out to ascertain their engineering properties. Twelve unweathered (fresh) soil samples were collected at designated locations within the sites as shown in table 2 above. The natural moisture content of the samples collected from the field was determined in the laboratory within a period of 24 hours after collection. This was followed by air drying of the samples by spreading them out on trays in a fairly warm room for four days. Large soil particles (clods) in the samples were broken with a wooden mallet. Care was taken not to crush the individual particles. The entire laboratory tests were carried out in accordance with standard procedures, such as those recommended by the American Society for Test and Material (ASTM) or British Standard B.S. 1377 (BSI, 1975) for all the soil samples collected using well calibrated apparatus/equipment. The investigations of soil in the laboratory and the values required for calculation have led to the development of special equipment and procedure (Cheng and Jack, 1990). The tests conducted on the twelve different soil samples include: Atterberg limits: P-Index (Plasticity Index), L-Limit (Liquid Limit), Particle size Analysis (Hydrometer test), Moisture content, and California Bearing Ratio (CBR). The particle size distribution curve is used for classification of soil, determining the coefficient of permeability, provides an index

to the shear strength. Soil moisture content, shows the change or variation in the soil characteristics; compaction is done to improve the engineering properties of soil, it generally increases the shear strength of the soil, and hence the stability and bearing capacity.

It is also useful in reducing the compressibility and permeability of the soil. The Atterberg limits show the consistency of the soil, i.e. the degree of cohesion between particles of the soil at given moisture content. CBR is primarily intended for, but not limited to evaluating the strength of cohesive materials having maximum particle size less than 19mm (AASHTO, 2000). It helps to obtain the strength of the sub grade soil.

3.7 Geophysical Studies

3.7.1 Vertical Electric Sounding (VES)

In the course of this study, series of potential differences were acquired at successively greater electrode spacing while maintaining a fixed central reference point. The induced current was passed through progressive deeper layers at greater electrode spacing. From the VES carried out, apparent resistivity values for layers, thickness of layers and depth of layers were obtained. Below is atypical vertical electrical sounding design (Schlumberger array) used in this study.

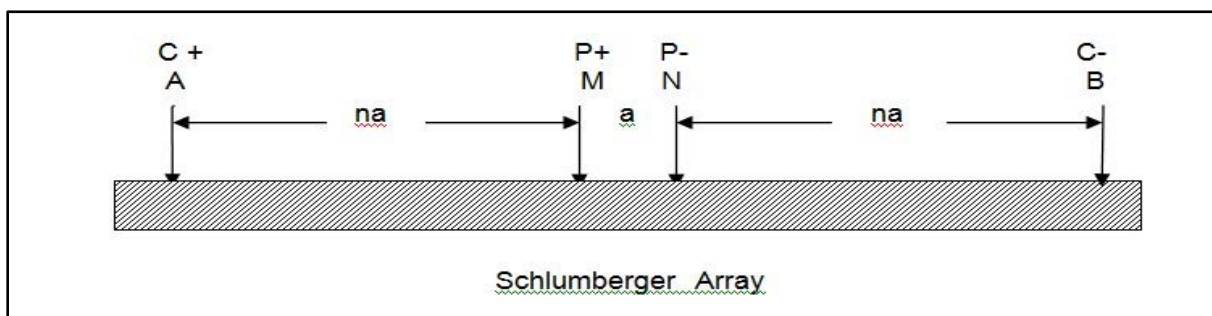


Fig. 3.0. Schlumberger array

During the sounding survey, electrodes were distributed along a line, centered about a midpoint that is considered the location of the sounding. In this process, two current electrodes A and B and two potential electrodes M and N were fixed, placed in line with another and

centered on a location, but the potential and current electrodes were not placed equidistant from one another. To acquire the resistivity data in the field, current was introduced into the ground through current electrodes and the potential electrodes were then used to quantitatively measure the voltage pattern on the surface resulting from current flow pattern of the first set of electrodes. The array was achieved by knowing the distance of the potential of MN as (a) and the distance of AB equals $a(2n + 1)$. The distance between the different electrodes is shown in the figure above. The value 'K' which is called the Geometric factor is calculated from the appropriate distances between the electrodes and for certain electrode configuration. Voltage and current were converted in millivolts and milliamperes respectively with distances in metres to obtain the apparent resistivity measured in Ohm-metre.

3.7.2 Azimuthal Resistivity Sounding (ARS)

For Azimuthal array, the location of measurement point is the centre point of the array. Azimuthal Resistivity Sounding (ARS) was carried out along four directions; N-S, E-W, NE-SW, NW-SE to ascertain the direction of structural weakness and fracture zones. Field arrangement for azimuthal array data collection is as shown in Figure 3.1.

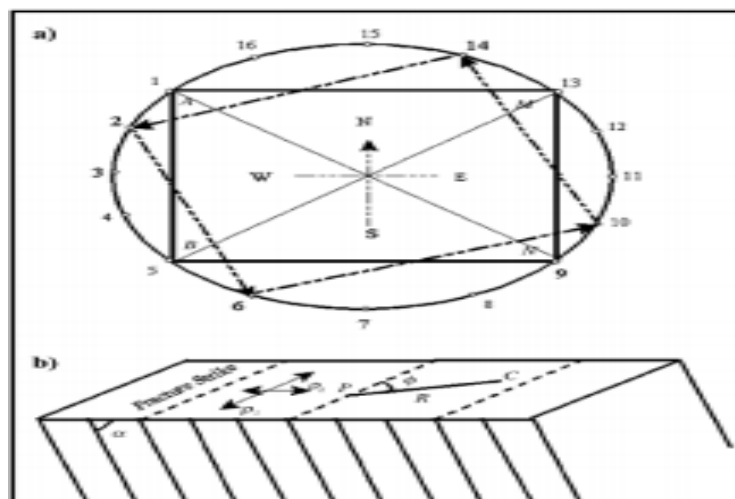


Fig. 3.1.Field array of Azimuthal Resistivity Sounding.

A total of eight (3) locations were sampled. The maximum spread of AB/2 in this area is 50 m. It is known that in any formation which is anisotropic due to the presence of fractures, the apparent resistivity (ρ_t) measured normal to its strike direction is greater than apparent resistivity (ρ_s) measured along the strike direction, when Schlumberger or Wenner array is used but contrary when crossed square array method is employed (Lane et al., 1995). The apparent resistivity was measured along four different azimuths N-S, NE-SW, NW-SE and E-W for a given AB/2 separations and were plotted along their corresponding azimuths. Lines of the resistivity of the same value along different azimuths were joined together, thus resulting in a polygon. A set of such polygons obtained corresponding to different AB/2 separations is known as a polar diagram or anisotropy polygon.

3.8 Landsat Imagery/Acquisition

A seven band landsat ETM image of Orlu and Environs was acquired from national space research and development center agency (NSRDA). A shuttle radar topographic mission (SRTM) image of the same area was also obtained. Ground control points (GCP's) and satellite orbit transformation were used to rectify the imagery. Thus image rectification was carried out using existing geo-coded Landsat MSS and SPOT Multispectral data (that is image to image geo-coding) utilizing the universal Transverse Mercator (UTM) coordinate system. Each scene was radiometrically corrected. Band 1 of ETM data penetrates water for bathymetric mapping along coastal areas and is useful for soil vegetation differentiation and for distinguishing forest types. ETM Band 2 detects green reflectance from healthy vegetation while ETM Band 3 is designed for detecting chlorophyll absorption in vegetation. ETM Band 4 is ideal for detecting near Infra- red reflectance peaks in healthy green vegetation and for detecting water bodies/land interfaces. The two mid –IR red bands on ETM (Bands 5 and 7) are useful for vegetation and soil moisture studies, and for

discriminating between rock and mineral types. The thermal –IR Band on ETM Band 6 is designed to assist in thermal mapping and is used for soil moisture and vegetation studies.

The landsat 5 ETM data of the study area was digitally processed and enhanced to produce single band images, band ratios, colour composites, and classified images complemented by digitized geologic maps for the study area. Drainage patterns and textures, bare rocks and vegetated areas were enhanced in single band images. The SRTM data was utilized in the production of a digital elevation model (DEM) which is valuable in the identification of sandstone ridges. The colour composites were used as background data for both supervised and unsupervised image classification.

A Digital Elevation Model (Fig.4.0) was created in IDRISI 32 by performing a colour shaded operation on Shuttle Radar Topographic Mission (SRTM) data. The DEM was converted into a contour map using the ERDAS and ArcView software. From the DEM, geomorphic units in study area were identified. Based on the image texture and tone; three geomorphic units: part of Orlu and Environs, scarp slope and low-lying plain were identified. The highest elevations represented as green patches, is interpreted as a sandstone ridge. This feature are seen towards the top right corner of the map is suspected to be part of the Awka-Orlu Cuesta, running in NE-SW direction. The scarp slope of the ridge is identified where light green, yellow and red colours are closely packed together; representing a sudden change in topography from 286 to 116 metres. The slope is characterized by numerous streams, gullies and a river. It will be correct to interpret the topographic high areas as characterized by sandstone. This is justified by the dendritic drainage pattern expressed in the low lying area. Geologically the area with dendritic pattern correlates to the Benin Formation. The sandstone ridge represents the watershed for the study area. Similarly, the elevation contour map (fig.16) reveals the highest elevation of the study area as green contours which correlate to the green patches on the DEM map. The low-lying plain of the study area is shown as blue on the DEM and the contour map. The slope of the ridge is similar to the interpreted one on the DEM imagery.

Linear features equal to or greater than 1km in length were considered. The longer lineaments have the greatest potential of being more fully developed and of penetrating greater depths. The lineaments reveal three groups of linear features. The maxima having NE-SW direction, others trend in N-S, E-w and NW-SE directions. Umeji (1988) recognized the Pan African Shield as characterized by NNW-SSE to NNE-SSW trending structures and varied intrusives and the lower Cretaceous characterized by NE-SW oriented shear zones and fractures controlled by volcanism. Murat (1972) described three tectonic trends: The first, of Albian age gave rise to Abakaliki-Benue trough with NE-SW trending faults.

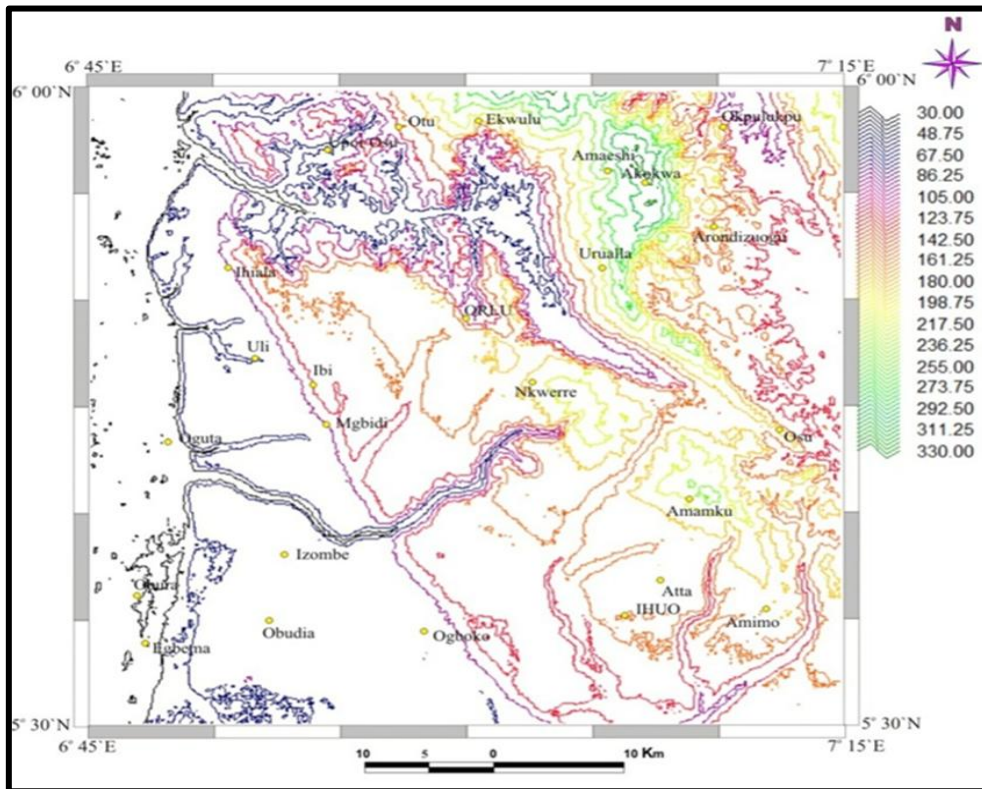


Fig.4.1: Topographical map of Orlu and Environs

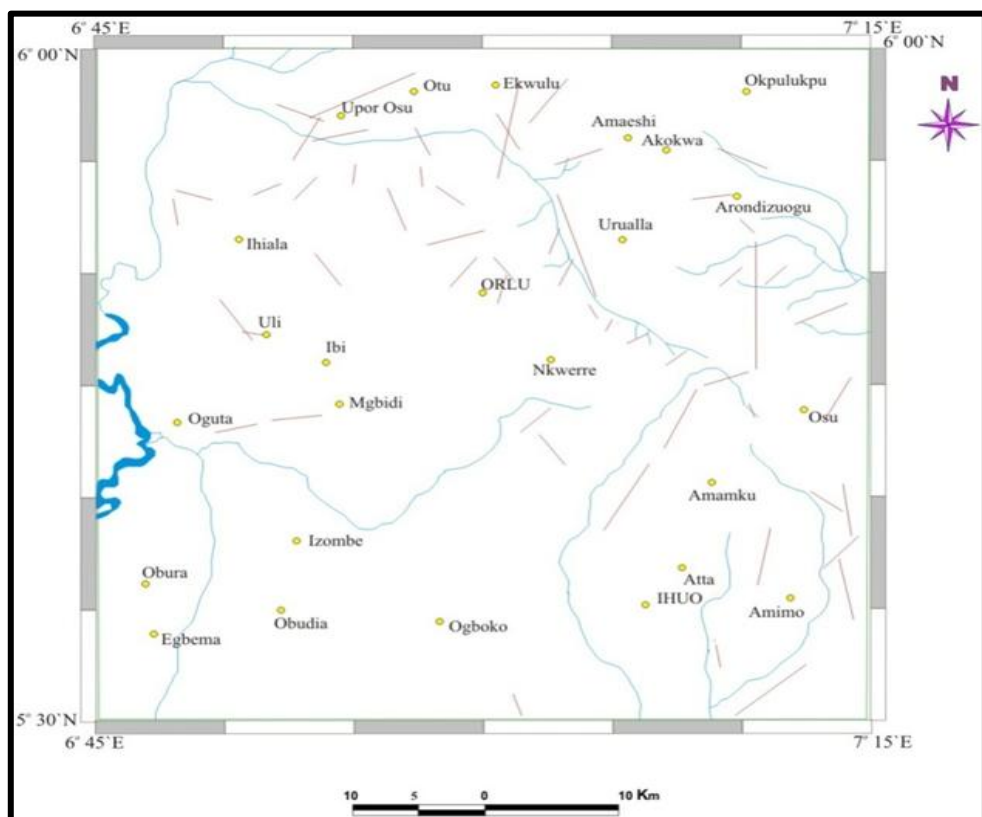


Fig. 4.2: Lineament on Drainage Map of the study area

The interpreted lineaments (Fig. 4.3) were superimposed on the edge enhanced map to show the relationship between geological formations and structural features. The lineament density map and enhanced filtered map (Fig.4.4) reveal a high density fracture zone 5km east of Urualla, Orlu town and also NNE of Orlu town. This zone is interpreted thus, because of the high density of lineaments seen in this area. This implies that there was intense effect tectonic activity that affected the area and weakened the structures. Around Orlu, existence of lineament is interpreted. Finally, Statistical trend analysis was applied to the interpreted structural lineaments.

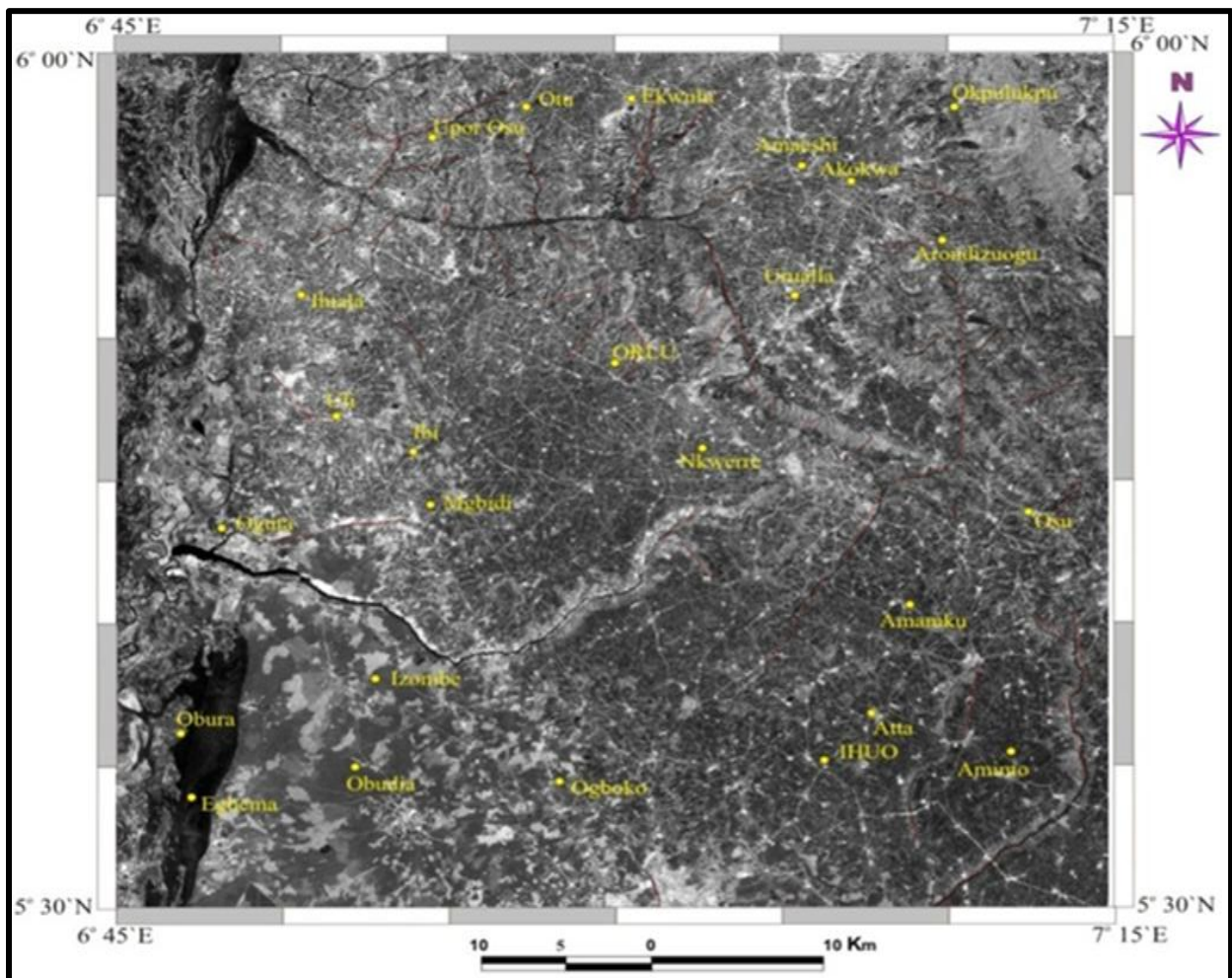


Fig. 4.3: Lineament on Edge Enhanced Band 5 Map of the study area

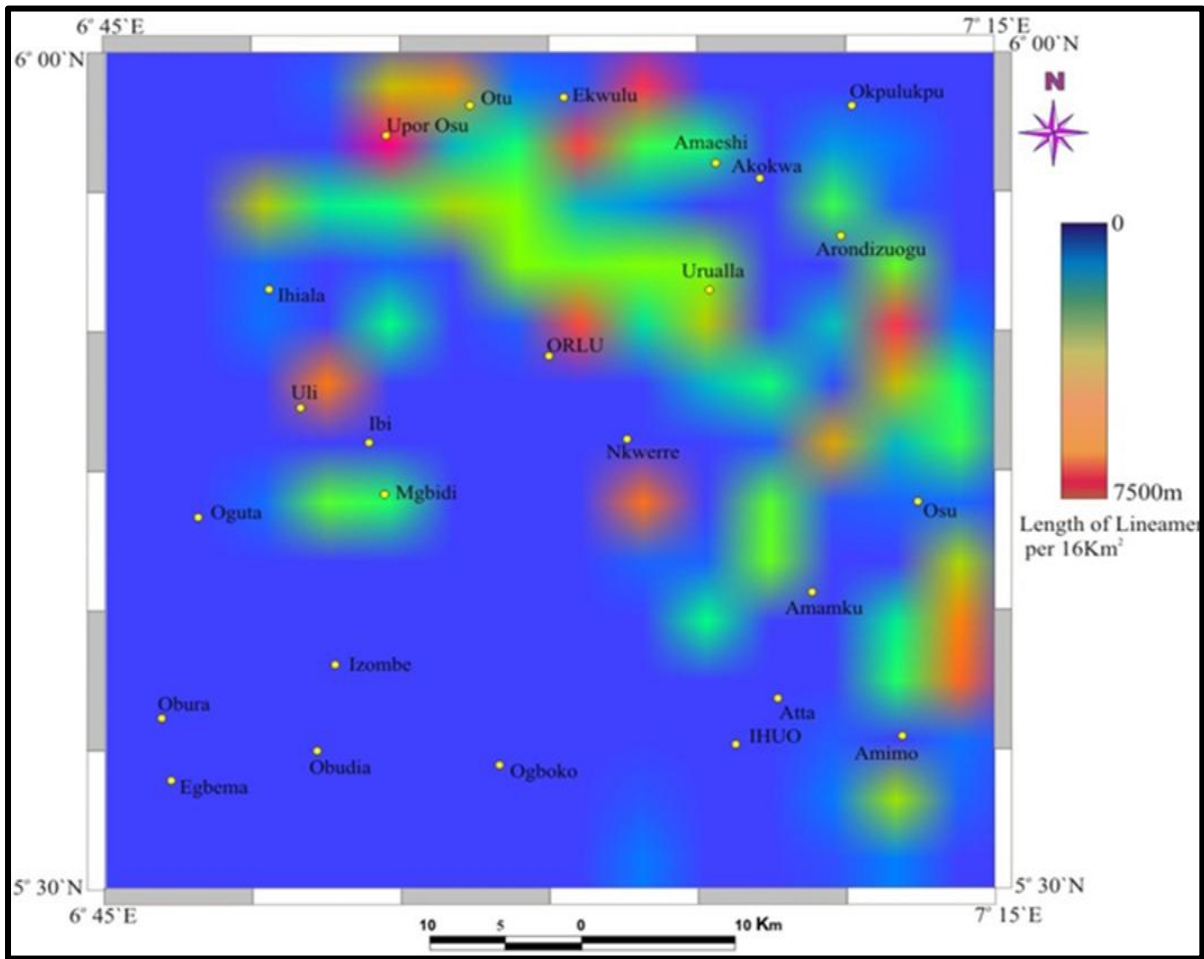


Fig. 4.4: Lineament Density Map of the study area

Normalized Difference Vegetation Index (NDVI) relies on the chlorophyll content of a plant. This was generated to delineate zones of vegetation and bare soil. Healthy plants have a higher value of NDVI because of their high reflectance of infrared (band 4) light and relatively low reflectance of red (band 3) light. The calculation of the NDVI is based on the formula:

$$NDVI = \frac{(NIR - R)}{(NIR + R)} \dots \dots \dots (1)$$

(Where NIR = Near Infrared and R = Red.)

A closer look at the NDVI imagery (Fig. 4.5) revealed that the brown areas (-0.22 to -0.04) correspond to bare soil which are found with Orlu, Urualla and toward the south eastern part of

Orlu. Yellow areas (-0.04 to 0.19) correspond to sparsely vegetated areas and green (0.19 to 0.51) correspond to thick vegetation areas.

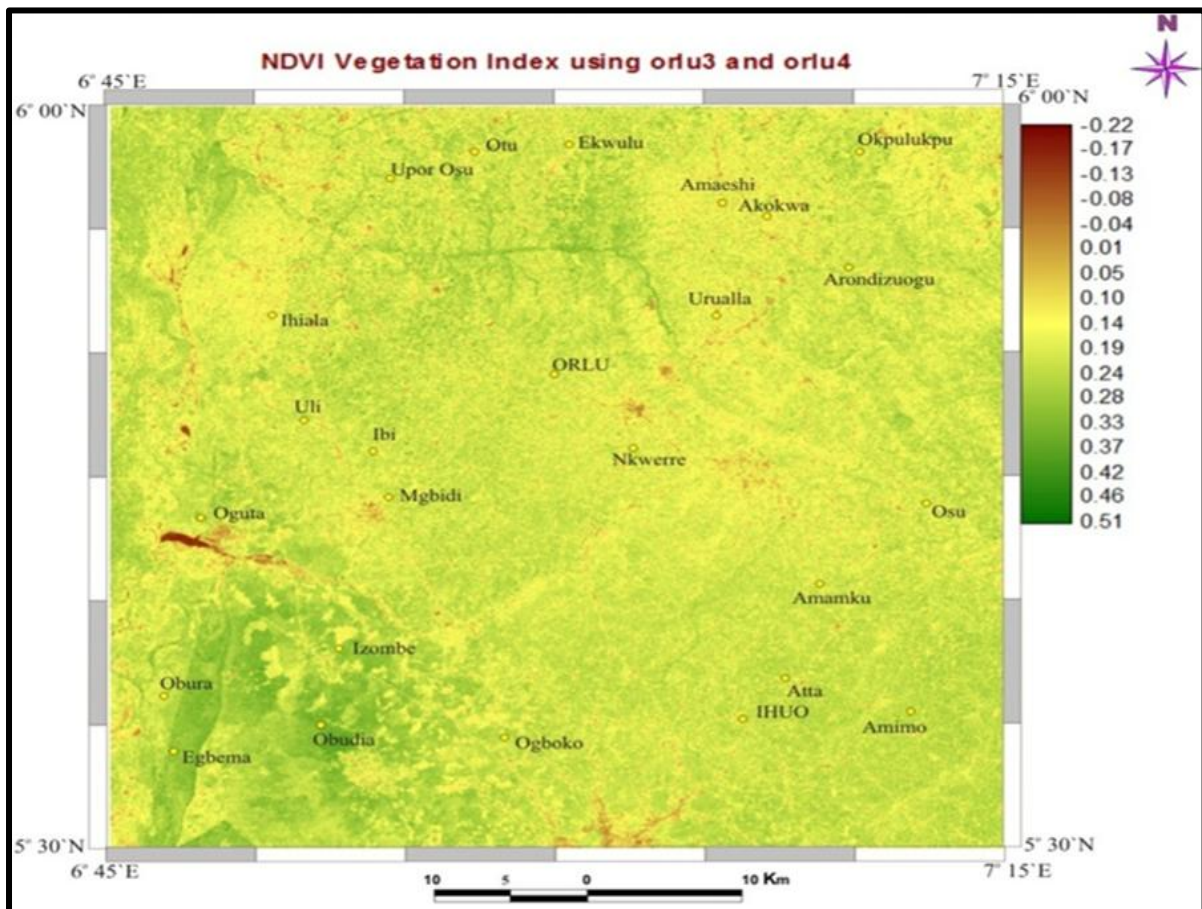


Fig. 4.5: Normalized Difference Vegetation Index (NDVI) map of the study area

The dendritic pattern suggests that the underlying sediment is a homogenous unit. Similarly, the dendritic pattern may reveal that the lithology has least resistance to erosive action of the river and streams. Such litho-unit includes laterites, sand, coarse grain etc. This implies that the stream channels are covered with vegetation. Red patterns are prominent along the river channel. RGB752 composite (Fig.4.6) is very descriptive, for it differentiates between the patterns. Bare soil area, interpreted as sandstone ridge from DEM are rendered as lavender and magenta, while urban areas are rendered in lavender pattern.

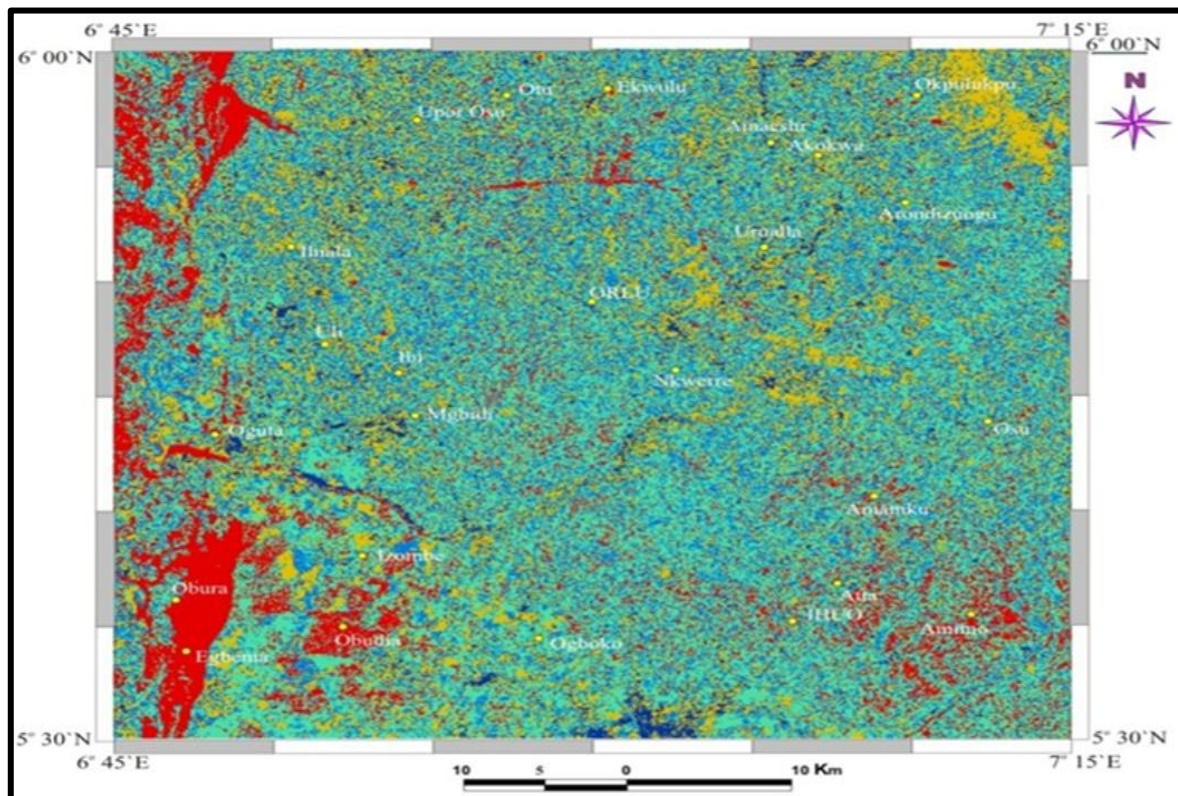


Fig. 4.9: Unsupervised Classification Map of the study area

The unsupervised classification map relies on image classification tied around tonal differences of the patterns seen. In the study area, nine tonal features were observed. Looking at the image (Fig. 4.9), blue and green colors are areas with mixed vegetation, shale and mudstones. The yellow areas observed within Orlu, Urualla and Umueshi. This has been interpreted previously from the DEM and colour composites as sandstone units.

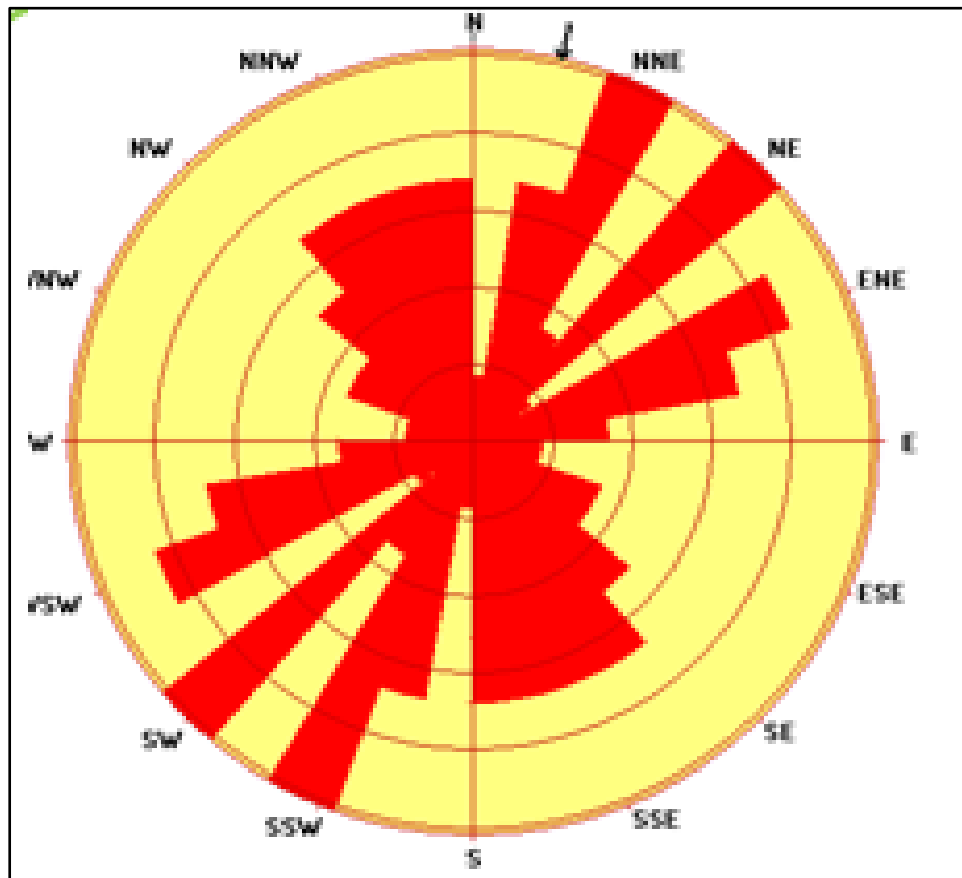


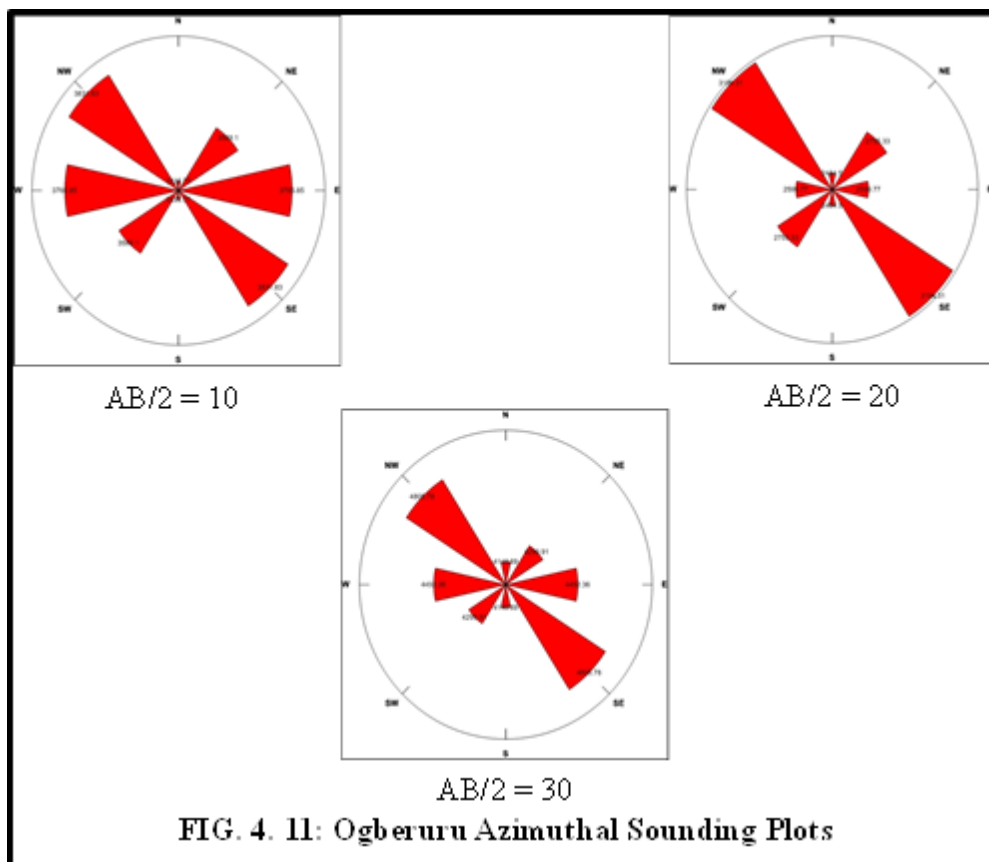
Fig. 4.10: Azimuth Frequency Diagram(Rose Diagram)

The results obtained are displayed on the rose diagrams (Fig.4.10). The azimuth frequency diagram (rose diagram) of the determined lineaments revealed that the commonest strikes of lineaments in the study area are in E-W, WNW-ESE, N-S and NE-SW trends. The E-W, WNW-ESE, and N-S, reflect the old and deeper tectonic trends. However, the NE-SW and NNE-SSW trend reflects the younger tectonic events, because the younger events are more pronounced and tends to obliterate the older events.

4.1.2 AZIMUTHAL RESISTIVITY SOUNDING RESULT

Table 4.0. Azimuthal Resistivity sounding valuesfor Ogberuru

AZIMUTHAL RESISTIVITY SOUNDING VALUE TABLE AT OGBERURU											
S/N	AB/2	MN/2	K	RESISTANCE(Ω)				RESISTIVITY (Ω m)			
				N-S	E-W	NE-SW	NW-SE	N-S	E-W	NE-SW	NW-SE
1	10	5	23.57	105.4	135.1	110.3	116.9	2484.28	3184.31	2599.77	2755.33
2	20	5	117.83	28.31	32.52	31.96	30.46	3335.77	3831.83	3765.85	3589.1
3	30	5	274.93	15.09	17.48	16.34	15.64	4148.69	4805.78	4492.36	4299.91

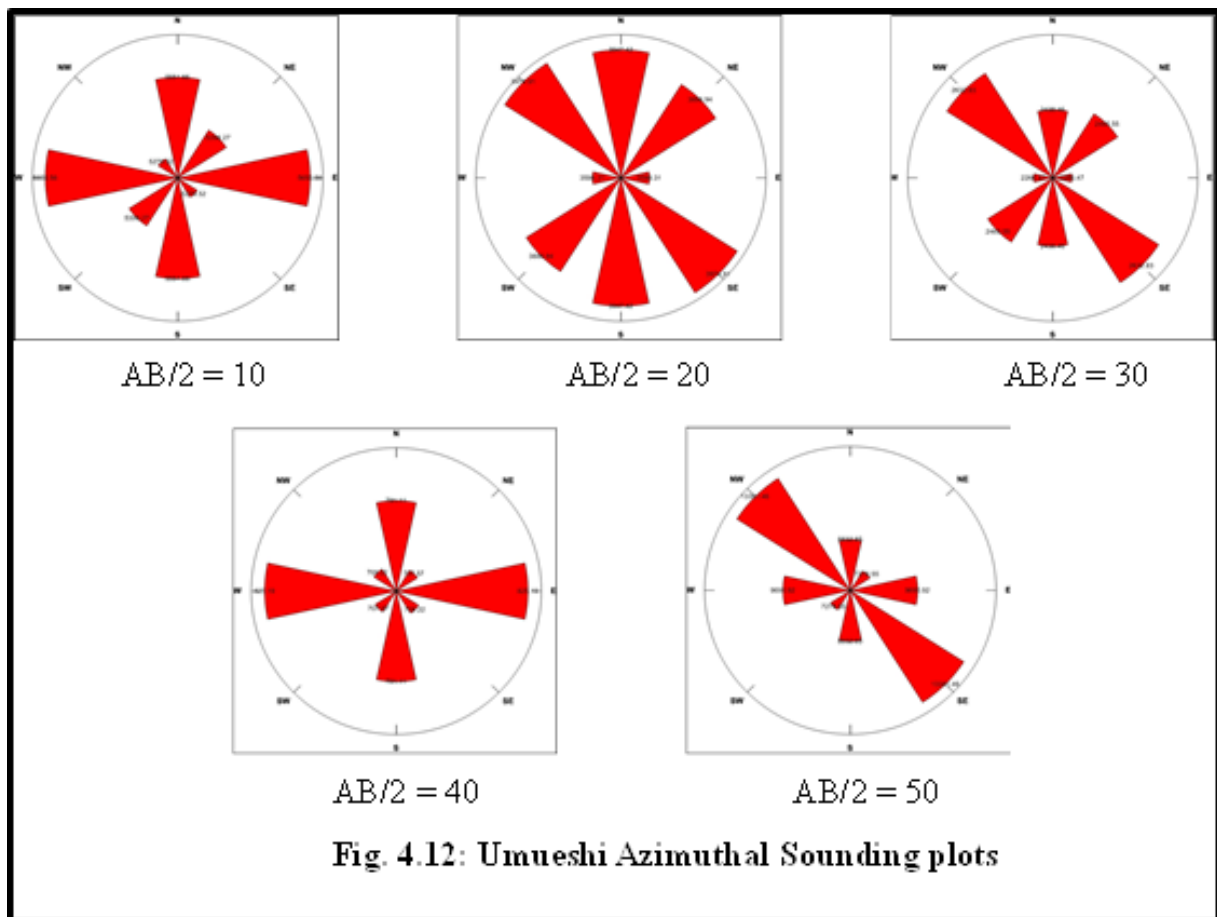


At Ogberuru, from figure 4.11 above, it was observed that the most dominant trend is in the NW – SE direction which coincided with the map in figure 1.0 showing that all the gullies in southeastern Nigeria lies in a straight line along the NW – SE direction which also corresponded with the azimuth frequency diagram in figure 4.10, showing the second most dominant trend to be the NW – SE direction. Therefore, it is obvious that, irrespective of the role formations play in aiding erosion within the area, the trends of these gullies in almost a

single direction suggests some sub-surface structural implications, (gullies in the area are structurally controlled).

Table 4.1. Azimuthal Resistivity Sounding Values for Umueshi

AZIMUTHAL RESISTIVITY SOUNDING VALUE TABLE AT UMUESHI											
S/N	AB/2	MN/2	K	RESISTANCE(Ω)				RESISTIVITY (Ω m)			
				N-S	E-W	NE-SW	NW-SE	N-S	E-W	NE-SW	NW-SE
1	10	5	23.57	33.14	30.09	35.01	30.02	781.11	709.22	825.19	707.57
2	20	5	117.8	20.9	22.35	19.24	20.93	2438.46	2632.83	2266.47	2465.55
3	30	5	274.89	14.36	14.46	13.09	14.14	3947.42	3974.91	3598.31	3886.94
4	40	5	494.8	11.22	10.67	11.43	10.91	5551.66	5279.52	5655.56	5398.27
5	50	5	777.54	11.36	17.21	12.47	9.361	8832.85	13,381.46	9695.92	7278.55



At Umueshi, the trends of the plots are multi-directional (E –W, N - S and NW – SE and NW – SE), with NW – SE trend being well pronounced at depth of AB/2 = 20, 30 and 50, thereby corresponding to the map in figure 1.0, which suggest all gullies within the south east to be in

the NW – SE direction. The Umueshi plots, when also compared to the azimuth frequency diagram of the study area in figure 4.10, have various levels of agreement and similarities.

Table 4.2. Azimuthal Resistivity Sounding Values for Umuomeji, Urualla

AZIMUTHAL RESISTIVITY SOUNDING VALUE TABLE AT UMUOMEJI, URUALLA											
S/N	AB/2	MN/2	K	RESISTANCE(Ω)				RESISTIVITY (Ω m)			
				N-S	E-W	NE-SW	NW-SE	N-S	E-W	NE-SW	NW-SE
1	10	5	23.57	141.2	101.2	115.1	107.5	3328.08	2385.28	2712.91	2533.78
2	20	5	117.8	35.61	30.26	28.64	30.81	4194.86	3564.63	3373.79	3629.42
3	30	5	274.89	13.97	15.27	13.7	15.56	3840.2	4197.57	3765.99	4277.29
4	40	5	494.8	7.341	8.251	10.66	7.461	3632.32	4082.59	5274.57	3691.7
5	50	5	777.54	4.814	5.867	5.74	3.914	3743.08	4,561.83	4463.08	3043.29

At Umuomeji, Urualla, another multi-directional trends of structural lines of weaknesses were observed (E–W, N-S, NE-SW, NW-SE directions) with E-W, N-S and NW–SE trends appearing significantly, twice at AB/2 = 10 and 50, AB/2 = 30 and 40, and AB/2 = 20 and 50 respectively. The NE–SW direction appeared significantly only once at depth of AB/2 = 20.

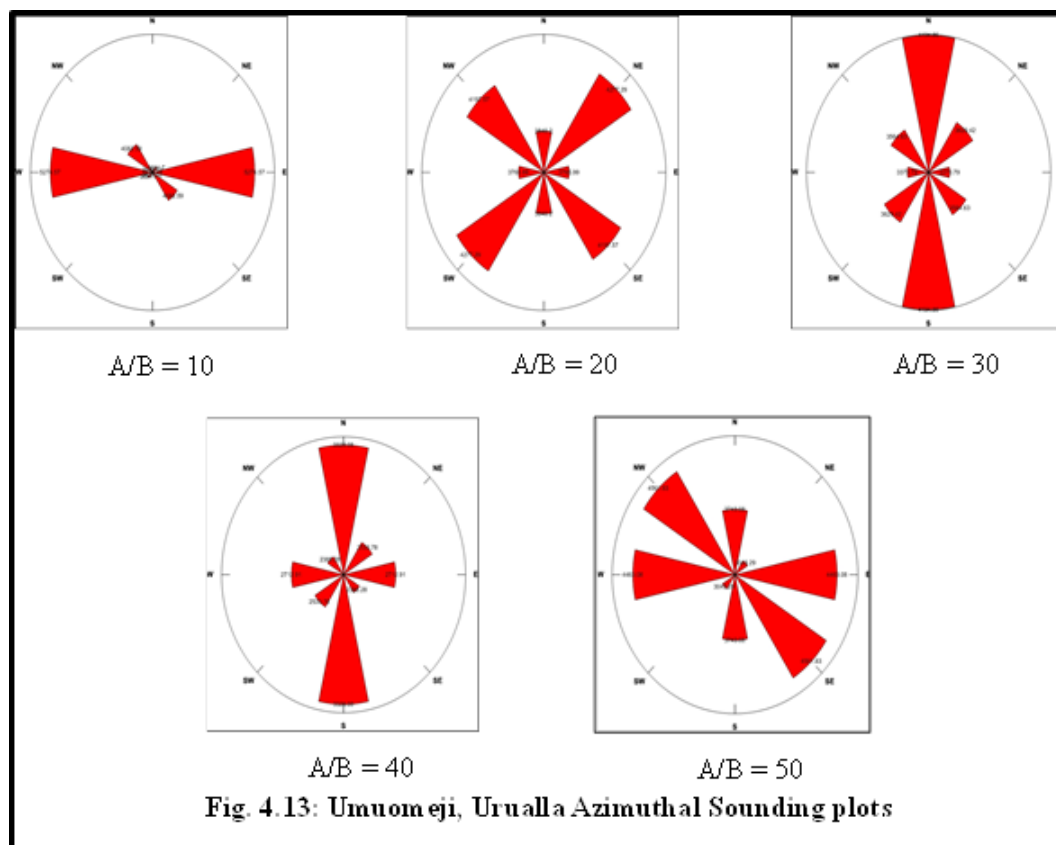


Table 4.3: Azimuthal Resistivity Sounding Values for Dimagu

AZIMUTHAL RESISTIVITY SOUNDING VALUE TABLE AT DIMAGU											
S/N	AB/2	MN/2	K	RESISTANCE(Ω)				RESISTIVITY (Ω m)			
				N-S	E-W	NW-SE	NE-SW	N-S	E-W	NW-SE	NE-SW
1	10	5	23.57	72.36	75.7	74.79	68.3	1705.525	1784.249	1762.8	1609.831
2	20	5	117.8	12.26	10.94	10.23	11.95	1444.228	1288.732	1205.094	1407.71
3	30	5	274.89	5.097	5.472	4.368	5,158	1401.114	1504.198	1200.72	1417883
4	40	5	494.8	3.091	3.314	2.807	3.06	1529.427	1639.767	1388.904	1514.088
5	50	5	777.54	2.665	2.219	2.047	2.148	2072.144	1725.361	1591.624	1670.156

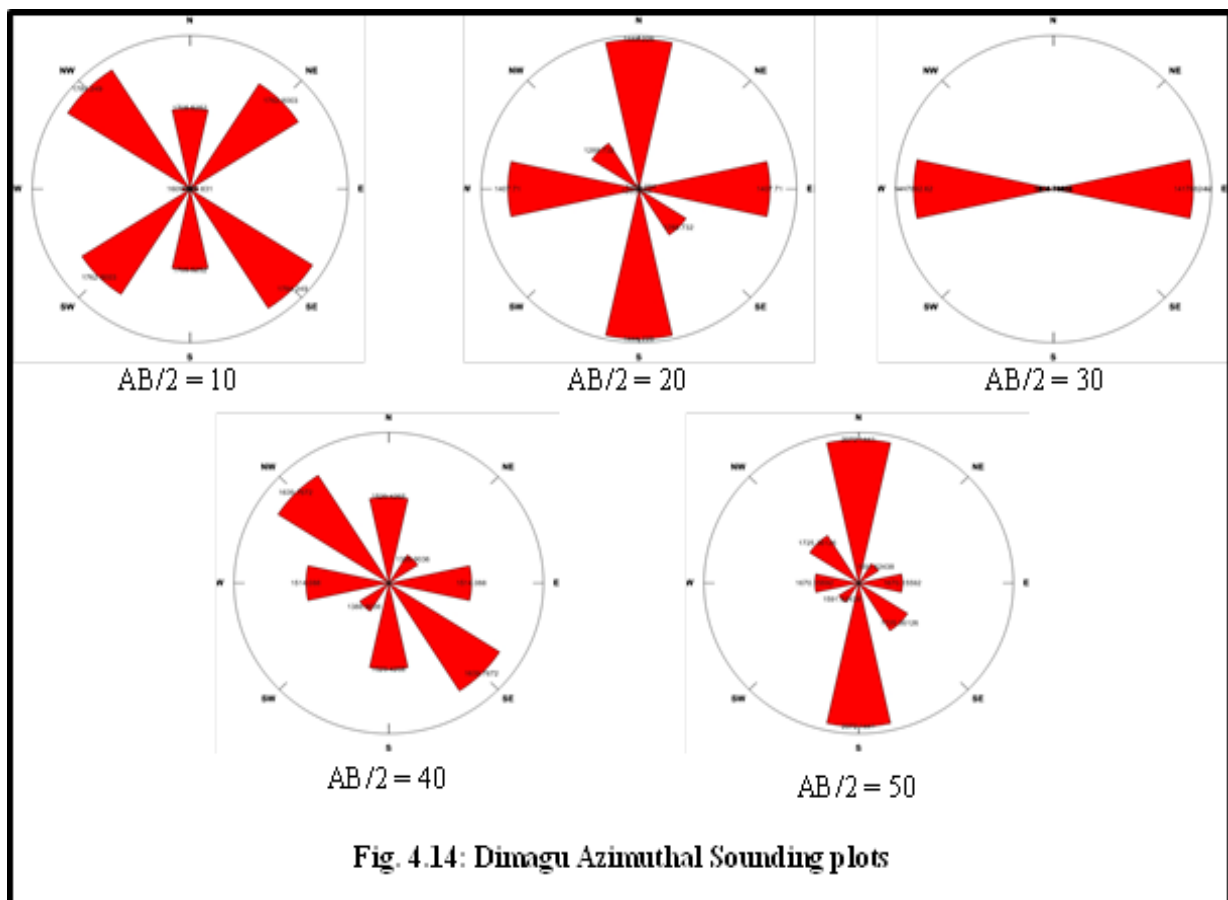


Fig. 4.14: Dimagu Azimuthal Sounding plots

Dimagu erosion site displayed another multi-directional trends of structural lines of weaknesses when plotted (that is E–W, N-S, NE-SW, NW-SE directions) with NW-SE, E-W and N-S directions appearing significantly twice at depths of AB/2 = 10, 40, AB/2 = 20, 30 and AB/2 = 20, 50 respectively. The NE-SW directions appeared significantly only once at depth of AB/2 = 10.

Table 4.4: Azimuthal Resistivity Sounding Values for Ihioma

AZIMUTHAL RESISTIVITY SOUNDING VALUE TABLE AT IHIOMA											
S/N	AB/2	MN/2	K	RESISTANCE(Ω)				RESISTIVITY (Ω m)			
				N-S	E-W	NW-SE	NE-SW	N-S	E-W	NW-SE	NE-SW
1	10	5	23.57	84.93	68.91	82.09	86.14	2001.8	1624.209	1934.861	2030.32
2	20	5	117.8	16.72	14.79	17.93	15.6	1969.616	1742.262	2112.154	1837.68
3	30	5	274.89	8.422	7.449	8.868	7.682	2315.124	2047.656	2437.725	2111.705
4	40	5	494.8	5.219	4.449	5.878	4.905	2582.361	2201.365	2908.434	2426.994
5	50	5	777.54	3.471	3.182	3.993	3.415	2698.841	2474.132	3104.717	2655.299

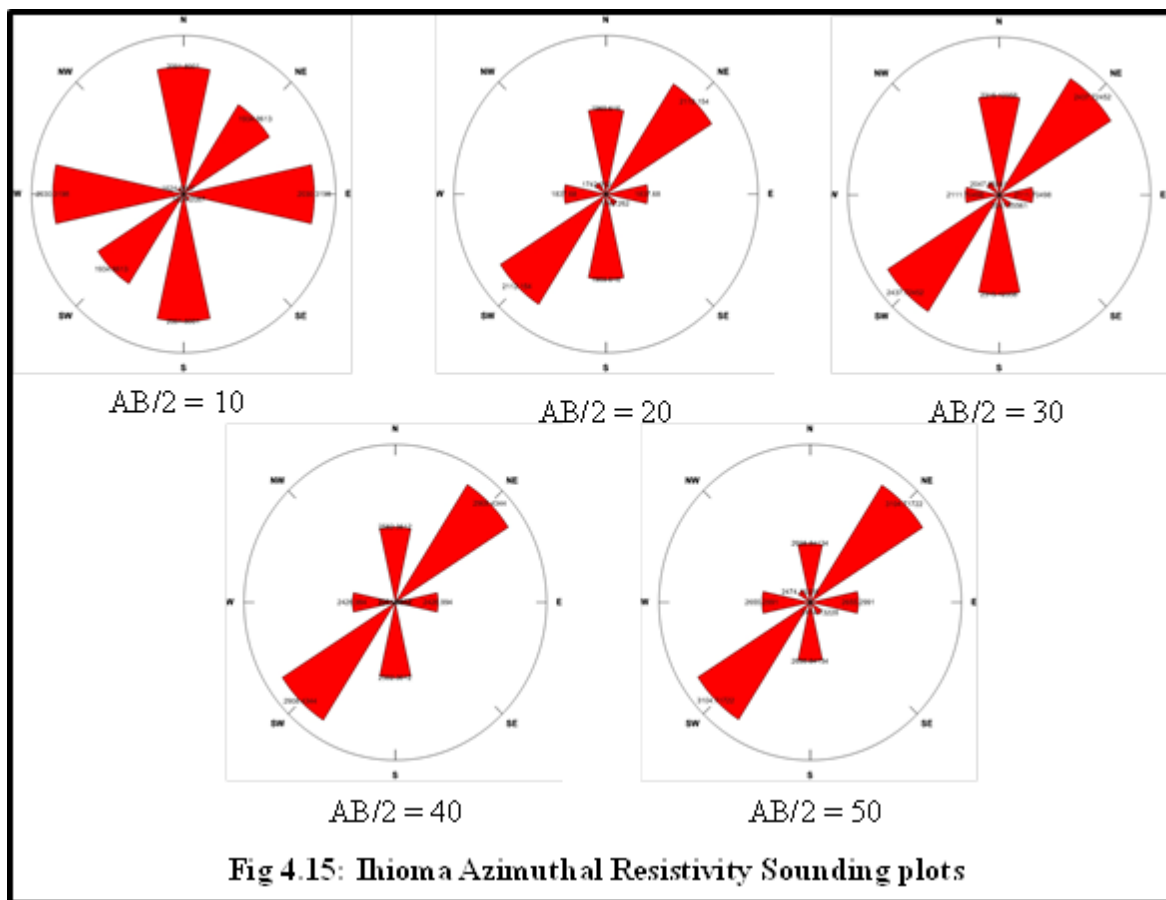


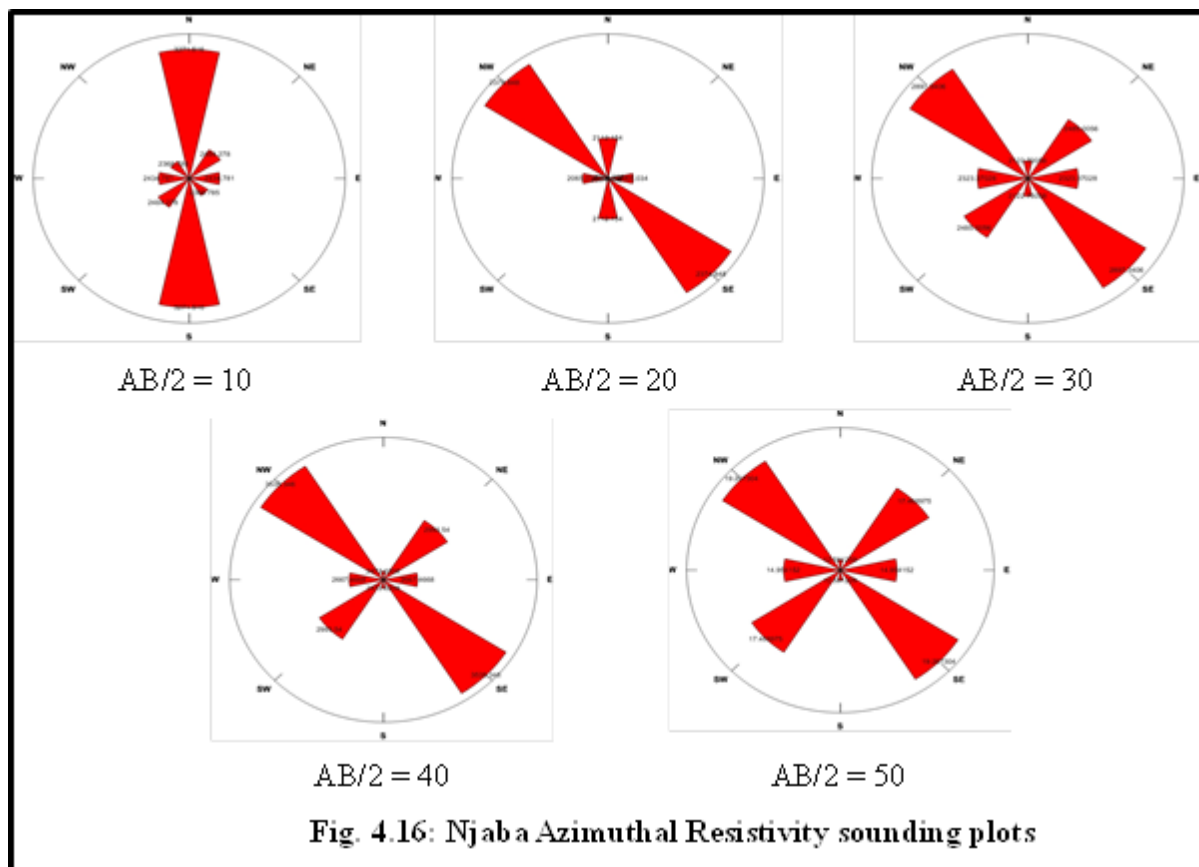
Fig 4.15: Ihioma Azimuthal Resistivity Sounding plots

Ihioma erosion site displayed a uni-directional trends of structural lines of weaknesses when plotted (that is NE-SW direction) at depths of $AB/2 = 20, 30, 40$ and 50 with an exception at the depth $AB/2 = 10$ whose trends are multi-directional. If figures 4.15 and 4.10 (Azimuth frequency diagram of the study area) are compared critically, it will be observed that the most

dominant trend in figure 4.10 is NE-SW which corresponds to the most dominant trend in the Ihioma.

Table 4.5: Azimuthal Resistivity Sounding Value Table at Njaba

AZIMUTHAL RESISTIVITY SOUNDING VALUE TABLE AT NJABA											
S/N	AB/2	MN/2	K	RESISTANCE(Ω)				RESISTIVITY (Ω m)			
				N-S	E-W	NE-SW	NW-SE	N-S	E-W	NE-SW	NW-SE
1	10	5	23.57	138.8	100.5	105.4	103.3	3271.516	2368.785	2484.278	2434.781
2	20	5	117.8	17.93	20.16	17.02	17.53	2112.154	2374.848	2004.956	2065.034
3	30	5	274.89	7.722	10.54	9.04	8.452	2122.701	2897.341	2485.006	2323.37
4	40	5	494.8	4.996	7.145	6.05	5.391	2472.021	3535.346	2993.54	2667.467
5	50	5	3.547	3.547	5.432	4.925	4.216	12.58121	19.2673	17.46898	14.95415

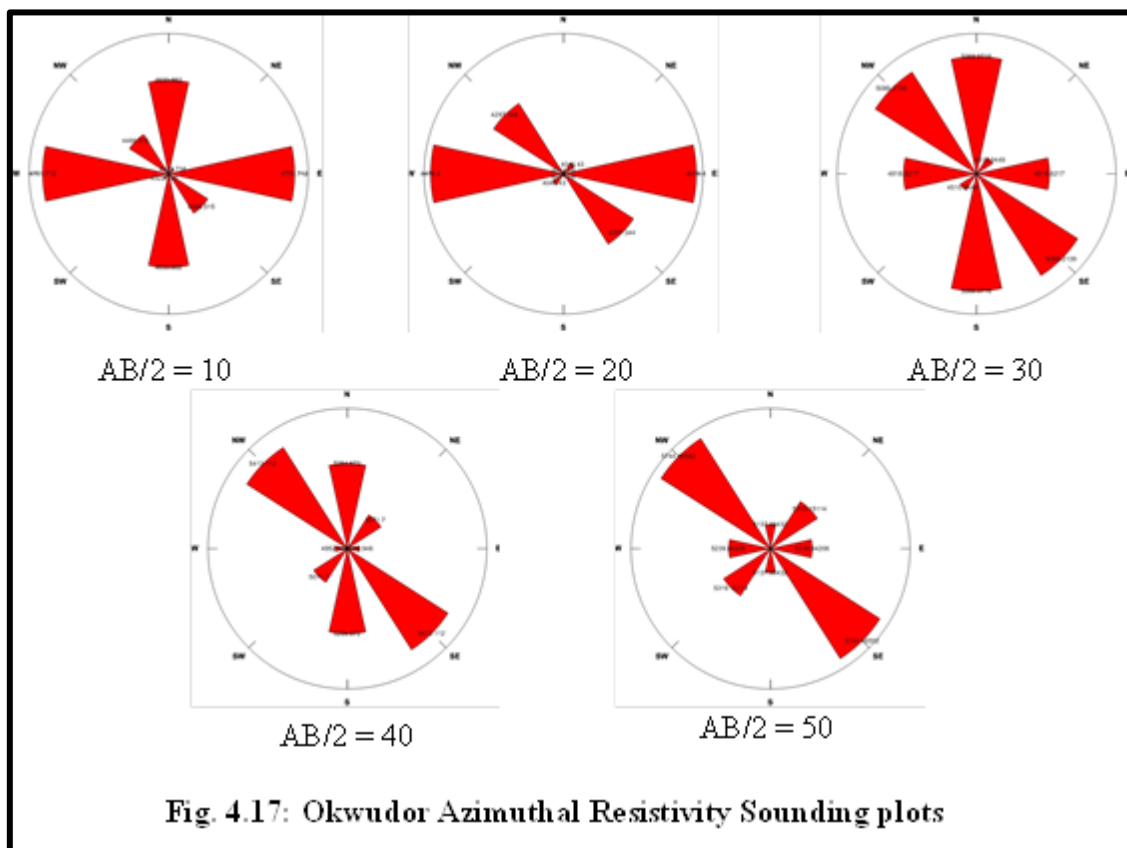


Njaba erosion site also displayed a uni-directional (NW-SE) trend of structural line of weakness when plotted. In this case, the direction is opposite to that of Ihioma which is also uni-directional, but corresponds to the second most dominant trend in figure 4.10 (Azimuth

frequency diagram of the study area). The unitary direction occurred at depths of $AB/2 = 20$, 30, 40 and 50 with an exception at the depth $AB/2 = 10$ whose trends is in the N-S direction.

Table 4.6: Azimuthal Resistivity Sounding Value Table at Okwudor

AZIMUTHAL RESISTIVITY SOUNDING VALUE TABLE AT OKWUDOR											
S/N	AB/2	MN/2	K	RESISTANCE(Ω)				RESISTIVITY (Ω m)			
				N-S	E-W	NE-SW	NW-SE	N-S	E-W	NE-SW	NW-SE
1	10	5	23.57	196.6	189.5	201.6	183.4	4633.862	4466.515	4751.712	4322.738
2	20	5	117.8	34.05	36.48	38	34.35	4011.09	4297.344	4476.4	4046.43
3	30	5	274.89	18.44	18.51	17.53	16.41	5068.972	5088.214	4818.822	4510.945
4	40	5	494.8	10.64	10.94	10.01	10.25	5264.672	5413.112	4952.948	5071.7
5	50	5	777.54	6.608	7.388	6.739	6.841	5137.984	5744.466	5239.842	5319.151



At Okwudor erosion site, three directional trends were observed which are E-W, N-S and NW-SE, which NW-SE being the most pronounced.

Table 4.7:Azimuthal Resistivity Sounding Value Table at Umuhuokabia

AZIMUTHAL RESISTIVITY SOUNDING VALUE TABLE AT UMUHUOKABIA											
S/N	AB/2	MN/2	K	RESISTANCE(Ω)				RESISTIVITY (Ω m)			
				N-S	E-W	NW-SE	NE-SW	N-S	E-W	NW-SE	NE-SW
1	10	5	23.57	31.22	28.58	27.46	25.74	735.8554	673.6306	647.2322	606.6918
2	20	5	117.8	5.453	6.587	6.699	3.071	642.3634	775.9486	789.1422	361.7638
3	30	5	274.89	2.676	3.263	2.949	3	735.6056	896.9661	810.6506	699.3202
4	40	5	494.8	1.996	1.996	1.662	2.235	987.6208	987.6208	822.3576	1105.878

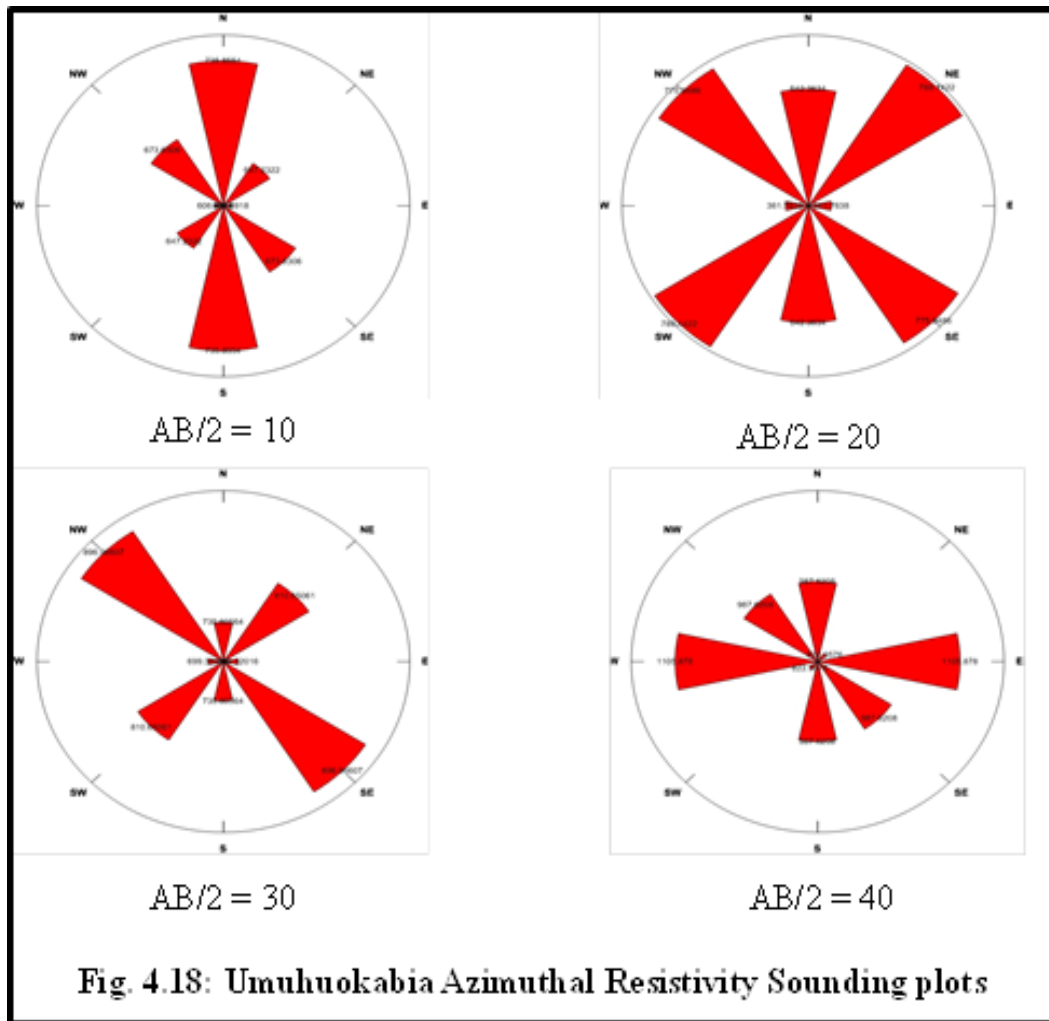


Fig. 4.18: Umuhuokabia Azimuthal Resistivity Sounding plots

At Umuhuokabia, another multi-directional trends of structural lines of weaknesses were observed with NW–SE trends being most prominent as it appeared twice at depths of AB/2 = 20 and 30 respectively.

These azimuthal plots show that there is more to the gullying within Orlu and environs as has been previously attributed to soil texture, compaction and rainfall. The consistence in the structural lines of weaknesses as observed in all the azimuthal plots points to a structural deformation in the subsurface which in turns, enhances a surface expression (gully) of the weaknesses underneath when exposed to agents of erosion, soil texture and compaction also being an unneglectable factor.

4.1.3 Vertical Electrical Sounding

4.1.3.1 Iso-resistivity (Resistivity Depth Slices) Interpretation

The Iso-Resistivity tables are as shown below

Table 4.8a: Iso-Resistivity value for AB/2 from 5 - 65

STATION	LONG.	LAT.	5	10	15	20	25	30	35	40	45	50	55	60	65
NJABA RIVER	7.193056	5.774167	550	1070	1330	1680	2070	2380	2500	2480	2450	2410	1900	2080	2310
ORLU/IHIALA RD	7.060278	5.878056	765	800	840	960	1140	1240	1240	1170	1153	1120	1200	1200	1200
OKWELLE/URUALLA RD	7.312500	5.886667	900	1180	1500	1660	1940	2260	2510	2740	2880	2940	3020	3340	3380
AFOR UKWU - AFOR NTA	7.360556	5.861944	1050	850	850	1100	1350	1600	1900	2250	3550	2750	2700	2850	3000
OKWELLE/URUALLA RD 2	7.322222	5.810833	1200	1900	3000	3700	4350	4900	5300	5450	5550	5650	4750	4750	4800
OWERRI/ORLU RD	7.253889	5.761111	10600	12200	13400	14200	14600	15800	16200	16180	16000	15800	14600	13800	12900
UMUNGUMA IHIOMA	7.263889	5.927222	2050	1525	1075	750	650	650	650	650	650	650	650	750	700
IKPA/IHIOMA	7.142778	5.960000	380	940	1360	1340	1100	880	680	580	490	410	360	570	460
UMUZZALA OGBERURU	7.028722	5.83039	3300	4700	6300	6200	6100	4900	3700	2700	1900	1550	1400	1370	1320
UMUESHI 1	7.110472	5.829000	135	440	760	1060	1400	1900	2420	2880	3210	3290	3100	2860	2600
UMUESHI 2	7.109669	5.83081	440	560	950	1250	1550	1900	2300	2650	2820	2850	2680	2410	2200
OGBERURU 2	7.015389	5.83203	300	550	900	1380	1450	1680	1750	1900	2240	2550	2720	2920	3050

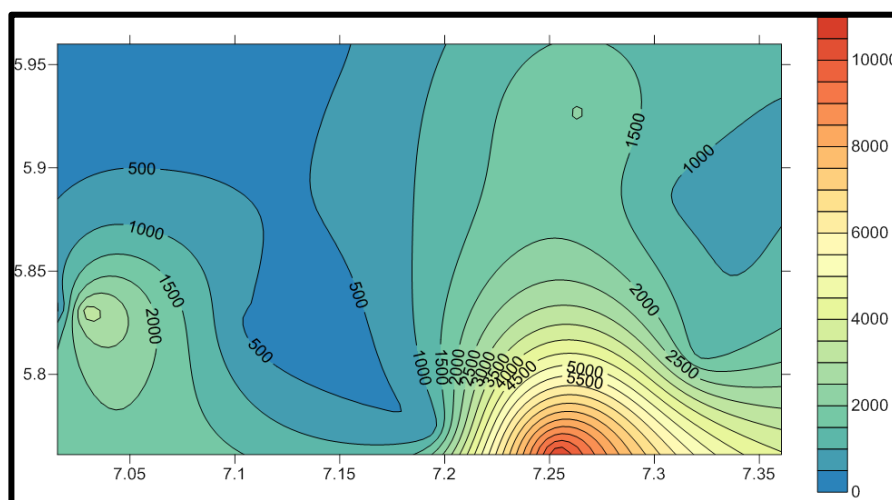


Fig. 4.19: Iso-Resistivity contour at the value AB/2 = 5

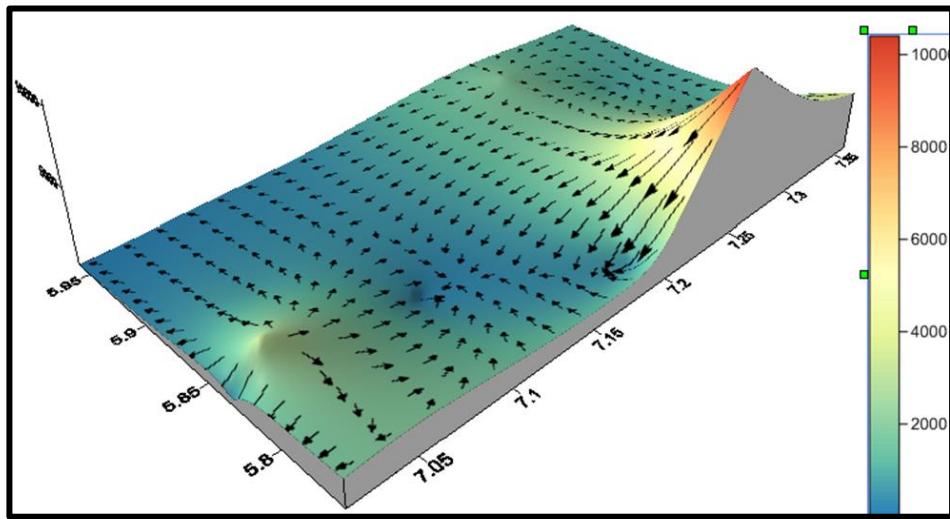


Fig. 4.20: 3D model with vector map of Iso-Resistivity at the value $AB/2 = 5$

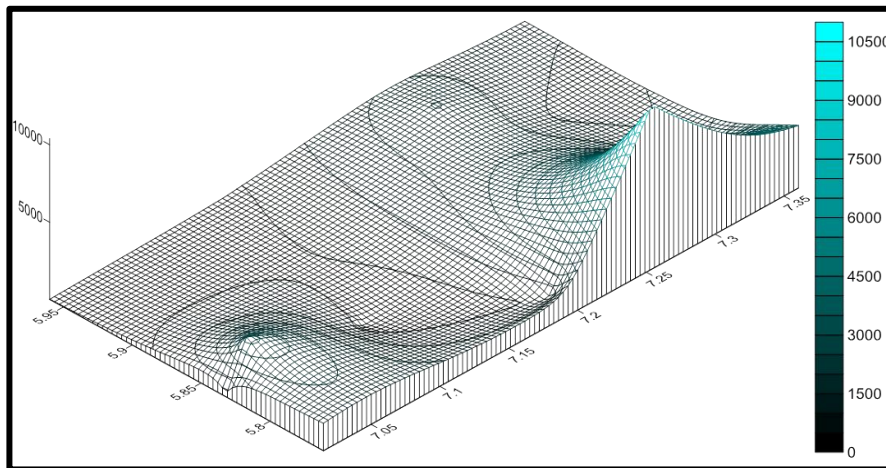


Fig. 4.21: Wired 3D model Iso-Resistivity at the value $AB/2 = 5$

Table 4.8b: Iso-Resistivity value for $AB/2$ from 70 - 135

STATION	LONG.	LAT.	70	75	80	85	90	95	100	105	110	115	120	125	130	135
NJABA RIVER	7.193056	5.774167	2580	2750	2820	2890	2900	2950	3040	3110	3220	3310	3420	3530	3645	3790
ORLU/IHIALA RD	7.060278	5.878056	1184	1180	1170	1160	1150	1120	1045	970	900	840	760	720	680	640
OKWELLE/URUALLA RD	7.312500	5.886667	3400	3450	3410	3380	3340	3320	3320	3340	3360	3340	3260	3180	3020	2860
AFOR UKWU - AFOR NTA	7.360556	5.861944	3200	3350	3500	3650	3750	3800	3800	3800	3750	3750	3700	3700	3750	3750
OKWELLE/URUALLA RD 2	7.322222	5.810833	4850	4900	5000	5050	5150	5190	5200	5280	5300	5300	5300	5280	5200	5100
OWERRI/ORLU RD	7.253889	5.761111	12400	12400	14000	16800	18800	19000	18000	15400	13000	10400	8400	6900	6000	5400
UMUNGUMA IHIOA	7.263889	5.927222	690	680	640	600	600	650	750	880	1025	1150	1250	1270	1250	1150
IKPA/IHIOA	7.142778	5.960000	360	280	230	215	200	195	190	195	200	200	195	190	180	160
UMUAZZALA OGBERURU	7.028722	5.83039	1300	1290	1220	1120	1100	1100	1120	1205	1300	1500	1600	1750	1900	2000
UMUESHI 1	7.110472	5.829000	2360	2190	2090	2030	1990	1960	1910	1860	1800	1750	1700	1640	1590	1550
UMUESHI 2	7.109669	5.83081	1995	1860	1860	1950	2080	2125	2120	2080	2005	1940	1850	1770	1690	1600
OGBERURU 2	7.015389	5.83203	3150	3120	2880	2400	1950	1650	1605	1700	1880	2095	2350	2550	2820	3050

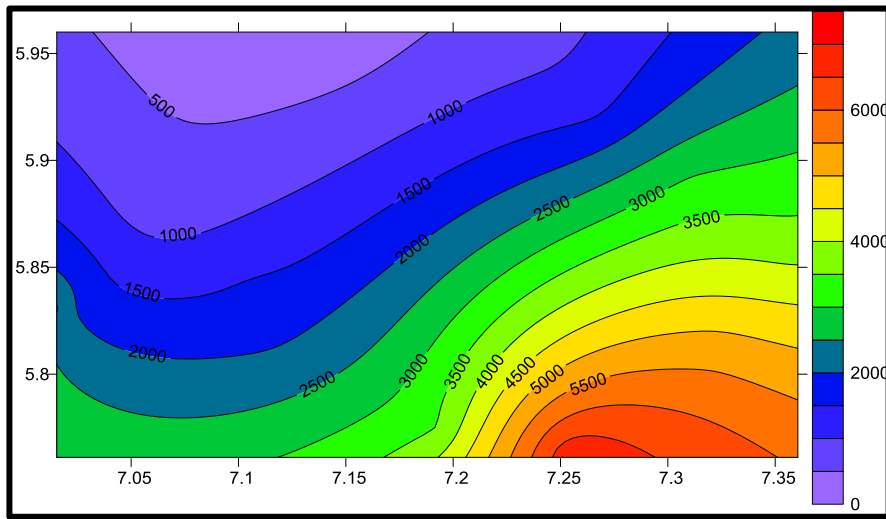


Fig. 4.22: Iso-Resistivity contour at the value $AB/2 = 125$

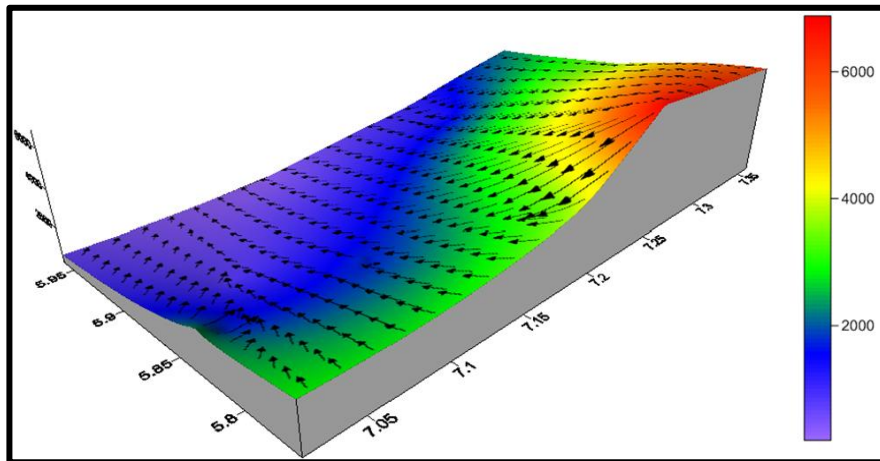


Fig. 4.23: 3D model with vector map of Iso-Resistivity at the value $AB/2 = 125$

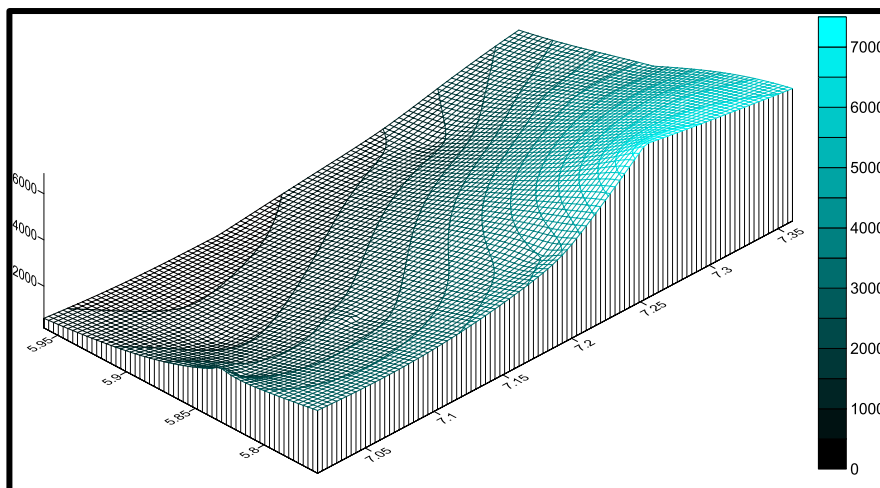


Fig. 4.24: Wired 3D model Iso-Resistivity at the value $AB/2 = 125$

Table 4.8c: Iso-Resistivity value for AB/2 from 135 - 195

STATION	LONG.	LAT.	135	140	145	150	155	160	165	170	175	180	185	190	195
NIABA RIVER	7.193056	5.774167	3790	3905	4225	4180	4290	4350	4400	4420	4430	4480	4500	4545	4590
ORLU/IHIALA RD	7.060278	5.878056	640	635	605	595	580	560	520	460	400	325	280	240	240
OKWELLE/URUALLA RD	7.312500	5.886667	2860	2700	2540	2380	2220	2060	1930	1780	1620	1500	1340	1220	1220
AFOR UKWU - AFOR NTA	7.360556	5.861944	3750	3800	3850	3900	3950	4100	4200	4300	4500	4600	4800	5000	5200
OKWELLE/URUALLA RD 2	7.322222	5.810833	5100	4850	4800	4650	4500	4400	4300	4200	4100	4000	3900	3800	3700
OWERRI/ORLU RD	7.253889	5.761111	5400	5100	5000	4955	4900	4800	4700	4600	4600	4600	4600	4600	4650
UMUNGUMA IHOMA	7.263889	5.927222	1150	1000	900	770	670	600	575	550	550	550	560	575	600
IKPA/IHIOMA	7.142778	5.960000	160	135	110	90	80	70	80	85	100	120	130	150	170
UMUJAZZALA OGBERURU	7.028722	5.83039	2000	2150	2250	2350	2405	2500	2550	2595	2605	2630	2650	2670	2695
UMUESHI 1	7.110472	5.829000	1550	1510	1480	1460	1450	1450	1460	1480	1500	1520	1550	1570	1590
UMUESHI 2	7.109669	5.83081	1600	1520	1460	1400	1360	1320	1290	1260	1240	1220	1200	1180	1160
OGBERURU 2	7.015389	5.83203	3050	3250	3430	3550	3610	3620	3615	3580	3520	3450	3390	3320	3250

Table 4.8d: Iso-Resistivity value for AB/2 from 200 – 250

STATION	LONG.	LAT.	200	205	210	215	220	225	230	235	240	245	250
NJABA RIVER	7.193056	5.774167	4685	5795	5810	5830	5865	5890	5905	5925	5985	6010	6100
ORLU/IHIALA RD	7.060278	5.878056	300	1960	1760	1560	1280	1145	840	620	420	250	150
OKWELLE/URUALLA RD	7.312500	5.886667	1940	2160	2020	2020	2020	2020	2000	1985	1980	1980	1950
AFOR UKWU - AFOR NTA	7.360556	5.861944	5550	7550	7500	7400	7350	7250	7200	7100	7050	7000	7000
OKWELLE/URUALLA RD 2	7.322222	5.810833	3700	4850	5000	5100	5150	5250	5300	5400	5500	5600	5700
OWERRI/ORLU RD	7.253889	5.761111	4700	4400	4100	3800	3600	3200	3000	2700	2400	2200	2000
UMUNGUMA IHOMA	7.263889	5.927222	650	1450	1550	1600	1650	1700	1750	1775	1825	1875	1925
IKPA/IHIOMA	7.142778	5.960000	180	180	180	180	185	187	190	200	200	210	220
UMUJAZZALA OGBERURU	7.028722	5.83039	2700	2705	2710	2720	2740	2750	2770	2780	2790	2795	2800
UMUESHI 1	7.110472	5.829000	1600	1620	1630	1650	1660	1680	1690	1705	1720	1740	1750
UMUESHI 2	7.109669	5.83081	1140										
OGBERURU 2	7.015389	5.83203	3220										

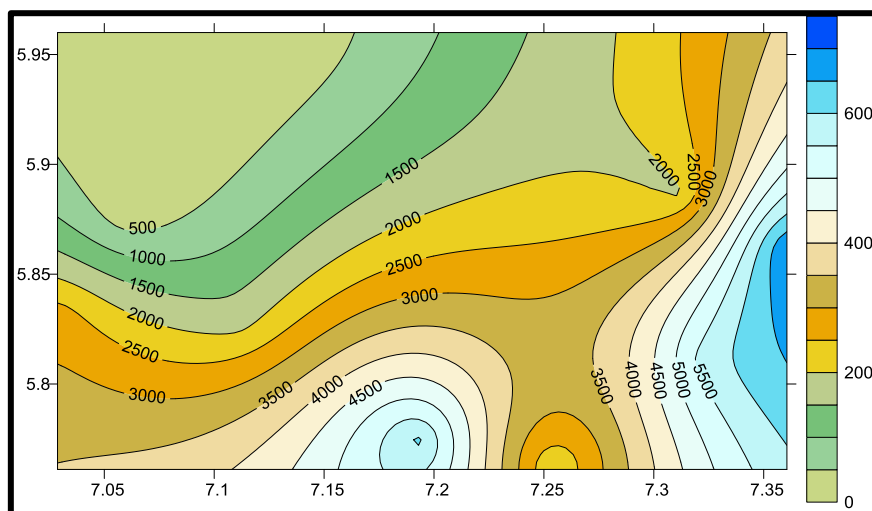


Fig. 4.25: Iso-Resistivity contour at the value AB/2 = 250

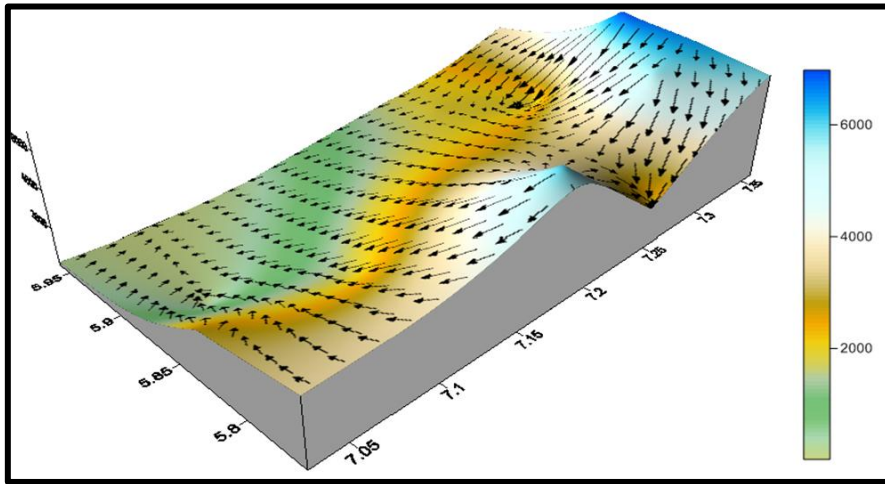


Fig. 4. 26: 3D model with vector map of Iso-Resistivity at the value $AB/2 = 250$

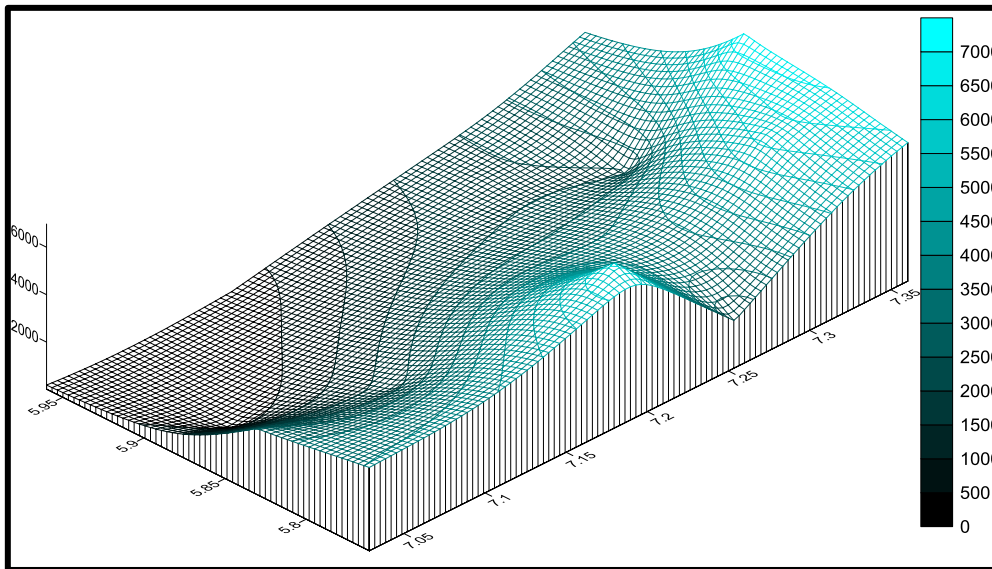


Fig. 4.27: Wired 3D model Iso-Resistivity at the value $AB/2 = 250$

4.1.3.2 Layer Resistivity, Depth and Thickness Values

Table 4.9: Table for Layer Resistivity, Depth of Layers and Thickness of Layers

STATIONS	LONG.	LAT.	LAYER RESISTIVITY						DEPTH OF LAYERS					THICKNESS OF LAYERS					ELEVATION
			R1	R2	R3	R4	R5	R6	D1	D2	D3	D4	D5	T1	T2	T3	T4	T5	
NJABA RIVER	7.193056	5.774167	186	10000	1090	9500	44800		1.6	8.7	33.6	65		1.6	7.1	24.9	31.4		115
ORLU/IHIALA RD	7.060278	5.878056	383	940	1810	1190	528	38.9	1.1	14.6	33	67.5	104	1.1	13.5	18.4	34.5	36.5	102
OKWELLE/URUALLA RD	7.312500	5.886667	650	5460	2870	910			4.8	34.5	61.8			4.8	29.7	27.3			152
AFOR UKWU - AFOR NTA	7.360556	5.861944	970	521	11600	3710	7330	25500	4.7	10.6	36.8	64.9	107	4.7	5.9	26.2	28.1	42.1	155
OKWELLE/URUALLA RD 2	7.322222	5.810833	643	11200	2210	3700	11000		2.5	24.8	66.7	110		2.5	22.3	41.9	43.3		137
OWERRI/ORLU RD	7.253889	5.761111	5970	12800	24900	6520	1020		0.9	16.8	53.6	78.7		0.9	15.9	36.8	25.1		107
UMJUNGUMA IHIDIOMA	7.263889	5.927222	1690	3100	560	748	621	7460	1.3	4.1	24.3	65.5	113	1.3	2.8	20.2	41.2	47.5	110
IKPA/IHIOMA	7.142778	5.960000	213	3040	76.2	152	1660		1.6	9.9	64.2	106		1.6	8.3	54.3	41.8		94
UMJAZZALA OGBERURU	7.028722	5.830389	2708.7	6736	536.21	4843.4	320.5		3.0227	12.49	34.73	212.08		3.0227	9.466	22.24	177.4		195
UMJESHI 1	7.110472	5.829000	179.22	3498.7	897.07				3.4263	90.66				3.4263	87.23				260
UMJESHI 2	7.109669	5.830806	65.168	471.34	1000.1	2999.2	2167	325.4	0.6106	1.544	2.843	14.822	105.6	0.6106	0.933	1.299	11.98	90.7	273
OGBERURU 2	7.015389	5.832028	204.43	4430.9	1883	601.7			2.9033	119.3	181.9			2.9033	116.4	62.57			121

Below is the contour, 3D model and wired 3D model of elevation of Orlu and Environs.

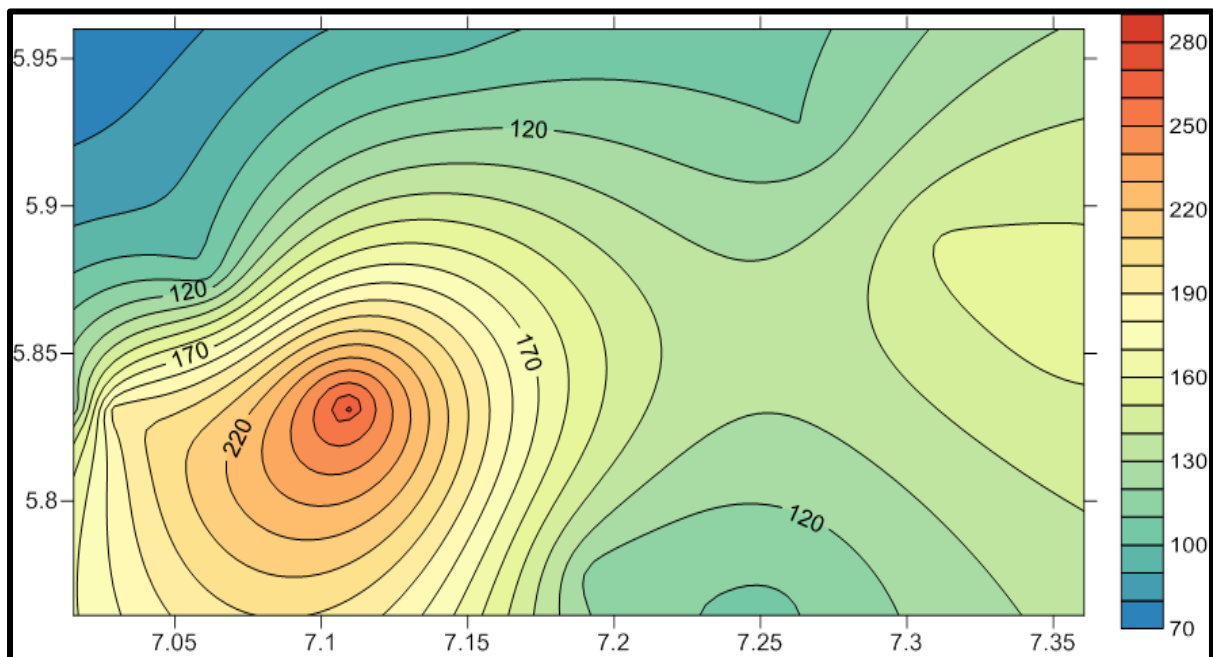


Fig. 4.28: The elevation contour of the study area

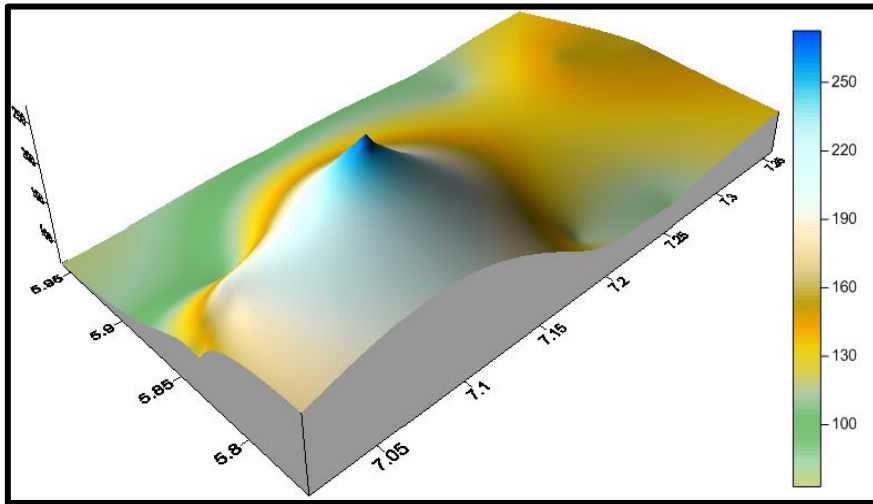


Fig 4.29: 3D Model of the elevation of the study area

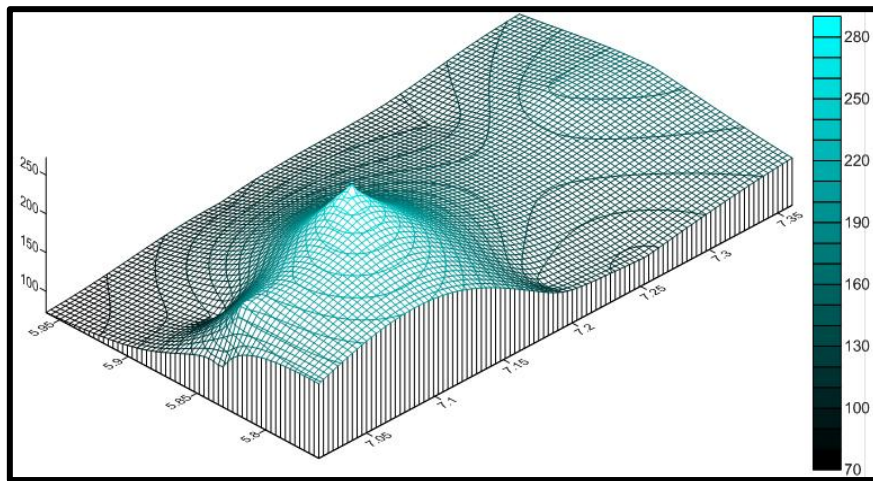


Fig 4.30: Wired 3D Model of the elevation of the study area

Below are the resistivity contours of layers within Orlu and Environs

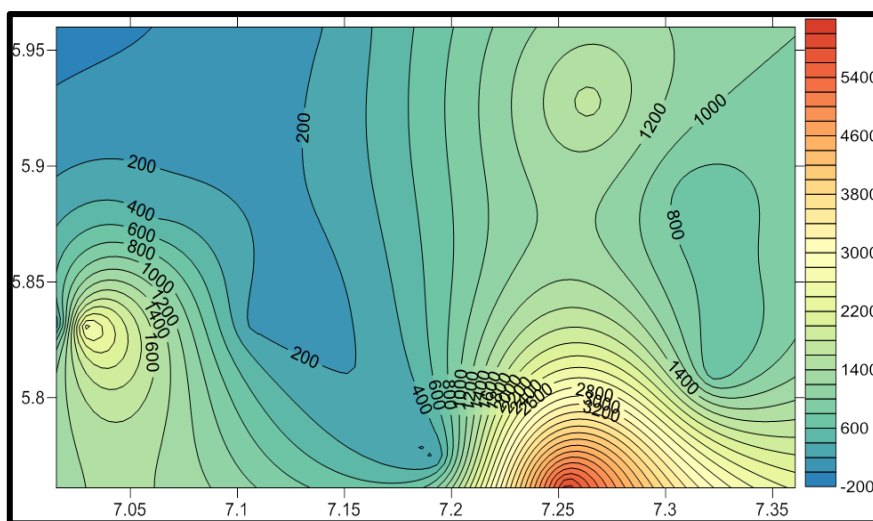


Fig 4.31: The Resistivity contour of the entire first (1st) – top most- layers

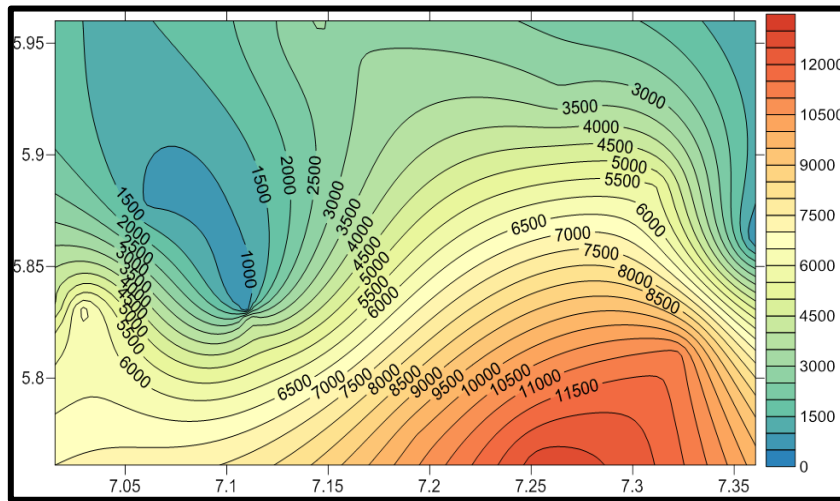


Fig 4.32: The Resistivity contour of the entire second (2nd) layers – i.e. 2nd from the top most layer

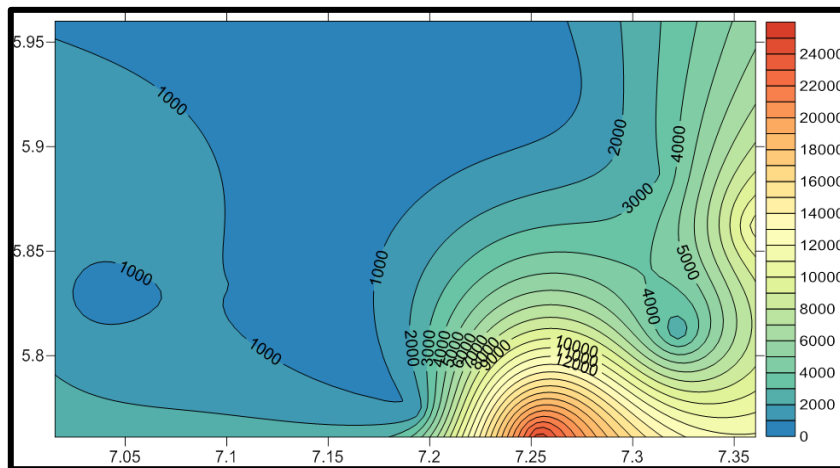


Fig 4.33: The Resistivity contour of the entire third (3rd) layers – i.e. 3rd from the top most layer

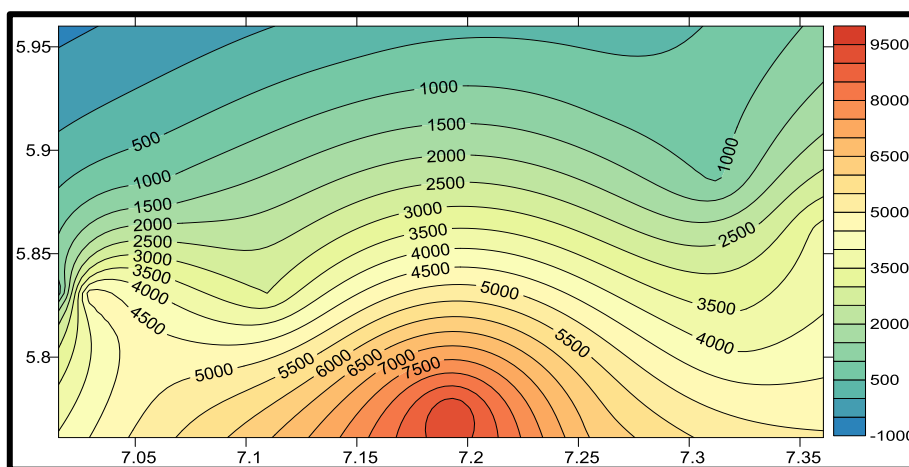


Fig 4.34: The Resistivity contour of the entire fourth (4th) layers – i.e. 4th from the top most layer

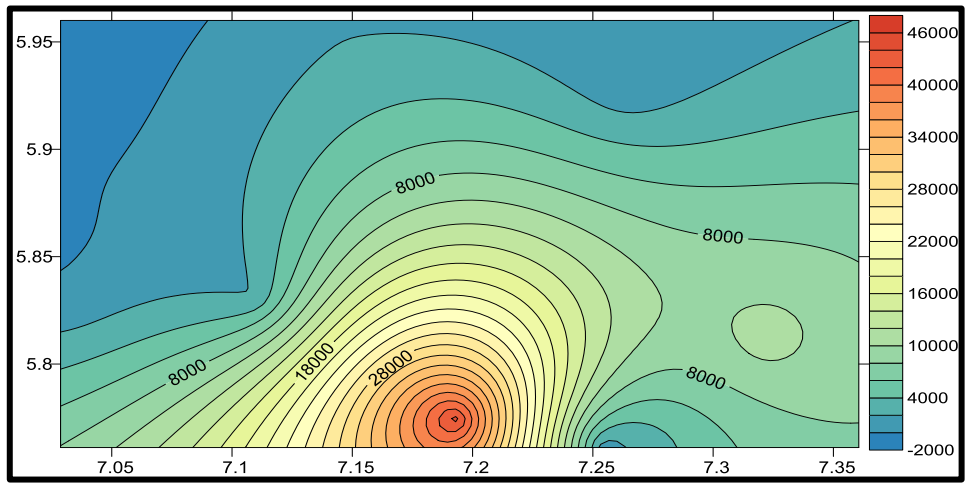


Fig 4.35: The Resistivity contour of the entire fifth (5th) layers – i.e. 5th from the top most layer

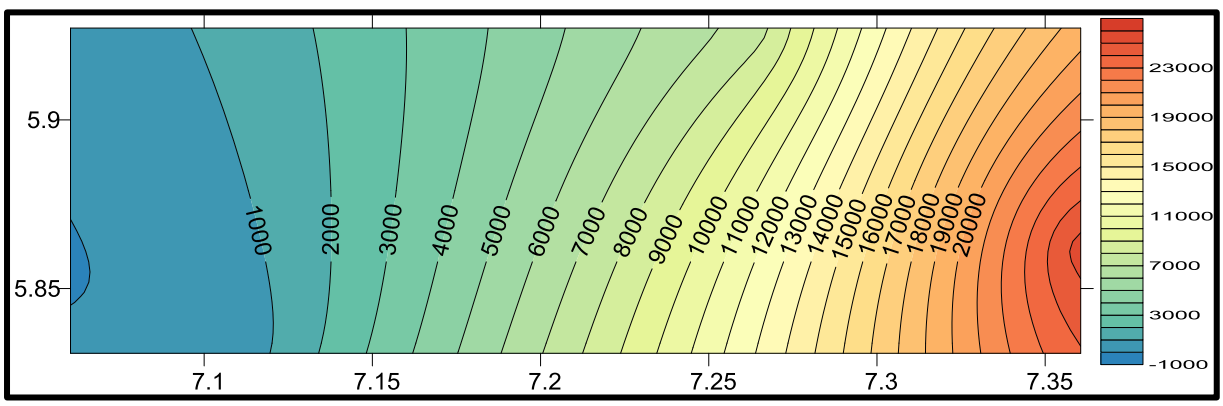


Fig 4.36: The Resistivity contour of the entire fifth (6th) layers – i.e. 6th from the top most layer

4.1.3.3 Geoelectric Sections

Below is the geo-electric sections and geo-electric profiling of the study locations.

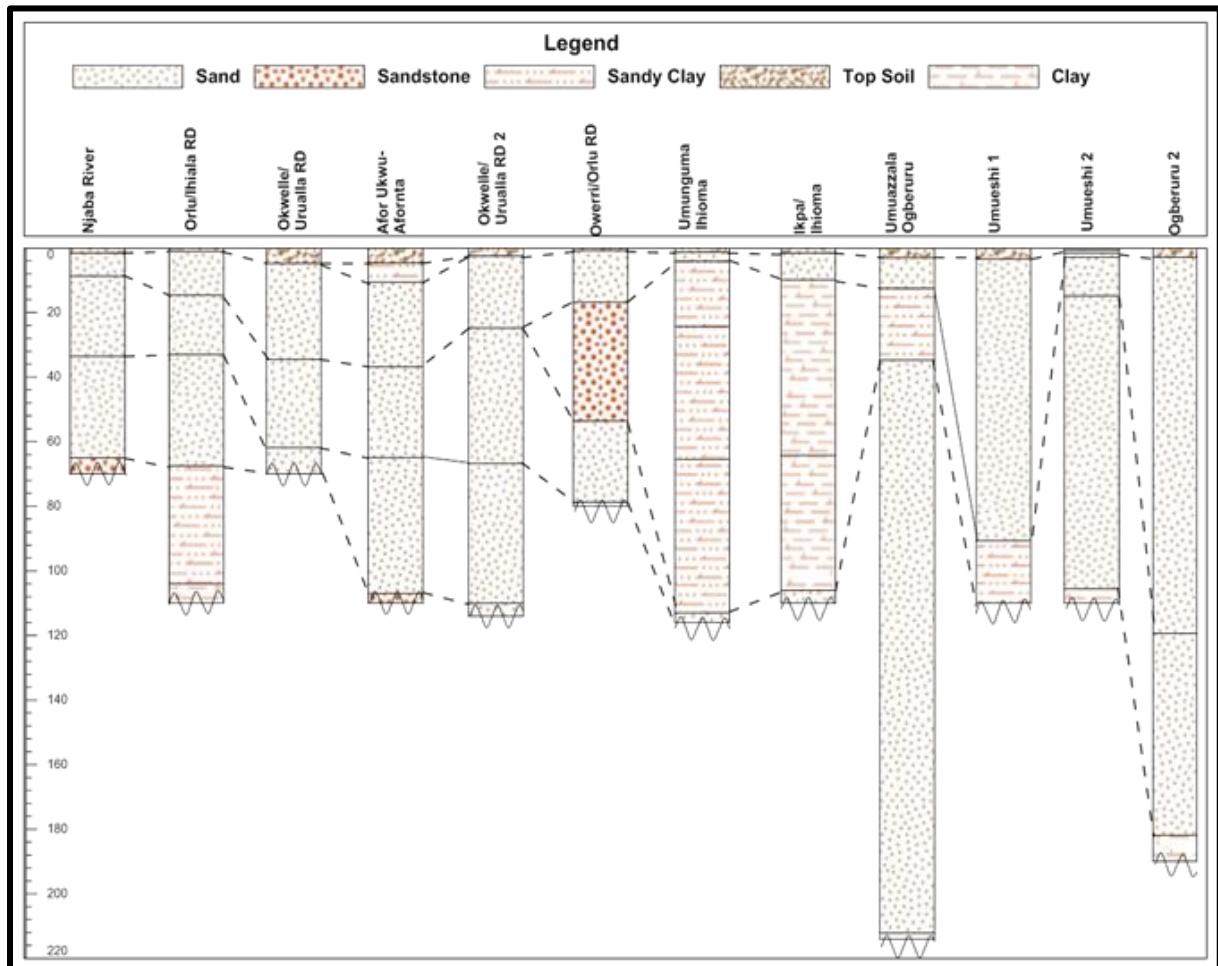


Fig 4.37: Geo-electric sections and profiling of the study locations

4.1.3.4 Geotechnical Analysis Result Presentation

The results from geotechnical analysis carried out within Orlu and environs are as shown below.

Please note the following: OMC = Optimum Moisture Content, MDD = Maximum Dry Density, LL = Liquid Limit, PL = Plasticity Limit, PI = Plasticity Index.

Grain Size Distribution of Afor-Ukwu Gully 1

Table 4.10: Sample statistics table for Afor-Ukwu gully Sample 1

SAMPLE STATISTICS						
SAMPLE IDENTITY: Afor-Ukwu Gully Sample 1			ANALYST & DATE: , 21/7/2014			
SAMPLE TYPE: Polymodal, Moderately Sorted			TEXTURAL GROUP: Sand			
SEDIMENT NAME: Moderately Sorted Medium Sand						
	μm	ϕ	GRAIN SIZE DISTRIBUTION			
MODE 1:	462.5	1.117	GRAVEL: 0.0%	COARSE SAND: 18.9%		
MODE 2:	327.5	1.616	SAND: 100.0%	MEDIUM SAND: 47.7%		
MODE 3:	231.0	2.119	MUD: 0.0%	FINE SAND: 26.2%		
D_{10} :	166.8	0.607	V FINE SAND: 6.1%			
MEDIAN or D_{50} :	340.4	1.555	V COARSE GRAVEL: 0.0%	V COARSE SILT: 0.0%		
D_{90} :	656.5	2.584	COARSE GRAVEL: 0.0%	COARSE SILT: 0.0%		
(D_{90} / D_{10}) :	3.936	4.256	MEDIUM GRAVEL: 0.0%	MEDIUM SILT: 0.0%		
$(D_{90} - D_{10})$:	489.7	1.977	FINE GRAVEL: 0.0%	FINE SILT: 0.0%		
(D_{75} / D_{25}) :	2.057	1.993	V FINE GRAVEL: 0.0%	V FINE SILT: 0.0%		
$(D_{75} - D_{25})$:	248.5	1.040	V COARSE SAND: 1.2%	CLAY: 0.0%		
			METHOD OF MOMENTS		FOLK & WARD METHOD	
	Arithmetic	Geometric	Logarithmic	Geometric	Logarithmic	Description
	μm	μm	ϕ	μm	ϕ	
MEAN (\bar{x}):	388.8	337.2	1.568	358.6	1.479	Medium Sand
SORTING (s):	198.3	1.748	0.805	1.777	0.830	Moderately Sorted
SKEWNESS (Sk):	1.181	-0.664	0.664	-0.085	0.085	Symmetrical
KURTOSIS (K):	6.321	3.499	3.499	1.173	1.173	Leptokurtic

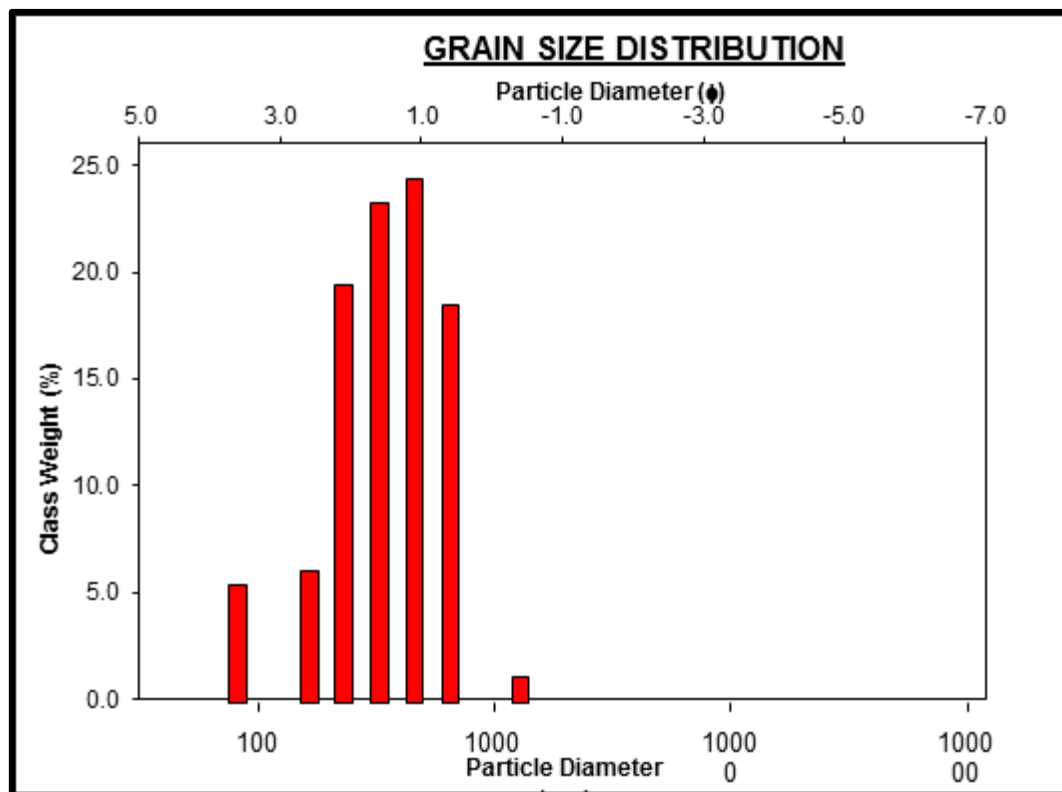


Fig. 4.38: Grain Size class of weight distribution chart for Afor-Ukwu gully sample 1.

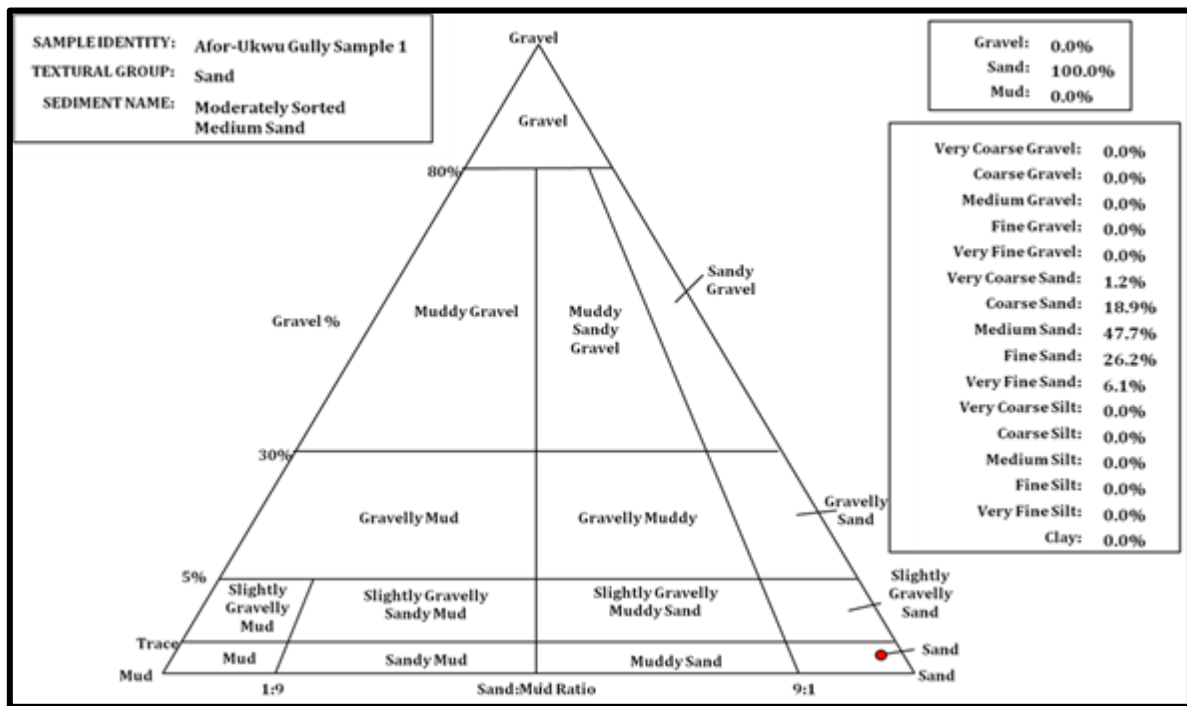


Fig. 4.39: Ternary chart of Afor-Ukwu Gully sample 1 grain size distribution

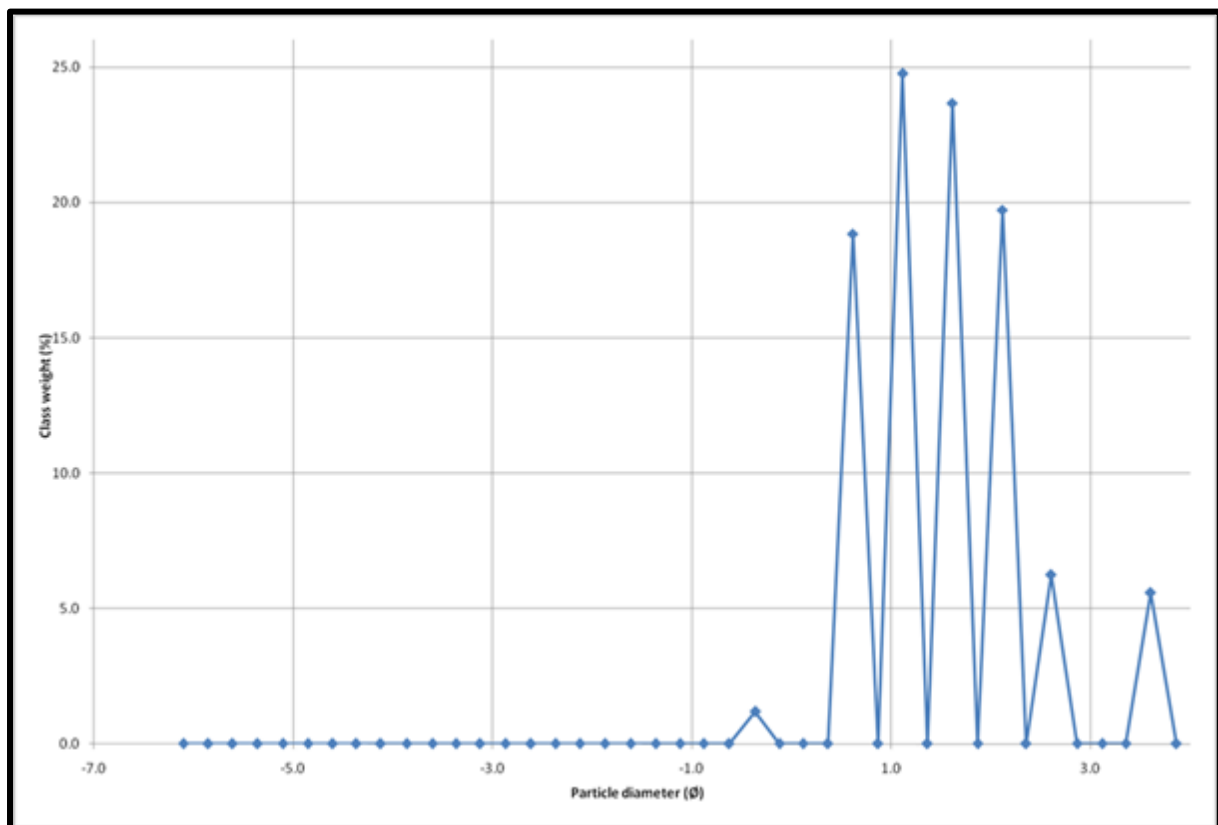


Fig. 4.40: Afor-Ukwu Gully Sample 1 grain size class of weight graph in phi

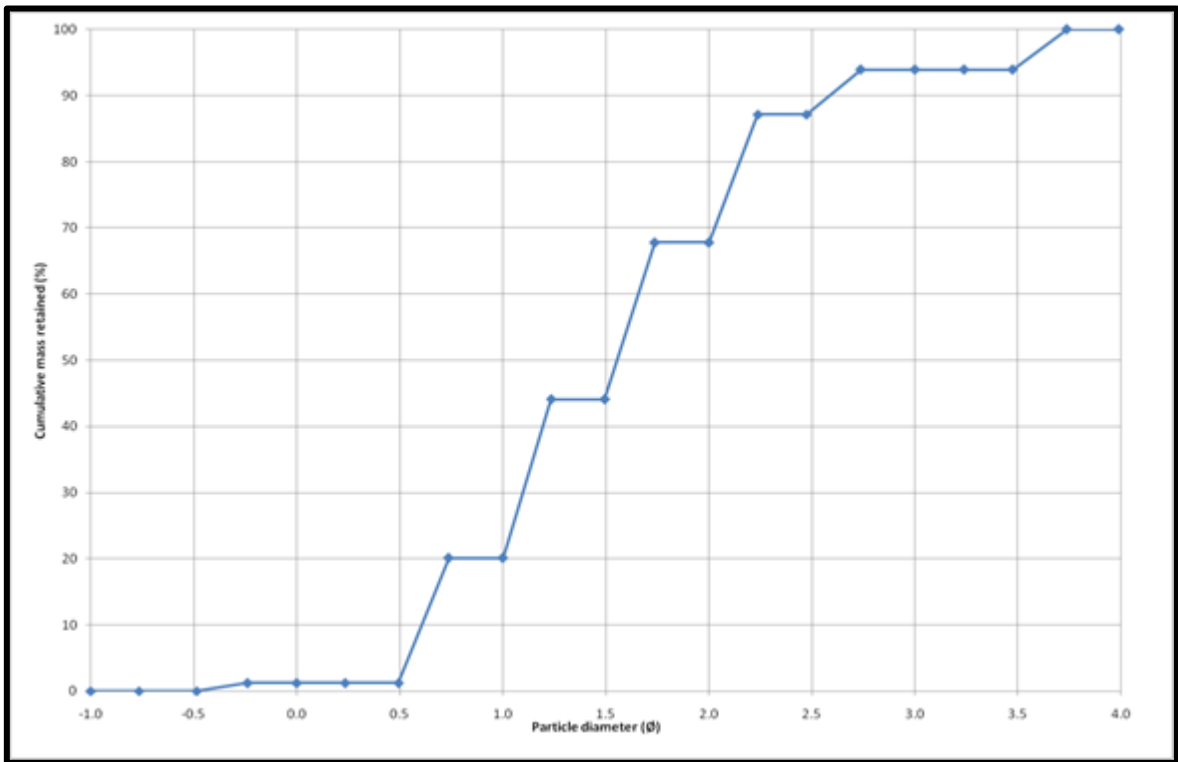


Fig. 4.41: Afor-Ukwu Gully Sample 1 Grain Size Cumulative mass Retained graph in phi

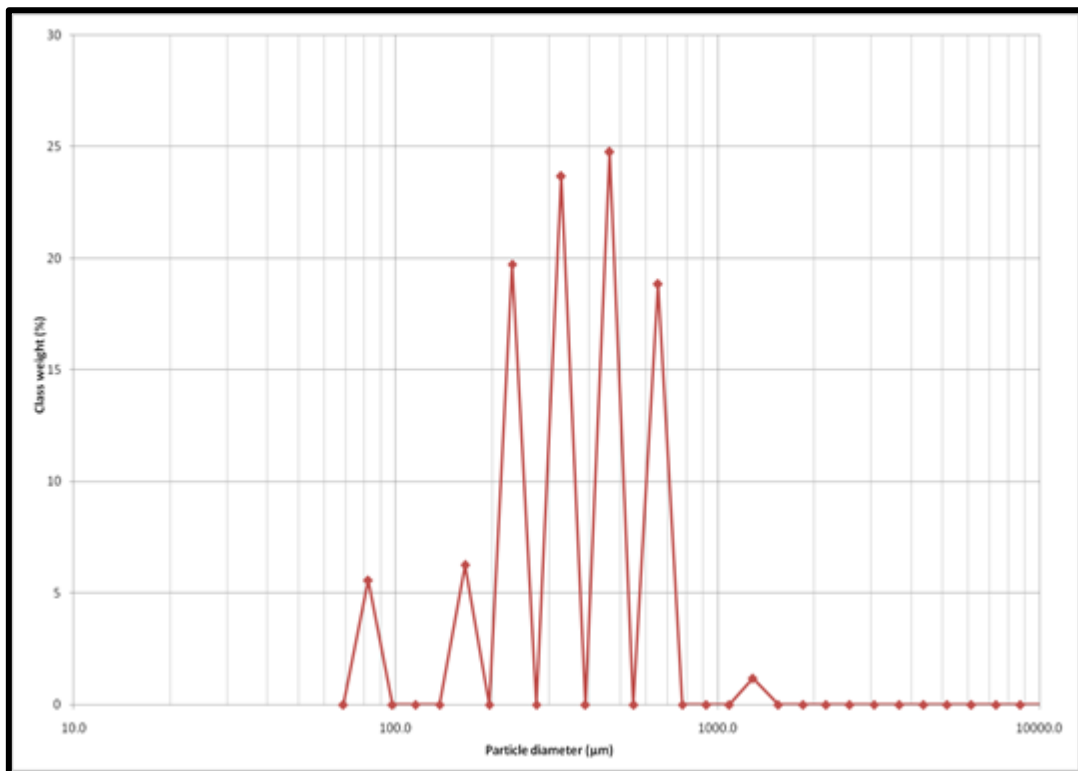


Fig. 4.42: Afor-Ukwu Gully Sample 1 class of weight graph in microns

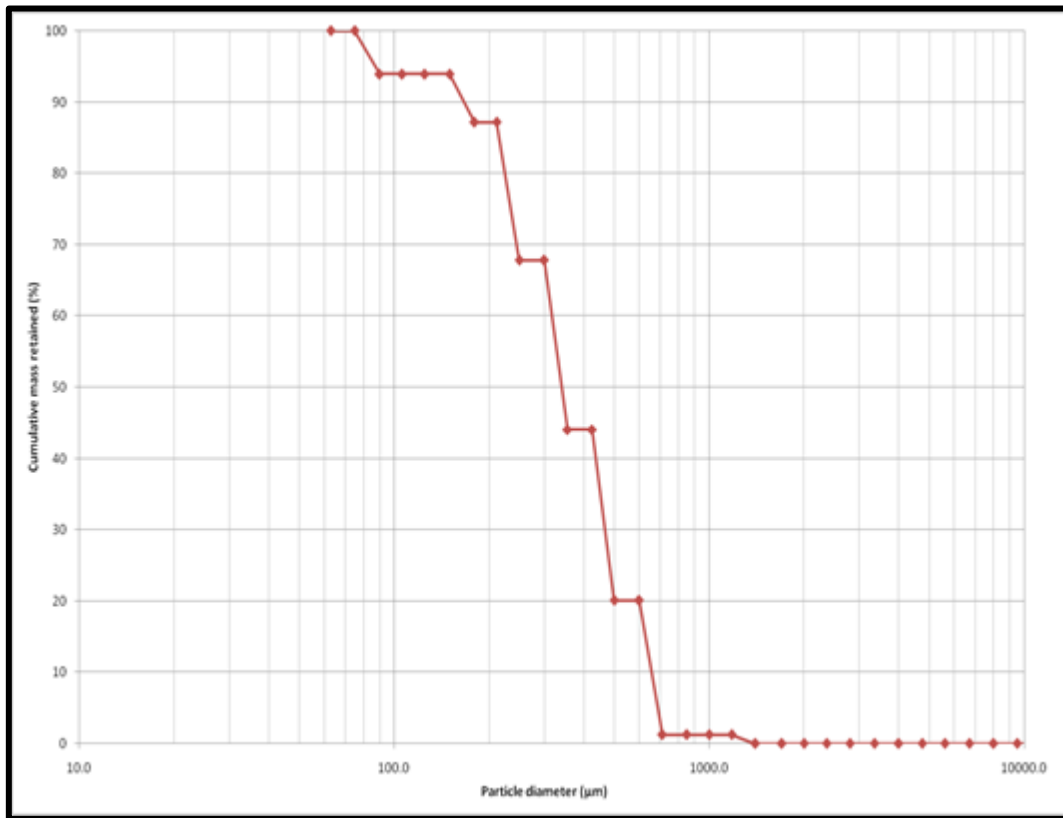


Fig. 4.43: Afor-Ukwu Gully Sample 1 cumulative mass retained graph in microns

The analysis of sample 1 collected at Afor Ukwu gully shows that Gavel and mud are 0% respectively while Sand is 100%. It also further revealed that the soil type within the area is polymodal, moderately sorted, symmetrical and also leptokurtic. This makes the area less compacted easily eroded in the presence of running water.

Grain Size Distribution of Afor-Ukwu Gully 2

The analysis of sample 2 collected at Afor Ukwu gully revealed that sand-sized particles are the predominant grains (100%), while mud (clay-sized particles) and gravel are absent (0%). These sand particles were found to be polymodal, moderately sorted, very fine skewed and leptokurtic. This makes the area easily prone to erosion in the presence of running water as no binding material (like muds) are present.

The analysis is as presented in table 9 below.

Table 4.11: Sample statistics table for Afor-Ukwu gully Sample 2

SAMPLE STATISTICS						
SAMPLE IDENTITY: Afor-Ukwu Gully Sample 2			ANALYST & DATE: , 21/7/2014			
SAMPLE TYPE: Polymodal, Moderately Sorted			TEXTURAL GROUP: Sand			
SEDIMENT NAME: Moderately Sorted Medium Sand						
	μm	ϕ	GRAIN SIZE DISTRIBUTION			
MODE 1:	462.5	1.117	GRAVEL: 0.0%	COARSE SAND: 19.5%		
MODE 2:	327.5	1.616	SAND: 100.0%	MEDIUM SAND: 52.8%		
MODE 3:	231.0	2.119	MUD: 0.0%	FINE SAND: 20.0%		
D ₁₀ :	174.3	0.592	V FINE SAND: 5.6%			
MEDIAN or D ₅₀ :	429.2	1.220	V COARSE GRAVEL: 0.0%	V COARSE SILT: 0.0%		
D ₉₀ :	663.6	2.521	COARSE GRAVEL: 0.0%	COARSE SILT: 0.0%		
(D ₉₀ / D ₁₀):	3.808	4.261	MEDIUM GRAVEL: 0.0%	MEDIUM SILT: 0.0%		
(D ₉₀ - D ₁₀):	489.4	1.929	FINE GRAVEL: 0.0%	FINE SILT: 0.0%		
(D ₇₅ / D ₂₅):	1.976	1.958	V FINE GRAVEL: 0.0%	V FINE SILT: 0.0%		
(D ₇₅ - D ₂₅):	242.6	0.983	V COARSE SAND: 2.2%	CLAY: 0.0%		
	METHOD OF MOMENTS			FOLK & WARD METHOD		
	Arithmetic	Geometric	Logarithmic	Geometric	Logarithmic	Description
	μm	μm	ϕ	μm	ϕ	
MEAN(\bar{x}):	416.6	362.2	1.465	393.0	1.347	Medium Sand
SORTING (s):	211.8	1.744	0.802	1.769	0.823	Moderately Sorted
SKEWNESS (Sk):	1.392	-0.783	0.783	-0.396	0.396	Very Fine Skewed
KURTOSIS (K):	7.191	3.963	3.963	1.240	1.240	Leptokurtic

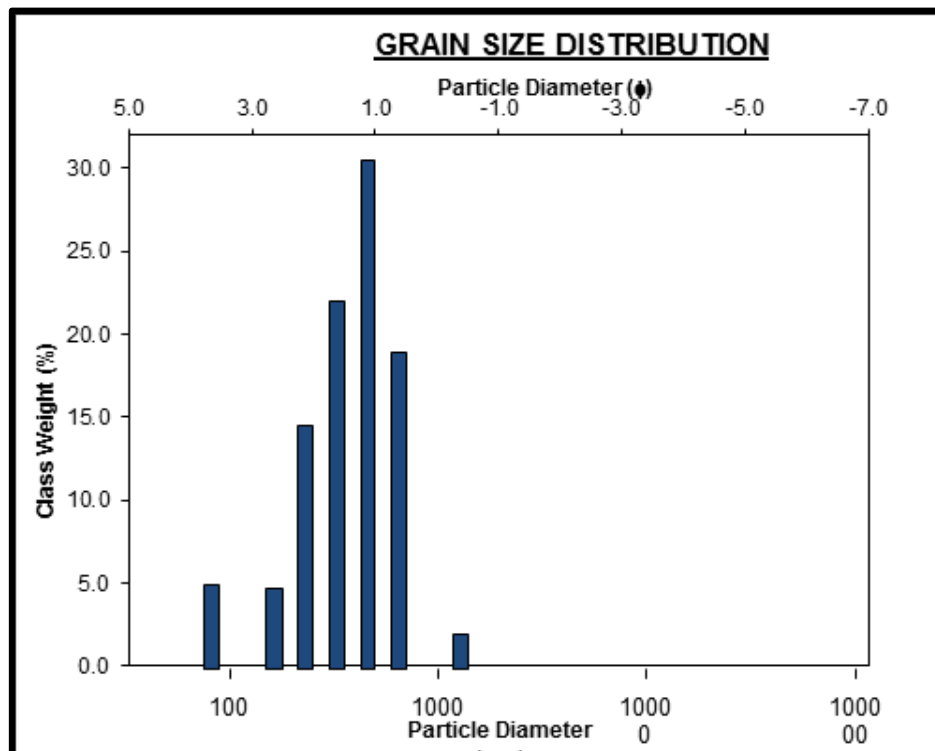


Fig. 4.44: Grain Size class of weight distribution chart for Afor-Ukwu gully sample 2.

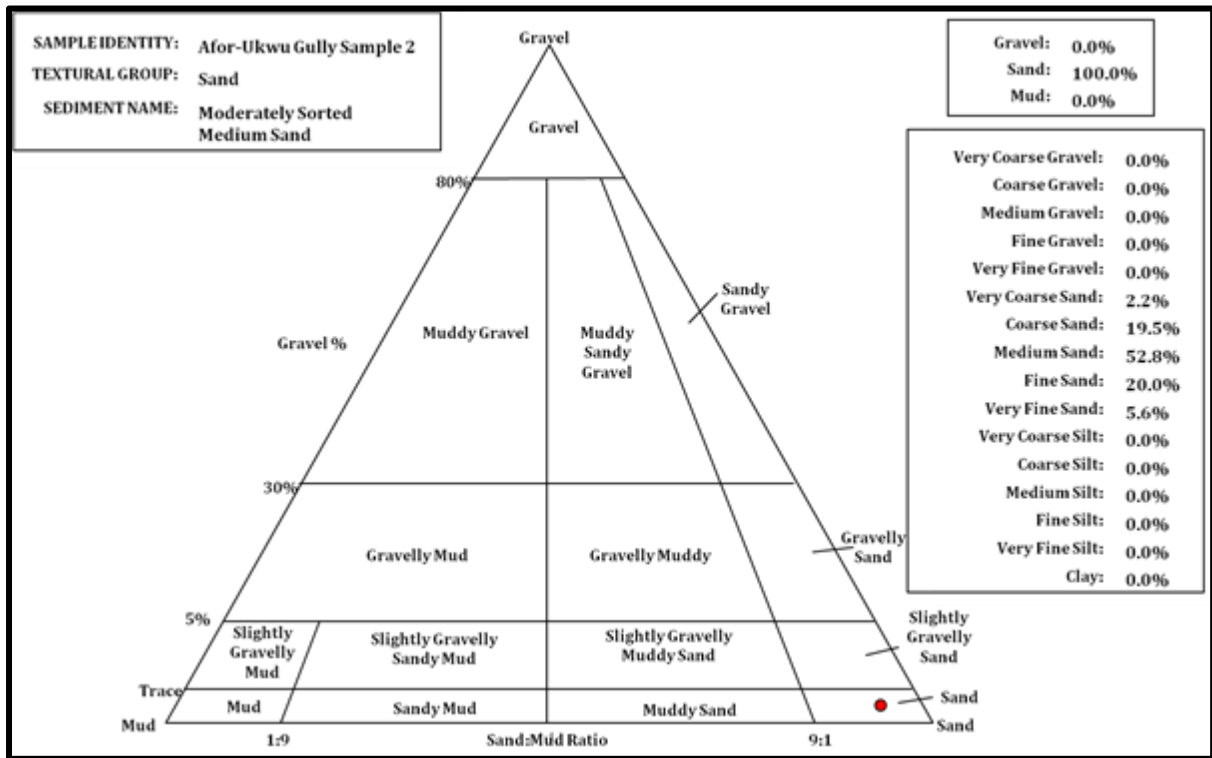


Fig. 4.45: Ternary chart of Afor-Ukwu Gully sample 2 grain size distribution

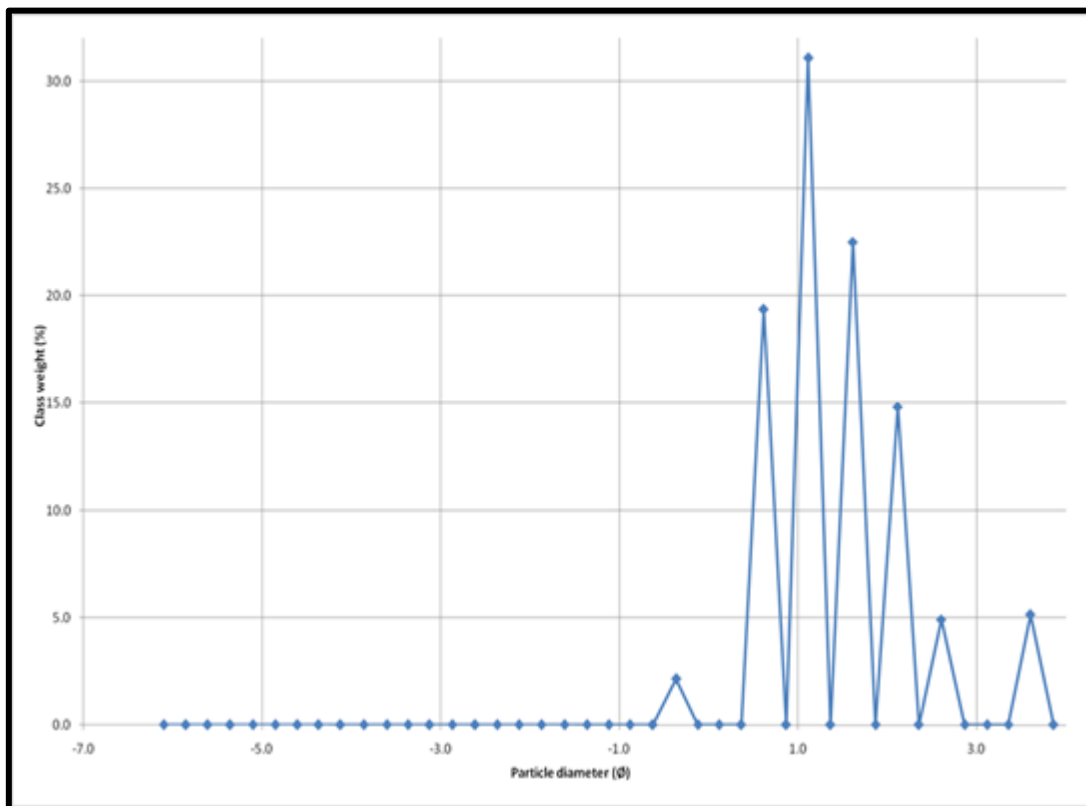


Fig. 4.46: Afor-Ukwu Gully Sample 2 Grain Distribution class of weight graph in phi

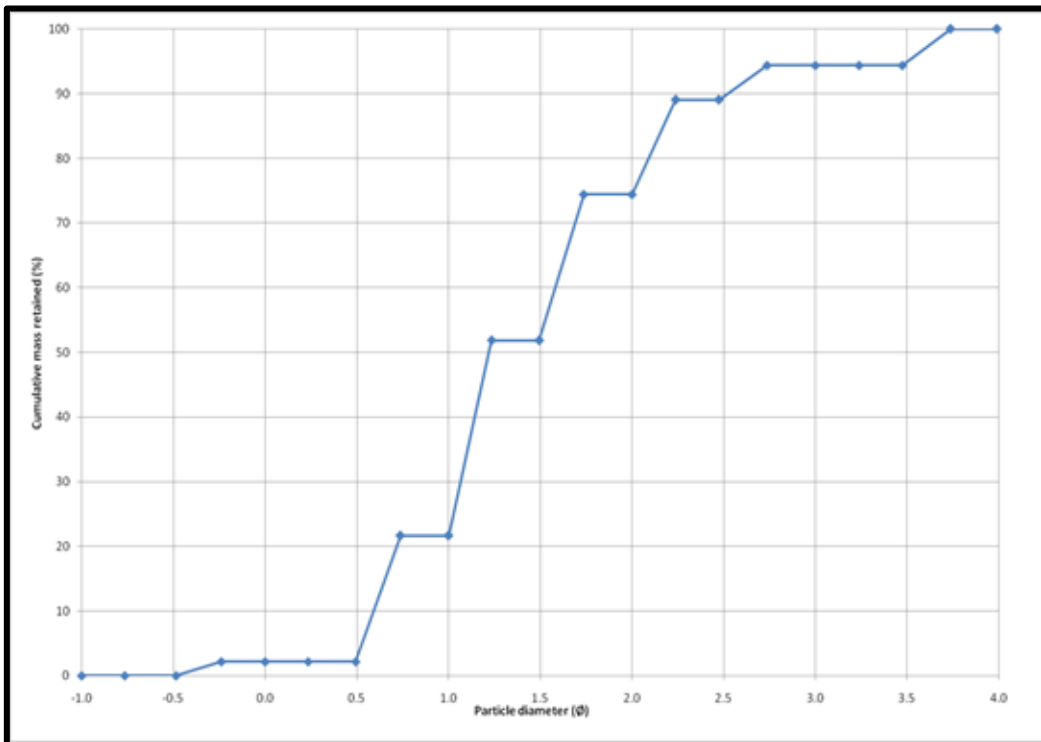


Fig. 4.47: Afor-Ukwu Gully Sample 2 Grain Size Cumulative mass Retained graph in phi

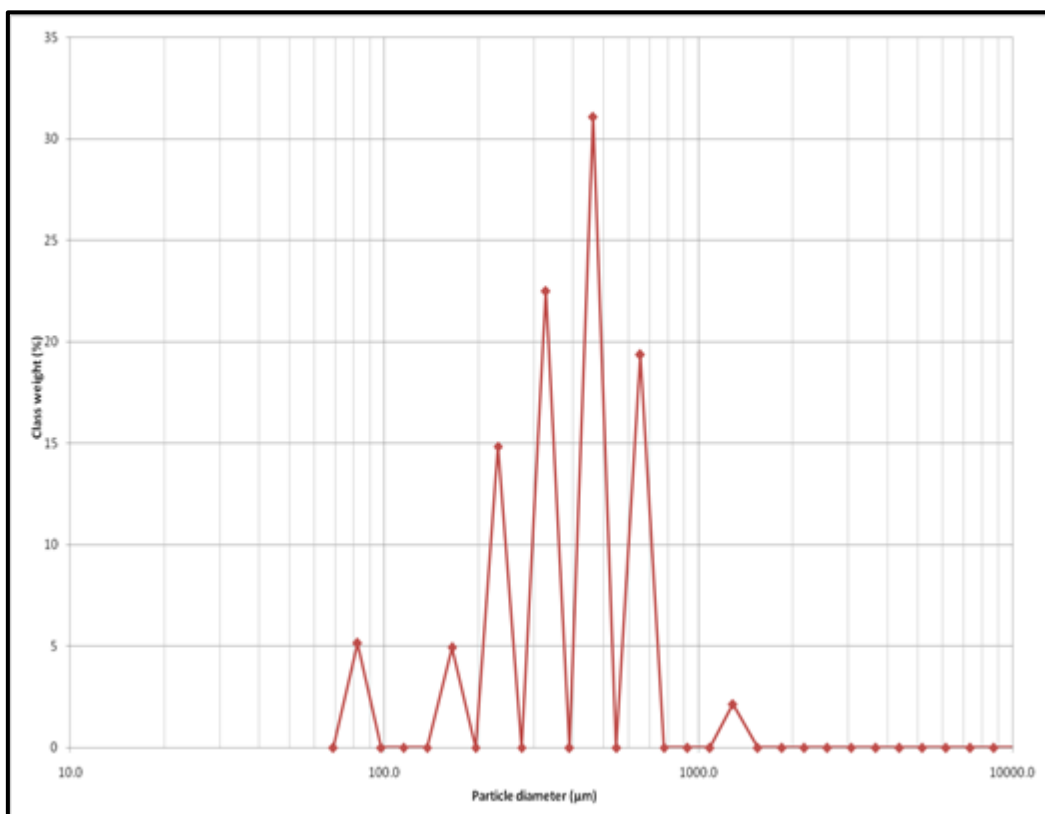


Fig. 4.48: Afor-Ukwu Gully Sample 2 class of weight graph in microns

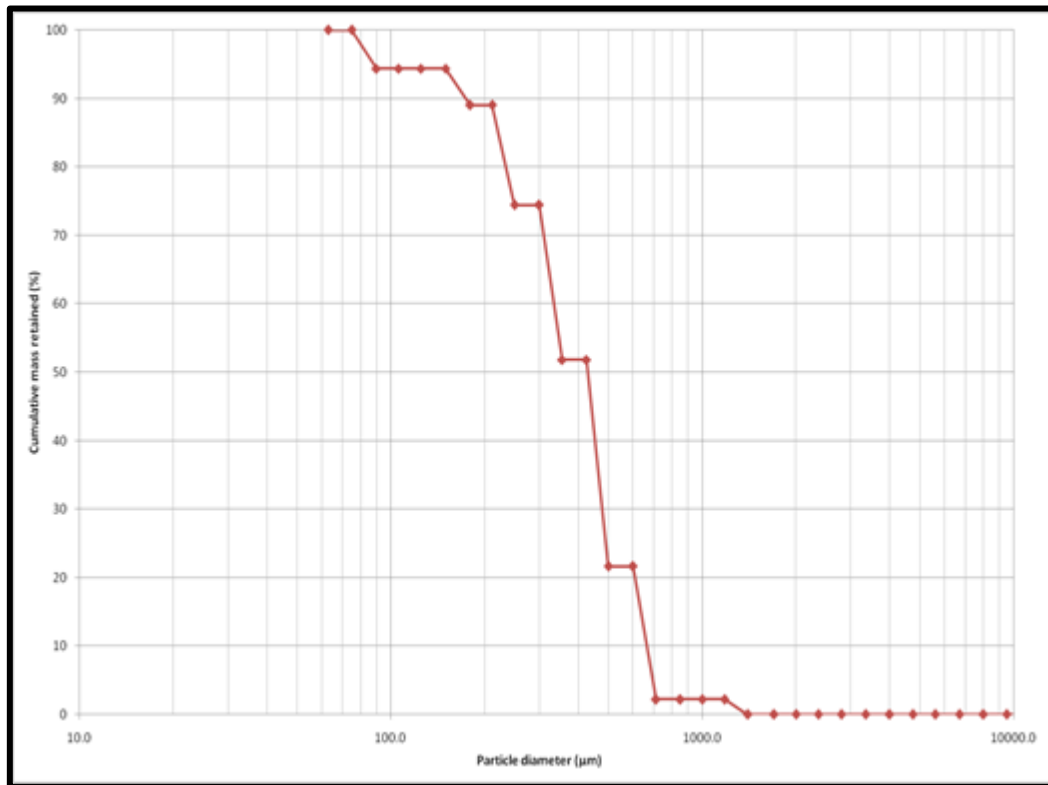


Fig. 4.49: Afor-Ukwu Gully Sample 1 cumulative mass retained graph in microns

Grain Size Distribution of Ihioma Gully Head

Table 4.12: Sample statistics table for Ihioma Gully Head

SAMPLE STATISTICS						
SAMPLE IDENTITY: Gully Head Ihioma Orlu			ANALYST & DATE: , 21/7/2014			
SAMPLE TYPE: Trimodal, Moderately Well Sorted			TEXTURAL GROUP: Sand			
SEDIMENT NAME: Moderately Well Sorted Medium Sand						
	µm	φ	GRAIN SIZE DISTRIBUTION			
MODE 1:	462.5	1.117	GRAVEL: 0.0%	COARSE SAND: 12.7%		
MODE 2:	327.5	1.616	SAND: 100.0%	MEDIUM SAND: 70.3%		
MODE 3:	655.0	0.616	MUD: 0.0%	FINE SAND: 9.8%		
D ₁₀ :	179.3	0.671		V FINE SAND: 6.5%		
MEDIAN or D ₅₀ :	441.9	1.178	V COARSE GRAVEL: 0.0%	V COARSE SILT: 0.0%		
D ₉₀ :	628.1	2.480	COARSE GRAVEL: 0.0%	COARSE SILT: 0.0%		
(D ₉₀ / D ₁₀):	3.503	3.695	MEDIUM GRAVEL: 0.0%	MEDIUM SILT: 0.0%		
(D ₉₀ - D ₁₀):	448.8	1.809	FINE GRAVEL: 0.0%	FINE SILT: 0.0%		
(D ₇₅ / D ₂₅):	1.500	1.554	V FINE GRAVEL: 0.0%	V FINE SILT: 0.0%		
(D ₇₅ - D ₂₅):	160.3	0.585	V COARSE SAND: 0.8%	CLAY: 0.0%		
	METHOD OF MOMENTS			FOLK & WARD METHOD		
	Arithmetic	Geometric	Logarithmic	Geometric	Logarithmic	Description
	µm	µm	φ	µm	φ	
MEAN(\bar{x}):	413.6	371.2	1.430	378.8	1.401	Medium Sand
SORTING (s):	165.9	1.671	0.741	1.622	0.698	Moderately Well Sorted
SKEWNESS (Sk):	0.796	-1.521	1.521	-0.630	0.630	Very Fine Skewed
KURTOSIS (K):	7.927	5.551	5.551	2.072	2.072	Very Leptokurtic

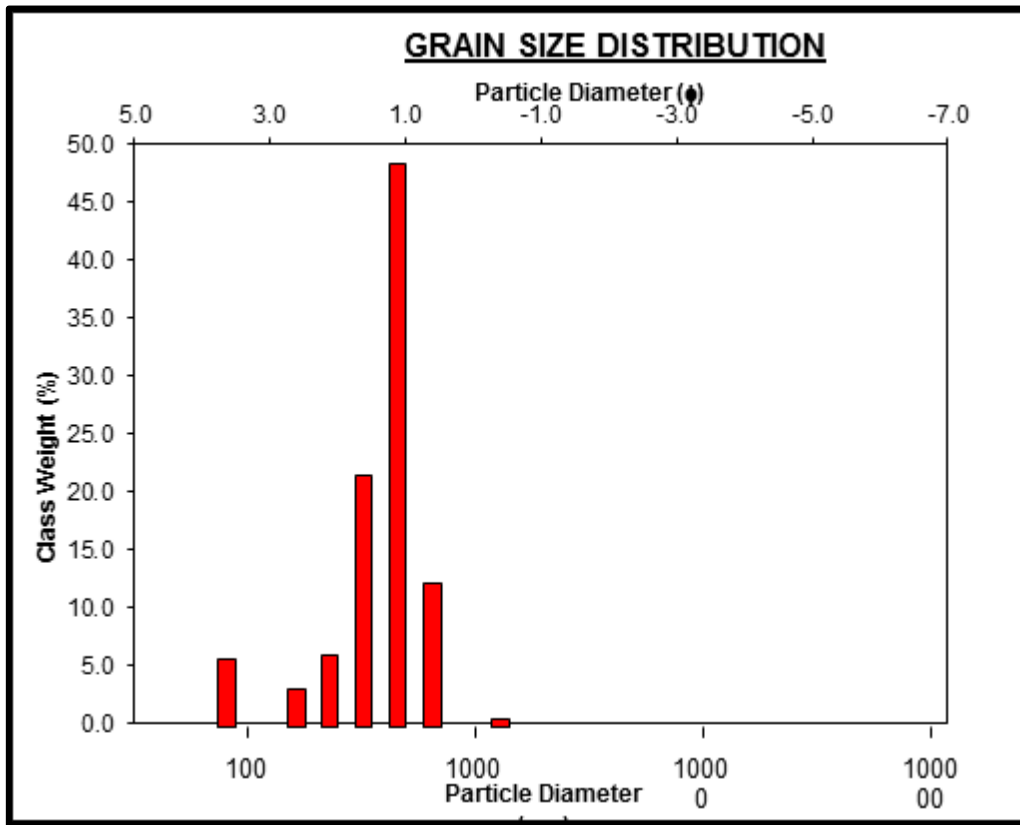


Fig. 4.50: Grain Size class of weight distribution chart for Ihoma Gully Head.

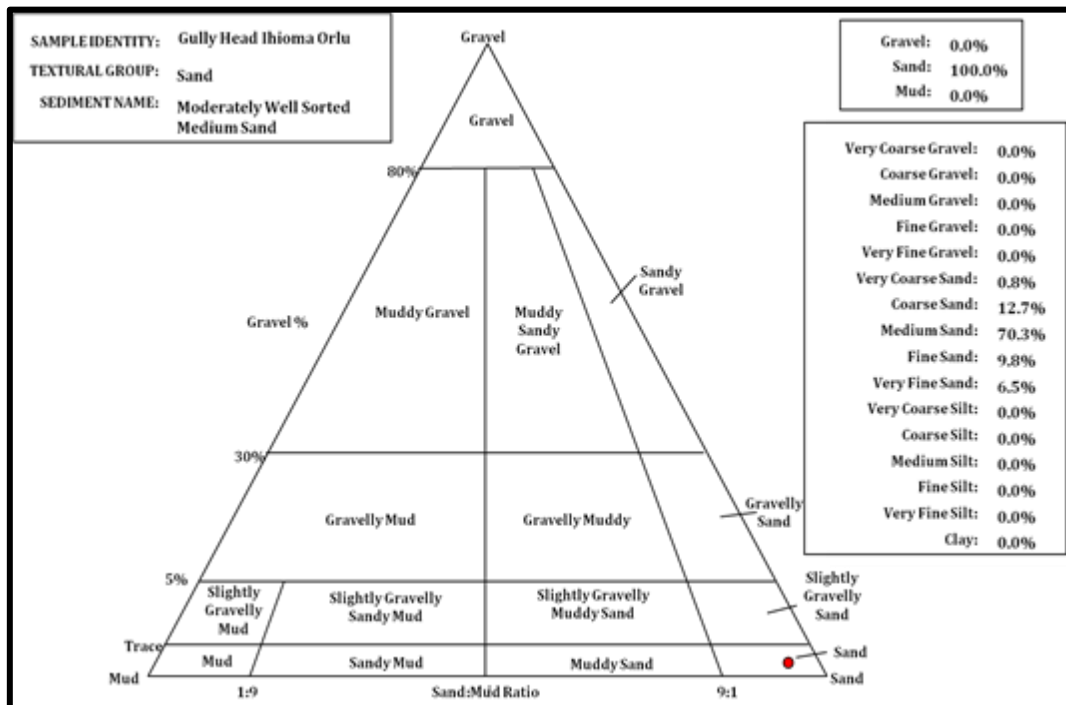


Fig. 4.51: Ternary chart of Ihoma Gully Head grain size distribution

Ihioma gully head sample shows that mud and gravel are 0% present, while sand is 100%. Furthermore, the sand in the area is trimodal, and contains moderately well sorted medium sand, very fine skewed and very leptokurtic. This makes the area easily prone to erosion in the presence of running water as a result of low compaction and no binding material. Table 4.12 and figure 4.51 above explained all these in detail.

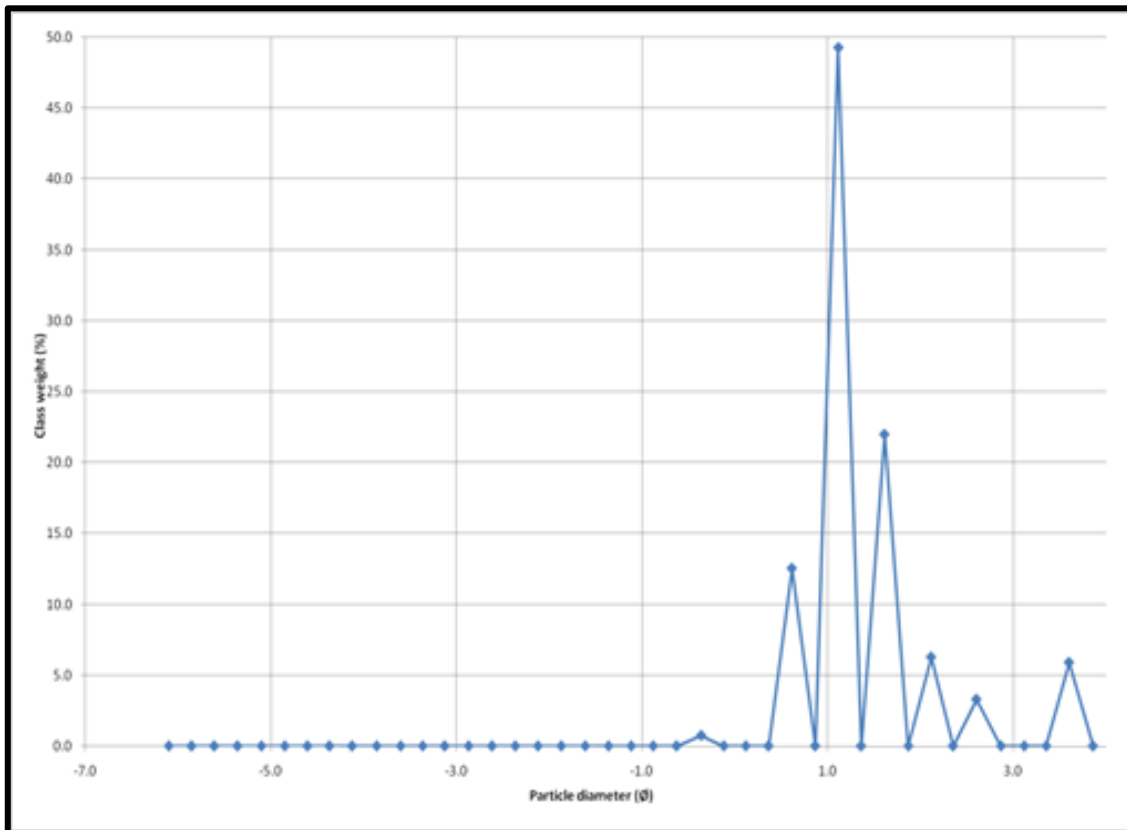


Fig. 4.52: Ihioma Gully Head Grain Size Distribution class of weight graph in phi

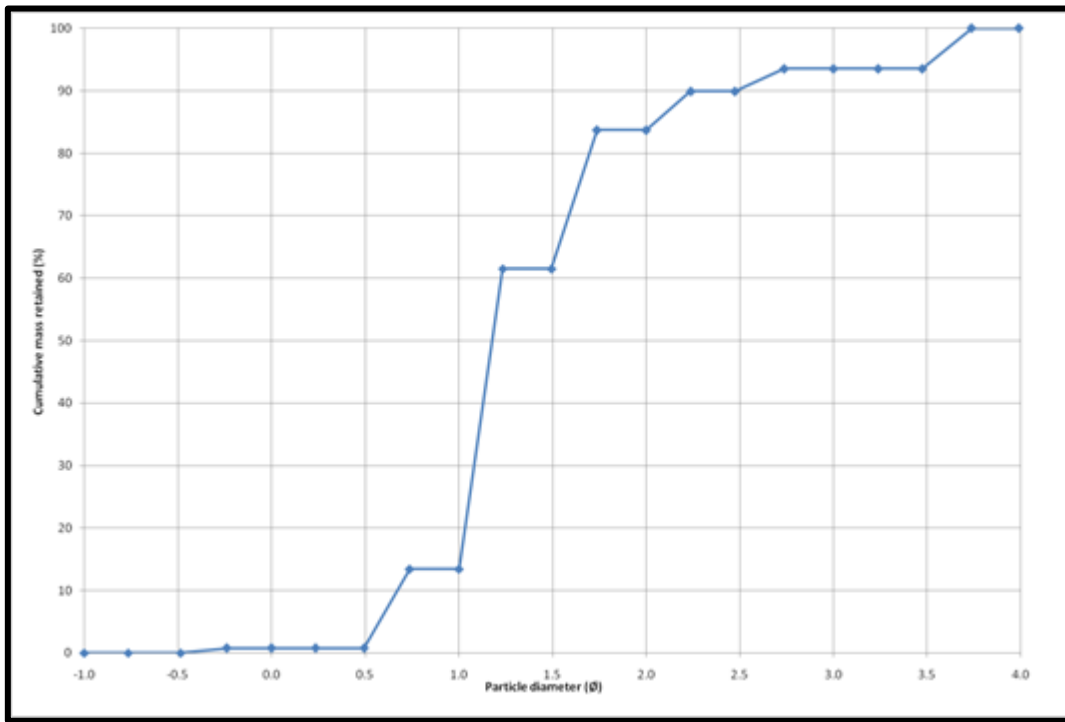


Fig. 4.53: Ihioma Gully Head Grain Size Cumulative mass Retained graph in phi

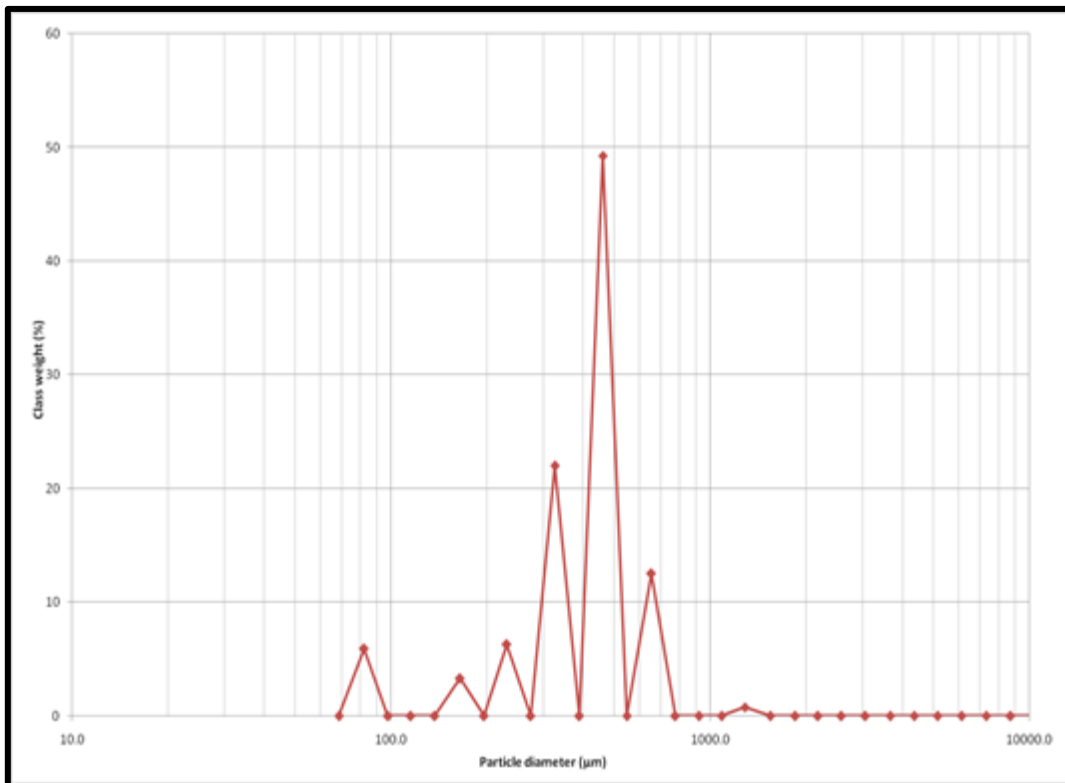


Fig. 4.54: Ihioma Gully Head class of weight graph in microns

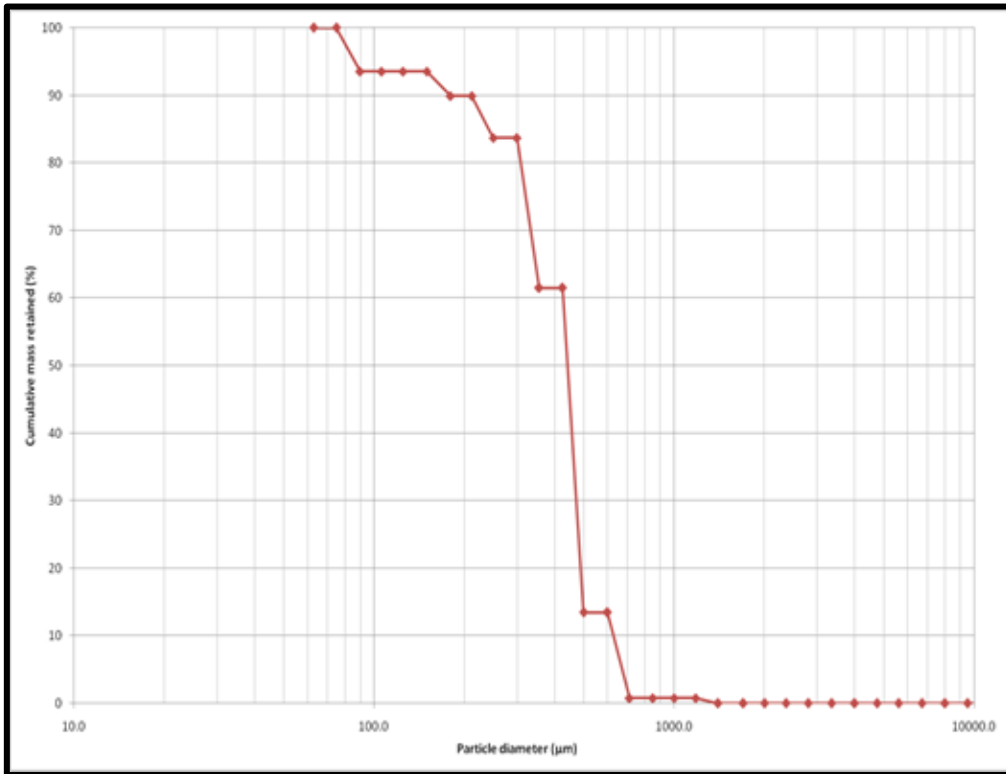


Fig. 4.55: Ihioma Gully Head cumulative mass retained graph in microns

Grain Size Distribution for Middle of Ihioma Gully

Table 4.13: Sample statistics table for Middle of Ihioma Gully

SAMPLE STATISTICS						
SAMPLE IDENTITY: Middle Gully Ihioma Orlu			ANALYST & DATE: , 21/7/2014			
SAMPLE TYPE: Polymodal, Moderately Sorted			TEXTURAL GROUP: Slightly Gravelly Sand			
SEDIMENT NAME: Slightly Very Fine Gravelly Medium Sand						
	μm	ϕ	GRAIN SIZE DISTRIBUTION			
MODE 1:	462.5	1.117	GRAVEL: 0.5%	COARSE SAND: 20.7%		
MODE 2:	327.5	1.616	SAND: 99.5%	MEDIUM SAND: 44.8%		
MODE 3:	231.0	2.119	MUD: 0.0%	FINE SAND: 21.7%		
D ₁₀ :	89.26	0.584		V FINE SAND: 10.5%		
MEDIAN or D ₅₀ :	348.8	1.520	V COARSE GRAVEL: 0.0%	V COARSE SILT: 0.0%		
D ₉₀ :	667.2	3.486	COARSE GRAVEL: 0.0%	COARSE SILT: 0.0%		
(D ₉₀ / D ₁₀):	7.474	5.970	MEDIUM GRAVEL: 0.0%	MEDIUM SILT: 0.0%		
(D ₉₀ - D ₁₀):	577.9	2.902	FINE GRAVEL: 0.0%	FINE SILT: 0.0%		
(D ₇₅ / D ₂₅):	2.154	2.087	V FINE GRAVEL: 0.5%	V FINE SILT: 0.0%		
(D ₇₅ - D ₂₅):	264.5	1.107	V COARSE SAND: 1.8%	CLAY: 0.0%		
	METHOD OF MOMENTS			FOLK & WARD METHOD		
	Arithmetic	Geometric	Logarithmic	Geometric	Logarithmic	Description
	μm	μm	ϕ	μm	ϕ	
MEAN(\bar{x}):	406.3	332.1	1.590	335.1	1.577	Medium Sand
SORTING (s):	271.6	1.940	0.956	1.923	0.943	Moderately Sorted
SKEWNESS (Sk):	3.202	-0.541	0.541	-0.223	0.223	Fine Skewed
KURTOSIS (K):	23.98	3.212	3.212	1.142	1.142	Leptokurtic

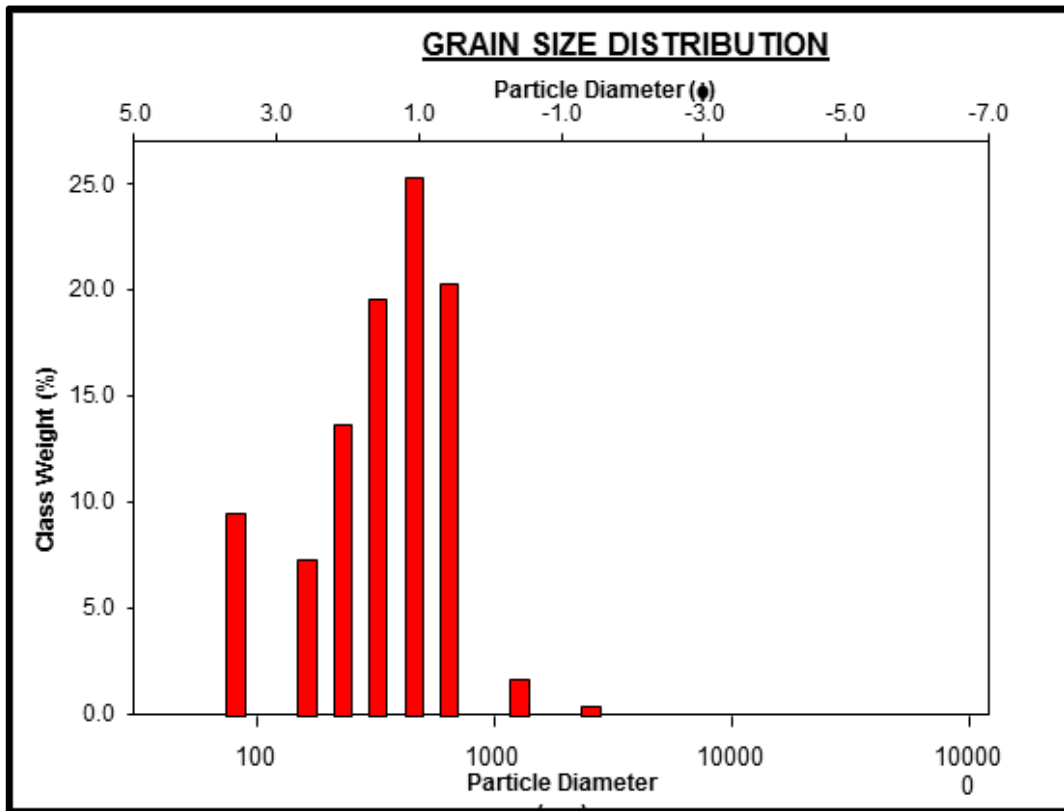


Fig. 4.56: Grain Size class of weight distribution chart for Middle of Ihioma Gully.

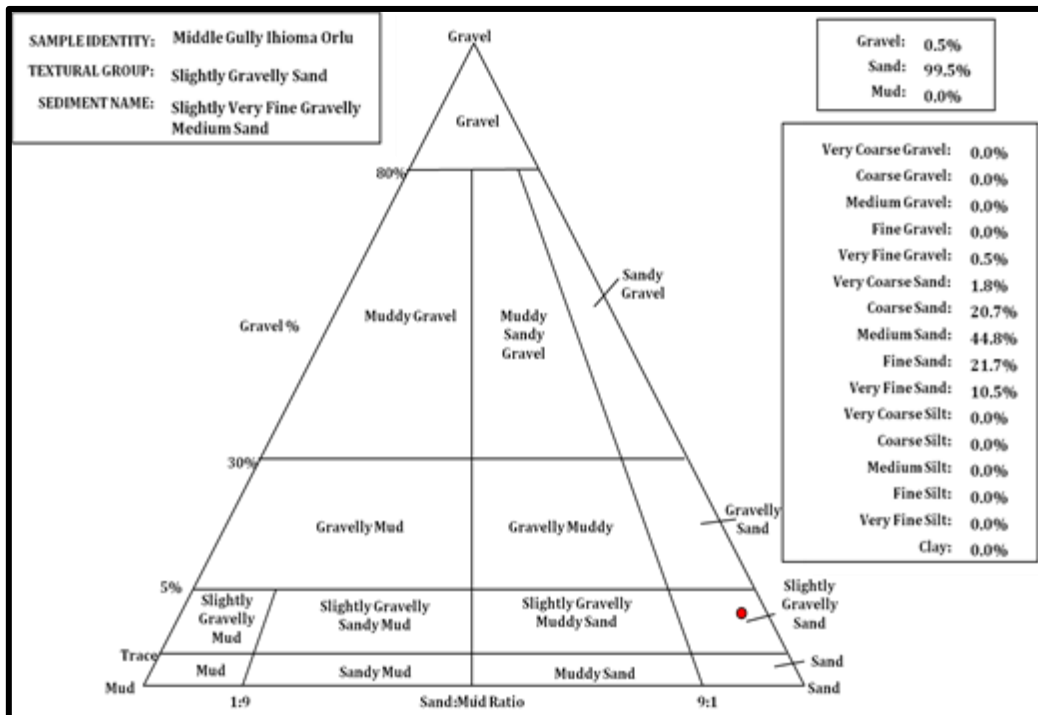


Fig. 4.57: Ternary chart of Middle of Ihioma Gully grain size distribution

Middle of Ihioma gully Sample shows that gravel is 0.5%, mud is 0% and sand is 99.5%. It is polymodal, moderately sorted; fine skewed and leptokurtic as seen in the result presented in Table 4.13 and figure 4.57 above.

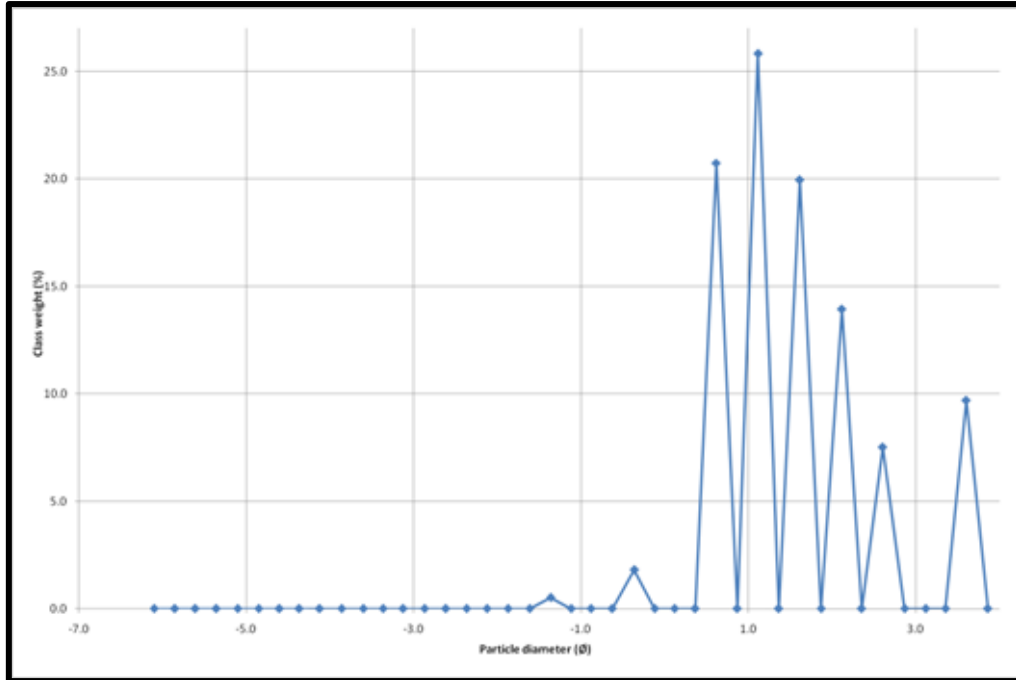


Fig. 4.58: Middle of Ihioma Gully Grain Size Distribution class of weight graph in phi

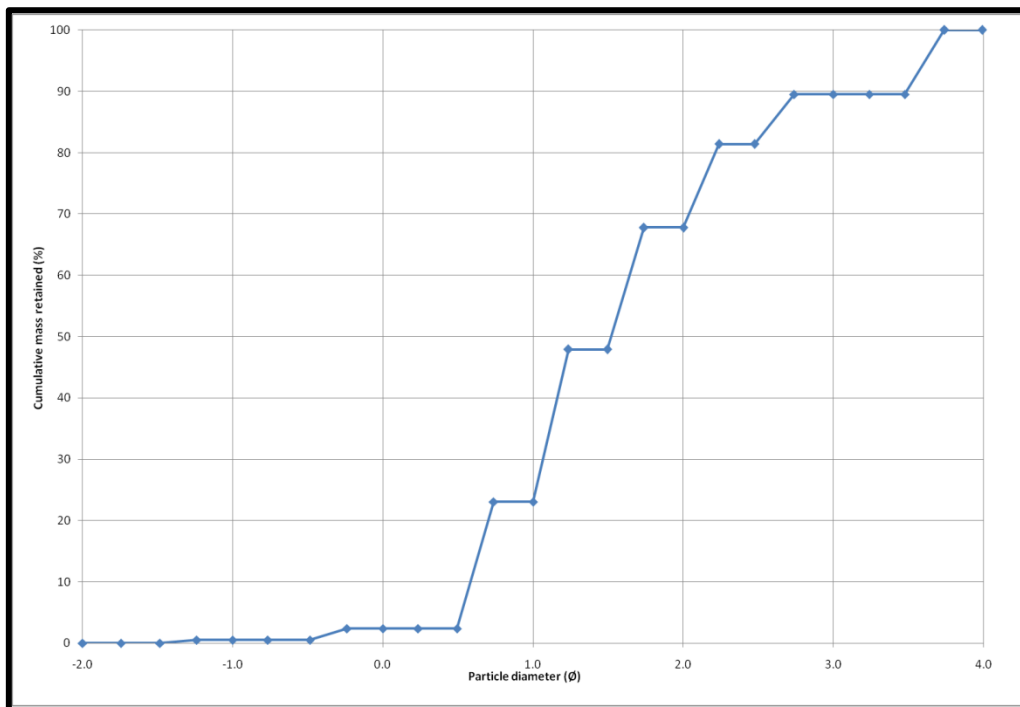


Fig. 4.59: Middle of Ihioma Gully Grain Size Cumulative mass Retained graph in phi

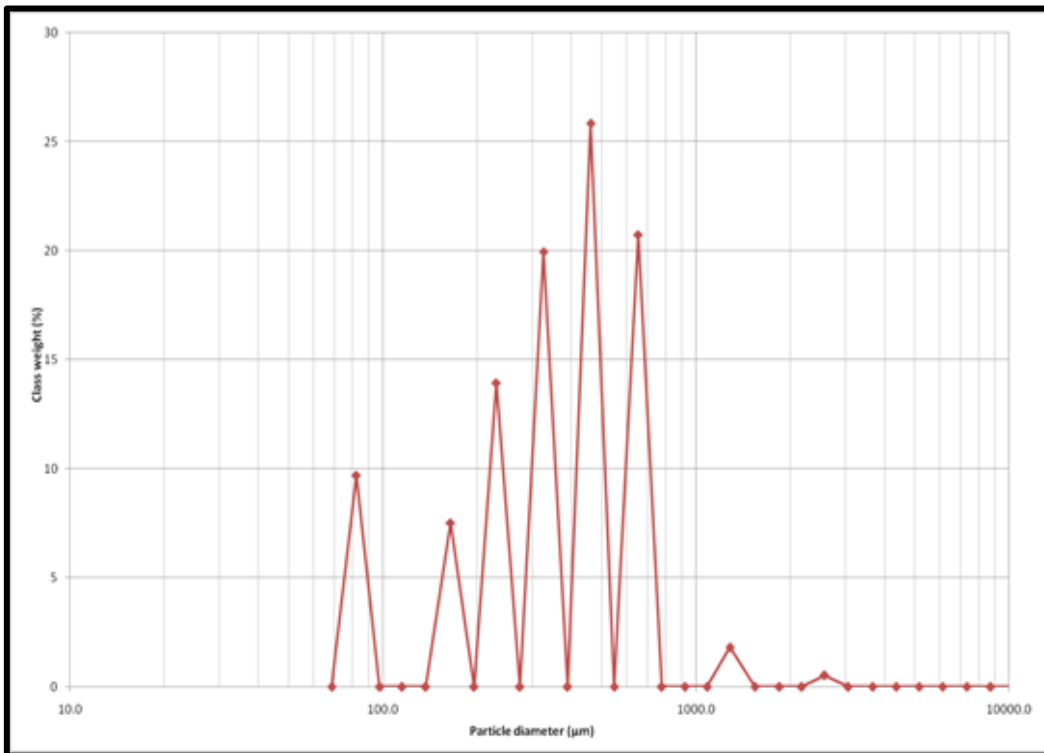


Fig. 4.60: Middle of Ihioma Gully class of weight graph in microns

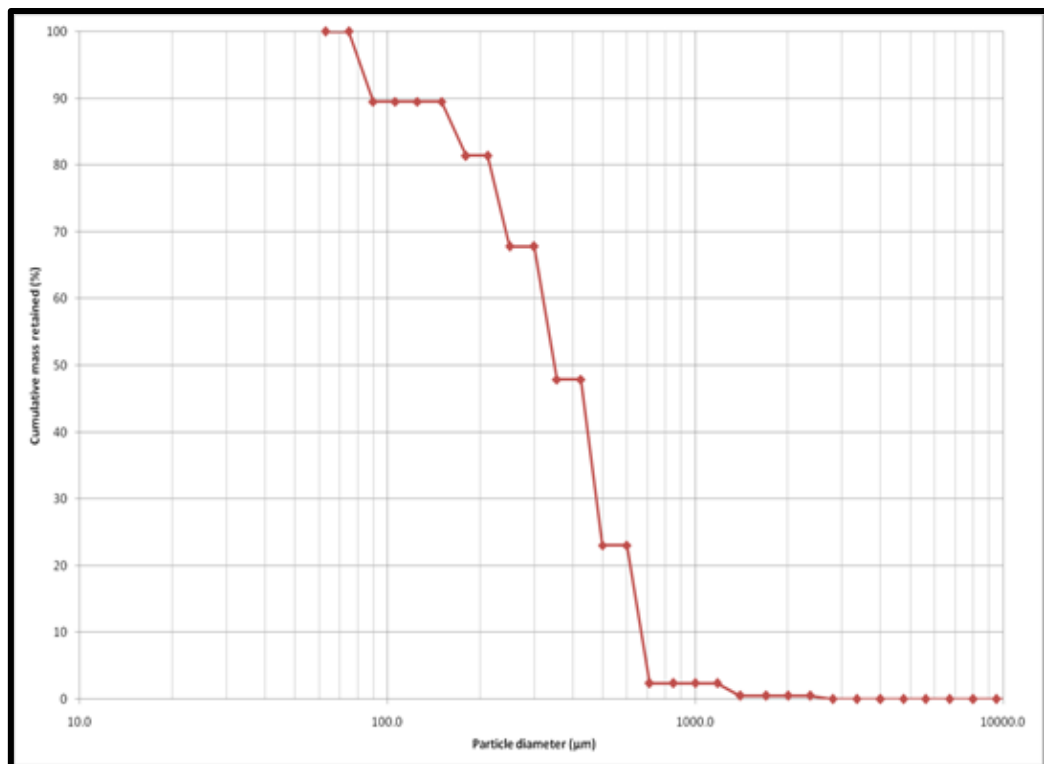


Fig. 4.61: Middle of Ihioma Gully cumulative mass retained graph in microns

Grain Size Distribution of Njaba Gully Sample 1

Table 4.14: Sample statistics table for Njaba gully Sample 1

SAMPLE STATISTICS						
SAMPLE IDENTITY: Njaba Gully Sample 1			ANALYST & DATE: , 18/7/2014			
SAMPLE TYPE: Polymodal, Moderately Sorted			TEXTURAL GROUP: Slightly Gravelly Sand			
SEDIMENT NAME: Slightly Very Fine Gravelly Medium Sand						
	μm	ϕ	GRAIN SIZE DISTRIBUTION			
MODE 1:	655.0	0.616	GRAVEL: 0.5%		COARSE SAND: 32.2%	
MODE 2:	462.5	1.117	SAND: 99.5%		MEDIUM SAND: 42.3%	
MODE 3:	327.5	1.616	MUD: 0.0%		FINE SAND: 13.2%	
D_{10} :	225.4	0.502			V FINE SAND: 3.3%	
MEDIAN or D_{50} :	473.3	1.079	V COARSE GRAVEL: 0.0%		V COARSE SILT: 0.0%	
D_{90} :	706.2	2.150	COARSE GRAVEL: 0.0%		COARSE SILT: 0.0%	
(D_{90} / D_{10}) :	3.134	4.284	MEDIUM GRAVEL: 0.0%		MEDIUM SILT: 0.0%	
$(D_{90} - D_{10})$:	480.9	1.648	FINE GRAVEL: 0.0%		FINE SILT: 0.0%	
(D_{75} / D_{25}) :	1.992	2.616	V FINE GRAVEL: 0.5%		V FINE SILT: 0.0%	
$(D_{75} - D_{25})$:	325.1	0.994	V COARSE SAND: 8.5%		CLAY: 0.0%	
	METHOD OF MOMENTS			FOLK & WARD METHOD		
	Arithmetic	Geometric	Logarithmic	Geometric	Logarithmic	Description
	μm	μm	ϕ	μm	ϕ	
MEAN (\bar{x}):	538.0	457.8	1.127	431.4	1.213	Medium Sand
SORTING (s):	318.6	1.792	0.842	1.754	0.811	Moderately Sorted
SKEWNESS (Sk):	2.095	-0.534	0.534	-0.148	0.148	Fine Skewed
KURTOSIS (K):	10.94	4.219	4.219	1.210	1.210	Leptokurtic

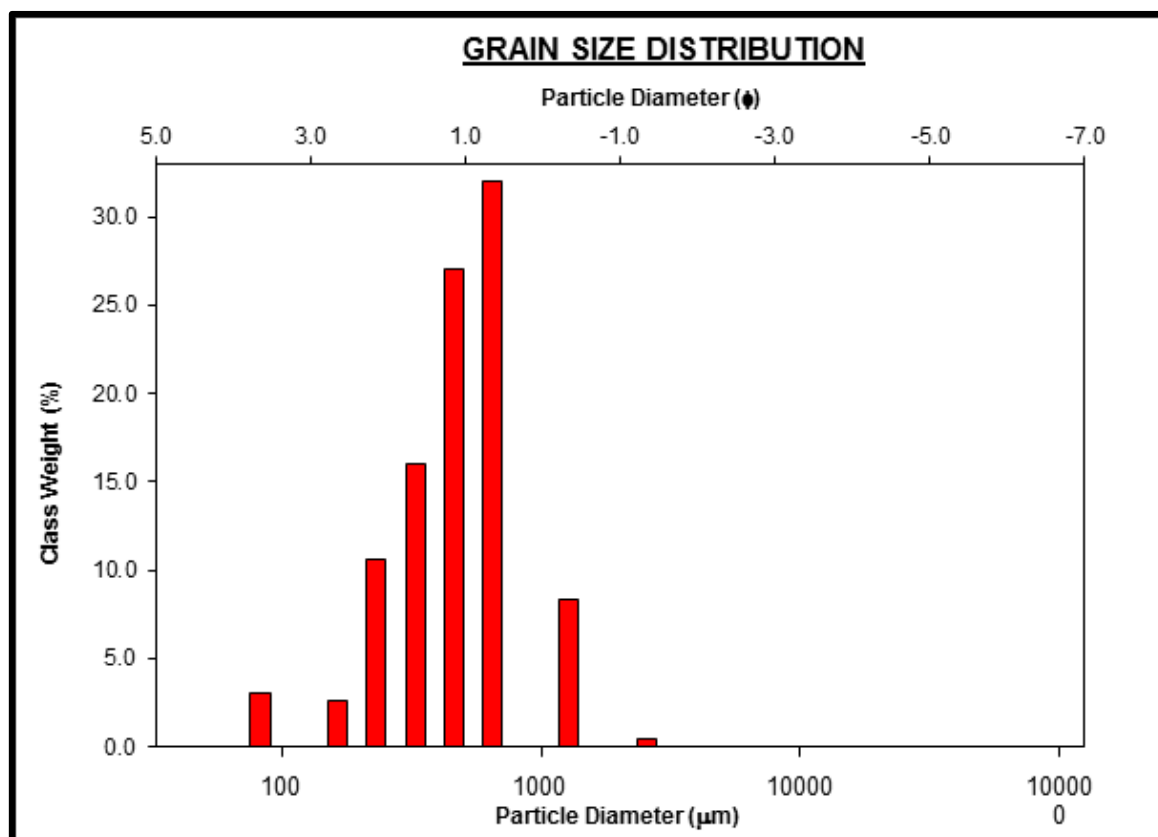


Fig. 4.62: Grain Size class of weight distribution chart of Njaba Gully sample 1.

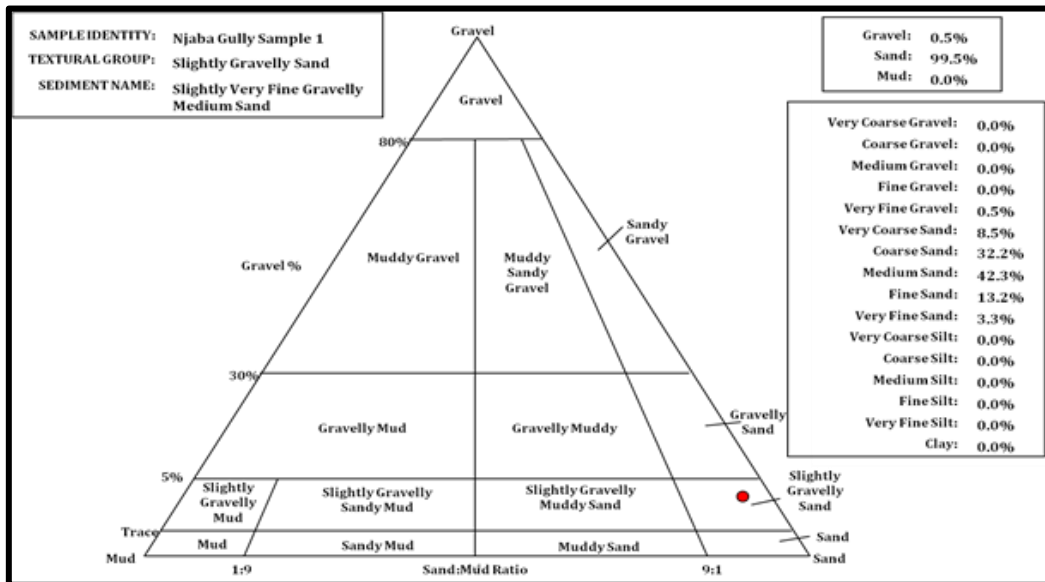


Fig. 4.63: Ternary chart of Njaba Gully sample 1 grain size distribution

Njaba gully sample 1 analysis shows no significant change as compared to the result of middle Ihioma gully sample. At Njaba gully sample 1, gravel is 0.5%, mud is 0% and sand is 99.5%. The soil is polymodal and contains slightly very fine gravel, moderately sorted; fine skewed and leptokurtic as seen in the analysis presented seen in Table 4.14 and figure 4.63 above.

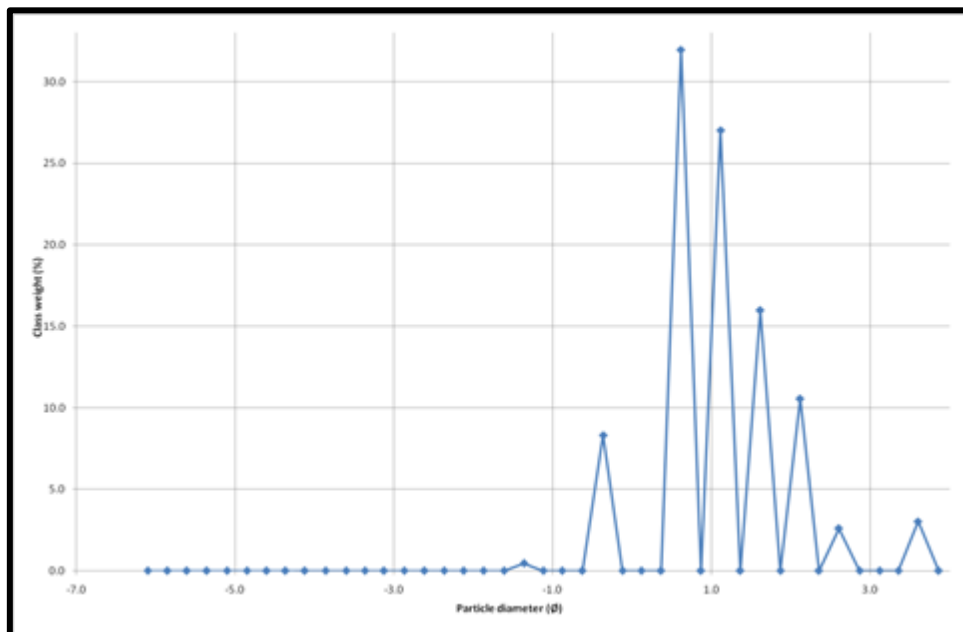


Fig. 4.64: Njaba Gully Sample 1 Grain Size Distribution class of weight graph in phi

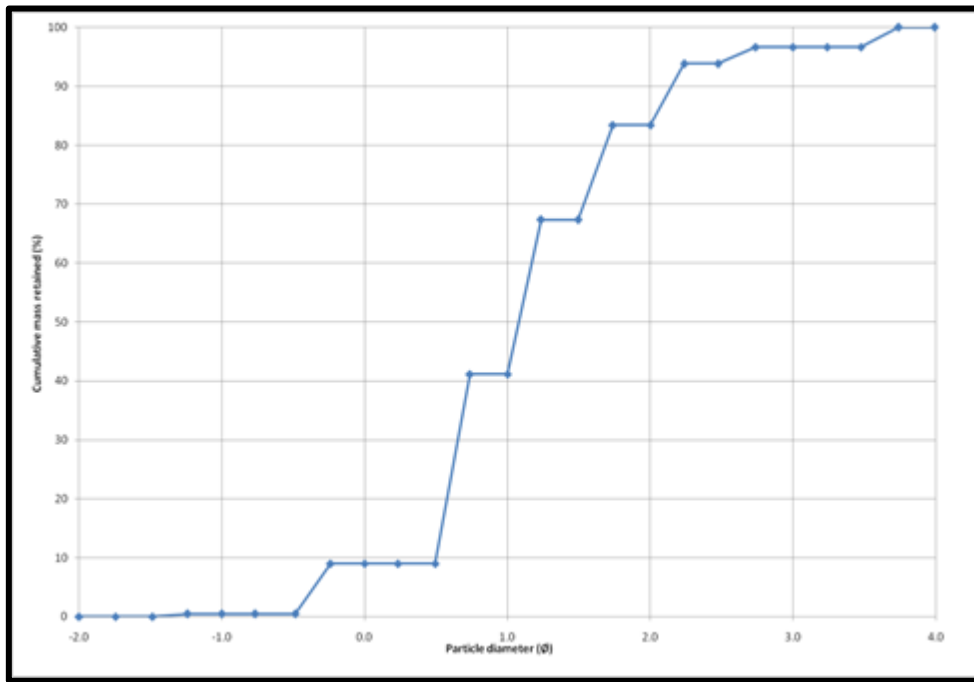


Fig. 4.65: Njaba Gully Sample 1 Grain Size Cumulative mass Retained graph in phi

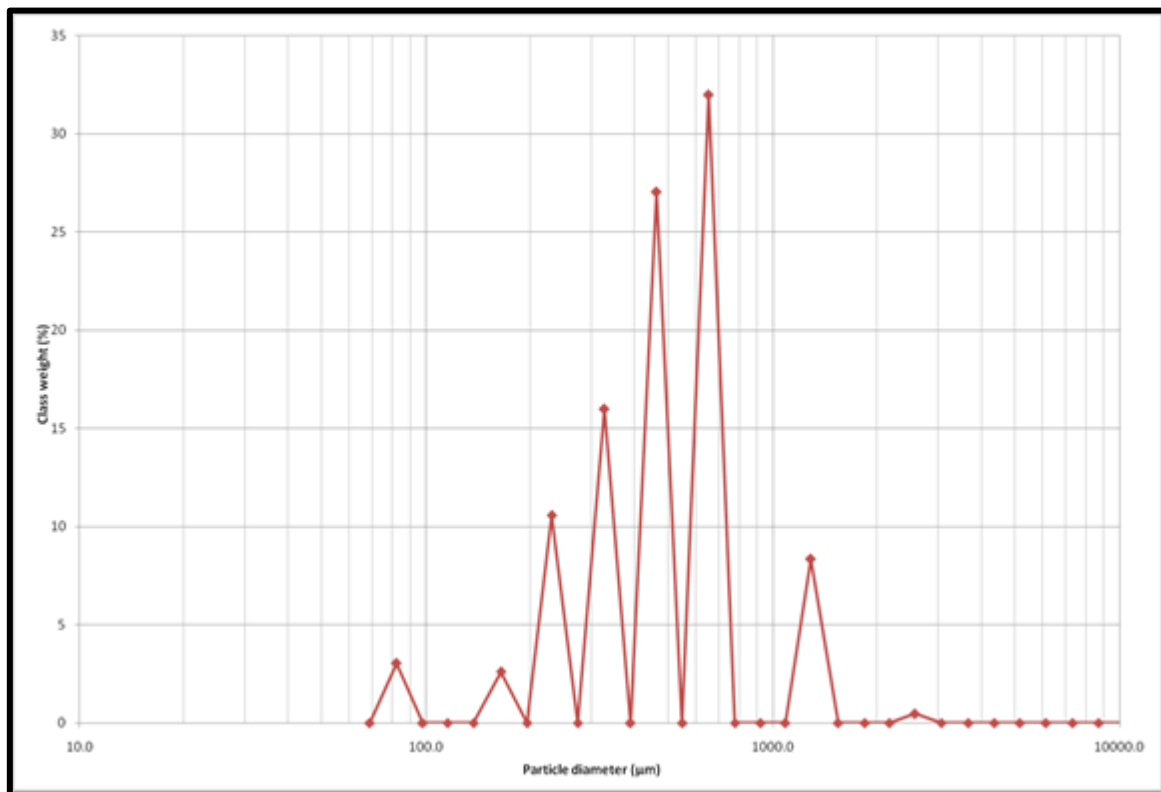


Fig. 4.66: Njaba Gully Sample 1 class of weight graph in microns

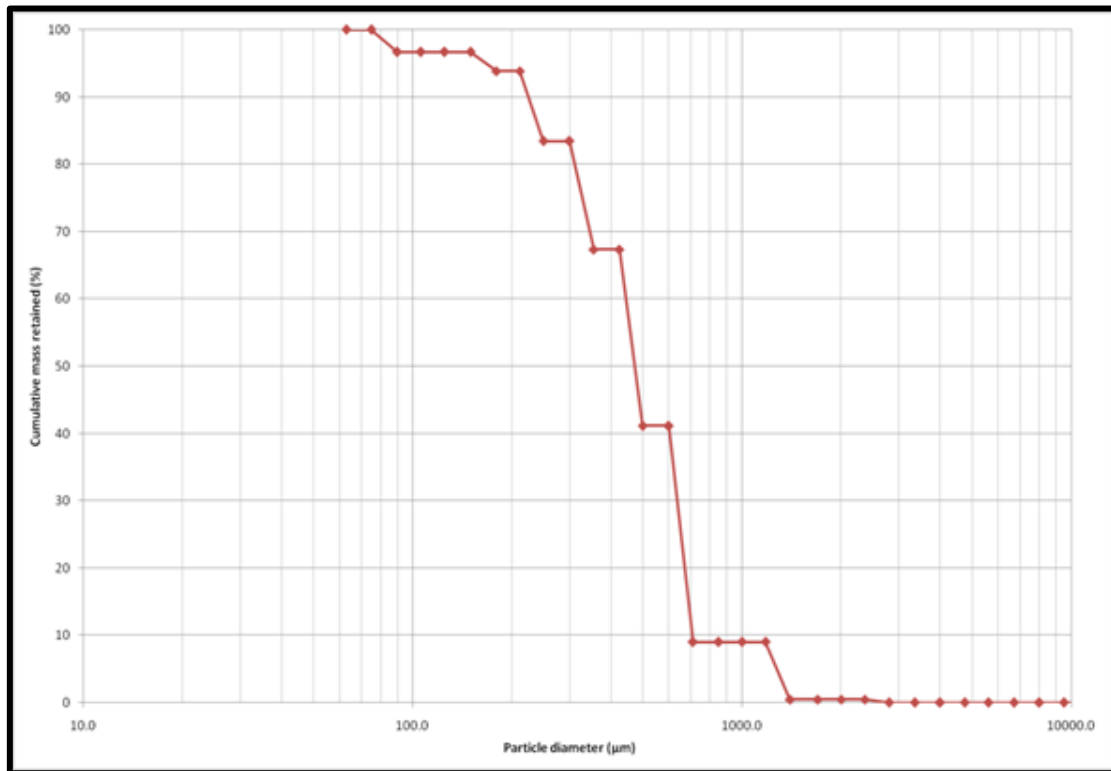


Fig. 4.67: Njaba Gully Sample 1 cumulative mass retained graph in microns

Grain Size Distribution of Njaba Gully Sample 2

Table 4.15: Sample statistics table of Njaba gully Sample 2

SAMPLE STATISTICS						
SAMPLE IDENTITY: Njaba Gully Sample 2			ANALYST & DATE: , 18/7/2014			
SAMPLE TYPE: Polymodal, Moderately Sorted			TEXTURAL GROUP: Slightly Gravelly Sand			
SEDIMENT NAME: Slightly Very Fine Gravelly Medium Sand						
	μm	ϕ	GRAIN SIZE DISTRIBUTION			
MODE 1:	655.0	0.616	GRAVEL: 0.2%	COARSE SAND: 30.1%		
MODE 2:	462.5	1.117	SAND: 99.8%	MEDIUM SAND: 43.8%		
MODE 3:	327.5	1.616	MUD: 0.0%	FINE SAND: 14.2%		
D ₁₀ :	220.8	0.507		V FINE SAND: 3.5%		
MEDIAN or D ₅₀ :	467.0	1.098	V COARSE GRAVEL: 0.0%	V COARSE SILT: 0.0%		
D ₉₀ :	703.6	2.179	COARSE GRAVEL: 0.0%	COARSE SILT: 0.0%		
(D ₉₀ / D ₁₀):	3.186	4.297	MEDIUM GRAVEL: 0.0%	MEDIUM SILT: 0.0%		
(D ₉₀ - D ₁₀):	482.8	1.672	FINE GRAVEL: 0.0%	FINE SILT: 0.0%		
(D ₇₅ / D ₂₅):	2.000	2.592	V FINE GRAVEL: 0.2%	V FINE SILT: 0.0%		
(D ₇₅ - D ₂₅):	323.5	1.000	V COARSE SAND: 8.2%	CLAY: 0.0%		
	METHOD OF MOMENTS			FOLK & WARD METHOD		
	Arithmetic	Geometric	Logarithmic	Geometric	Logarithmic	Description
	μm	μm	ϕ	μm	ϕ	
MEAN(\bar{x}):	522.0	444.4	1.170	426.0	1.231	Medium Sand
SORTING (s):	301.6	1.796	0.845	1.768	0.822	Moderately Sorted
SKEWNESS (Sk):	1.802	-0.567	0.567	-0.151	0.151	Fine Skewed
KURTOSIS (K):	8.851	4.051	4.051	1.220	1.220	Leptokurtic

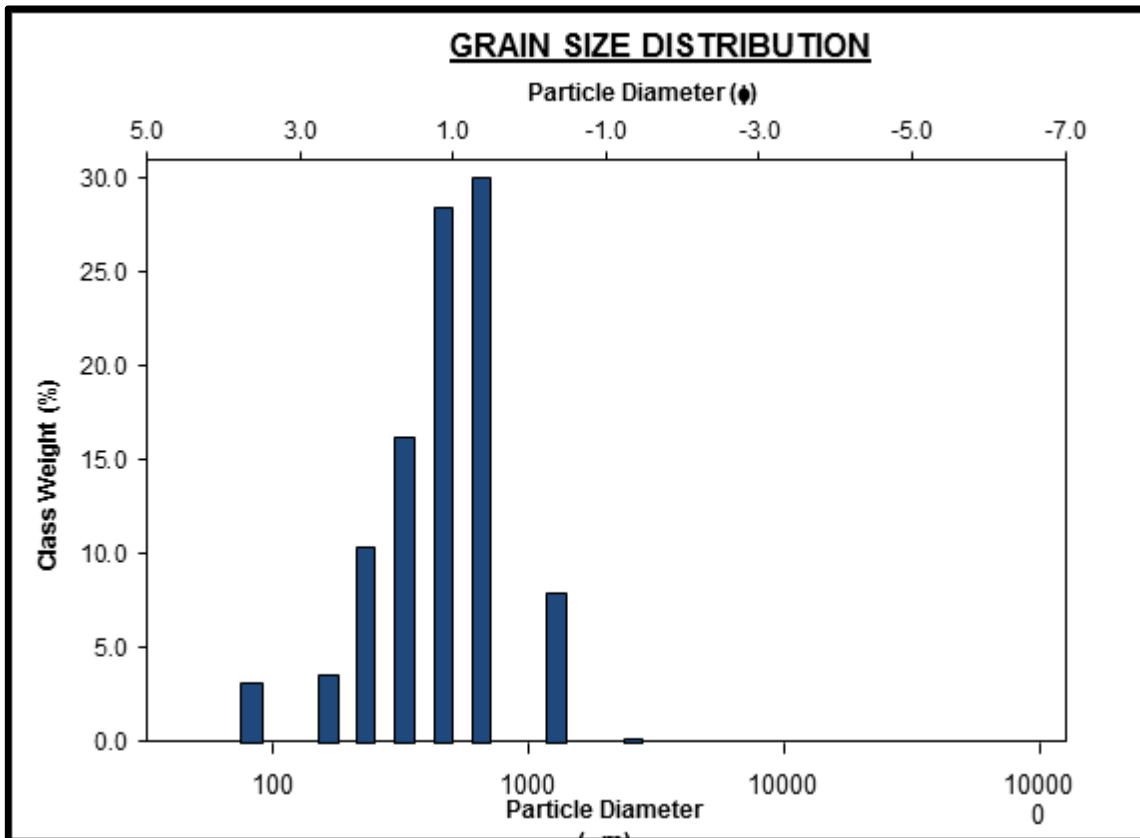


Fig. 4.68: Grain Size class of weight distribution chart for Njaba gully sample 2.

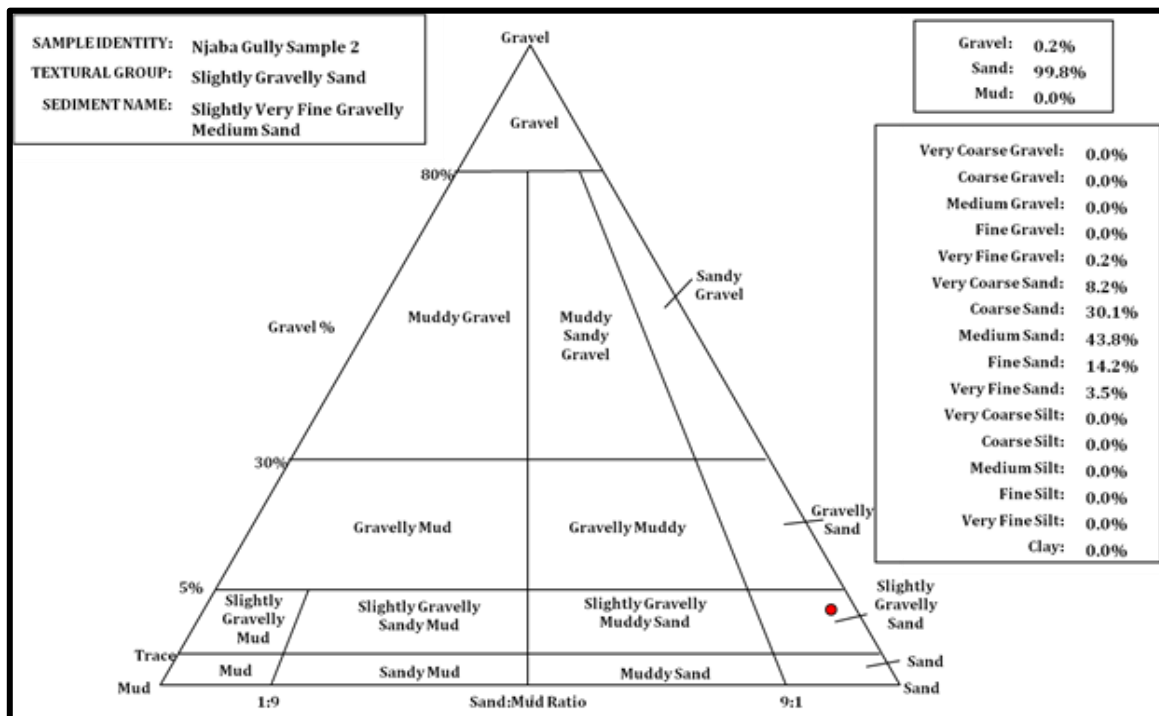


Fig. 4.69: Ternary diagram of Njaba Gully sample 2 grain size distribution

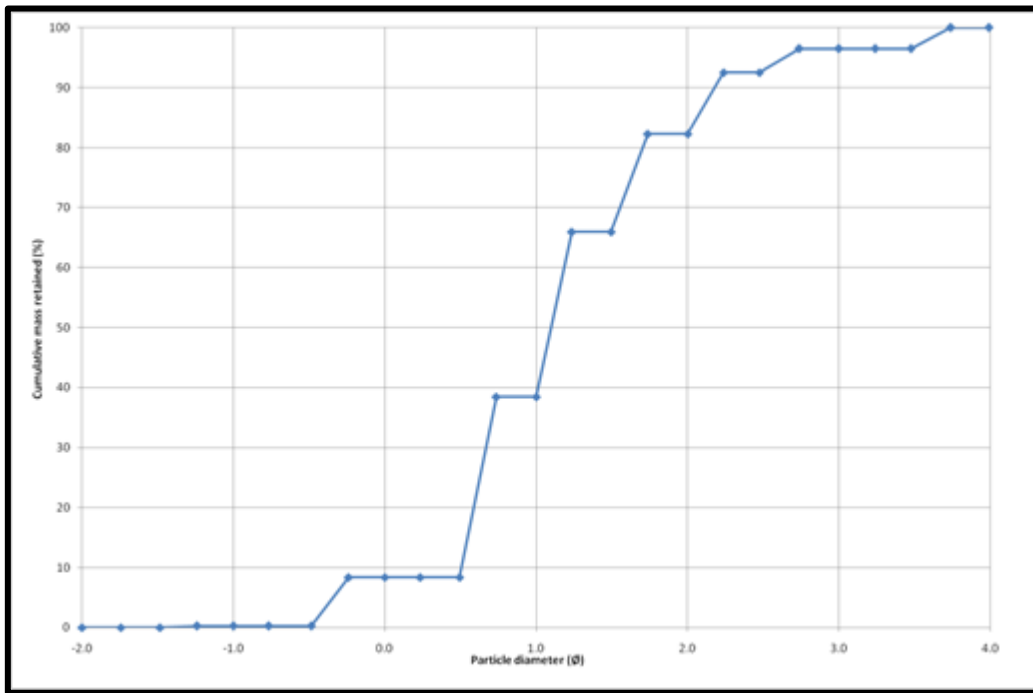


Fig. 4.70: Njaba Gully Sample 2 Grain Size Cumulative mass Retained graph in phi

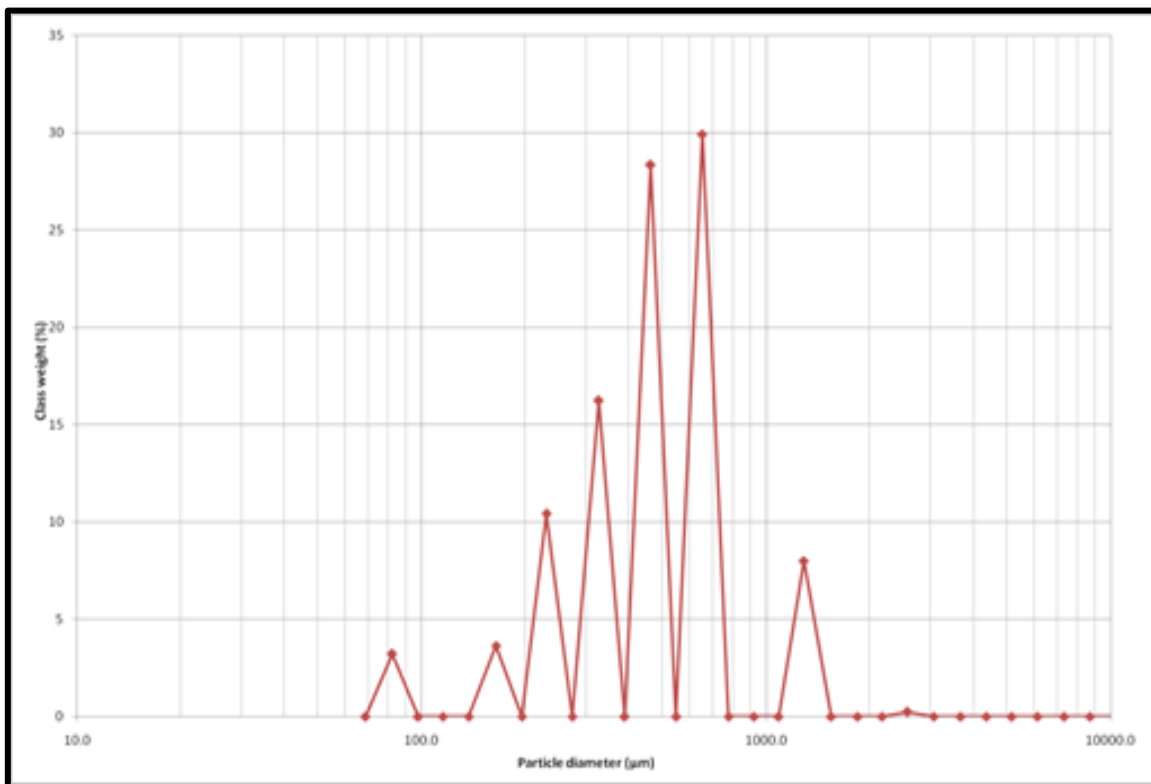


Fig. 4.71: Njaba Gully Sample 2 class of weight graph in microns

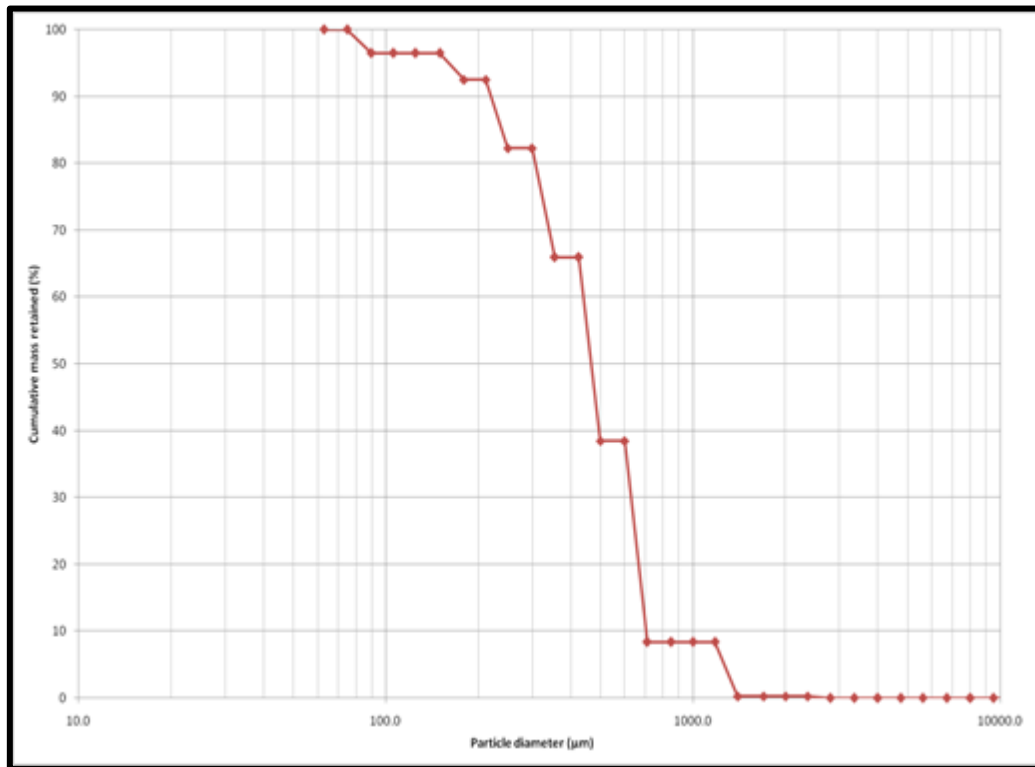


Fig. 4.72: Njaba Gully Sample 2 cumulative mass retained graph in microns

Njaba gully sample 2 and Sample 1 have almost the same result but just very slight difference in gravel and sand contents. Sample 1 has gravel content of 0.5% and sand content of 99.5% while sample 2 has 0.2% gravel and 99.8% sand. Just as in sample 1, sample 2 has 0% mud. The soil is polymodal and contains slightly very fine gravel, moderately sorted; fine skewed and leptokurtic as seen in the analysis presented seen in Table 4.15 and figure 4.69 above

4.2 DISCUSSION OF RESULTS

Since the primary objective of this study is to identify structures expressed as lineaments and classify them according to their spatial and directional attributes, it was necessary to process the Landsat -ETM data in a manner that would both enhance trends and facilitate the computation of locations and depths. Drainage pattern, termination of drainage line on linear trends and straight stream segments were some of the basic hypothetical models used to map

fractures. O'Leary et al. (1976) defines lineaments as a mappable, simple or composite linear feature of a surface whose parts are aligned in a rectilinear or slightly curvilinear relationship and which differ from the pattern of adjacent features and presumably reflects some subsurface phenomenon. The Landsat lineament map (fig.4.2) revealed the existence of lineaments around Orlu and environs. Similarly, lineament density and the filtered maps show heavy concentration of lineaments around the areas mentioned. This implies that the basement around the study area has suffered serious deformation. The last major tectonic event in the study area was the Pan African orogeny (650 Ma). It produced geological structures trending NE-SW; some of the interpreted lineaments bear this strike while some deviate from it. The study area has been affected by the many sedimentary phases (Short and Stauble, 1967; Murat, 1972). The first phase produced two principal sets of faults trending NE-SW and NW-SE directions which are also visible in the azimuthal plots of the study area (Orlu and environs) and the azimuth frequency diagram of the study area as well gotten from landsat imagery. It is worthy to note that the initial rifting of the Southern Nigeria Continental Margin in the Mesozoic Era produced two principal sets of faults trending NE-SW and NW-SE. The NE-SW fault bound the Benue Trough, while the NW-SE faults define the Calabar Flank and Niger Delta (Zarboski, 1998). According to Uzuakpunwa (1974), the NE-SW trending Abakaliki-Benue trough is thought to be the result of a pre-Albian rifting of the African shield prior to the opening of the South Atlantic. Linear structures running NE-SW observed from the study are suggested as the continental extension of the known pre Cretaceous oceanic fracture zones viz Charcot and Chain fracture zones (Ananaba, 1991; Burke et al 1971; 1972) which run along the trough axis beneath the sedimentary cover. The DEM (fig. 4.0) reveal the presence of a topographic high interpreted as sandstone ridge suspected to be the Awka-Orlu cuesta. The presence of lineaments around the Orlu area revealed that the erosion is structurally and lithologically controlled. It is possible that the

fault traces have provided a migration pathway for the top soil. This suggests that the rivers within the area are structurally controlled as well.

The azimuths of the major axes of the anisotropy diagrams above correlate significantly with the trends of the gullies within the area. The coefficient of anisotropy obtained from the survey varies from 1.17 to 1.58, indicating that structural in-homogeneities exist. The evidence from the acquired geophysical data indicates and the azimuthal plots show that the directions of gullies within the area are poly-directional in most cases just as seen in the azimuth frequency (rose) diagram. This suggests a juxtaposition of sediments of different degrees of saturation and resistance to shear and probably separated by a fractured region which may be a fault. The early cretaceous tectonic movement in the sedimentary basin of Southeastern Nigeria guided a major marine transgression across the continent and later determined the course of the Niger and Benue Rivers and probably had tremendous influence on gulling and erosion (Hospers, 1965). Consistent NE-SW, NW-SE, N-S orientation of maximum axes of electrical anisotropy and the form of the gully and its orientation which coincides with the regional geologic trend, narrow down wide range of other possible causes and have led to the speculation that the gully is structurally controlled and may indeed be running along the geologic contact between the Benin Formation and the Ameki Formation. This conclusion however has supporting evidences from remote sensing data (Azimuth frequency Diagram) and geotechnical work carried out in the area and thus this study sets out to narrow exploration target on the causes of the gulling and erosion in this area.

A combination of the interpreted sounding results together with information from lithological logs of existing boreholes in the study area were used to arrive at the conclusions that the top of the geoelectric sections (fig.4.37) constitute the lateritic overburden. The upper segment of this overburden contains laterite while the immediate lower segment of this overburden is made up of coarse (reddish) sand. The lower layers of the geoelectric sections whose

composition according to the lithological logs is mainly medium to coarse grained and white sand with relatively no clay identified. The resistivity varies from place to place but lies within the range of 65 – 44,800 ohm-m. The resistivity values indicated clean non saline groundwater.

Geo-electric sections of stratified layers which is deduced from electrical (resistivity) depth probing, where layers are identified by their apparent resistivities, in figures 4.37, shows variations in the apparent resistivity values of layers of different stations. The values of all the first layers of the entire stations did not coincide with each other as there are pronounced variations. This is also observed in the preceding layers of the entire stations, either in ascending or descending order to confirm the heterogeneity of the earth irrespective of being situated within the same geographical location. These differences in resistivities, shows areas with high pores to allow high rate of water penetrations and areas with minimal pores to permit water percolation or reduce the rate of penetrations. Areas with more retentive ability for fluids (waters) are suggested to have less resistive ability as conducting minerals may dissolve in them to aid conductivity or reduce resistivity. These areas with high resistivity are considered to be much loosed sand which is more often dry; and they are easily eroded in the presences of running water or any other erosion agent.

The result of the geotechnical analysis carried out on the eight soil samples collected from the study areas is presented in Table 4.16 below. From the samples collected, it was observed that moderately sorted sand of different categories, (medium sand being the most dominant and very fine sand the least) dominated the samples, with very negligible percentage of fine gravel. No atom of silt, clay or mud was observed, thereby reducing the bonding matrix between the soil particles. This makes it easy for running water to carry away top and loose soil particles depending on the topography of the area. Optimum moisture content determination for the eight samples as shown in Table 4.16 reveal that the moisture content of

earth materials from the erosion sites ranges from 8.8% to 12.5%, with an average of 10.70%. This low natural moisture content implies that the soil loses moisture easily in its natural state. It also implies that at about 10.7% optimum moisture content within the study areas, soil is compacted to its greatest density, thereby achieving its maximum dry density (the maximum dry density of the samples are approximately equal as they range between 1.90% and 1.99%). The Liquid Limits of the eight (8) samples collected ranges from 22.80% to 35%, with an average of 28.46%. Due to the low value of liquid limits within the area, soil easily gets saturated and thereby behaves like fluid and is transported out of their original positions. The plasticity limits of the eight (8) samples ranges between low values of 13.7% and 25%, with an average of 19.36%. Under this condition, the soil requires little or no much fluid to lose its cohesiveness or bonding. This makes the soil to be easily eroded. As plasticity limit and liquid limit are inseparable as both are directly proportional to each other, the plasticity Index of the samples ranges from 6% to 12.40% with an average of 9.1% (plasticity index is the difference between the two). With this very low index, it implies that the samples are above 90% sand dominated and will not swell or shrink as a result of increment or reduction in water content of the soil. This property makes the soil within the area very suitable for both road and building constructions as there will not be any form of cracking or deformity on the structures due to expansion and contraction of soil. The CBR values for soaked and unsoaked samples were also determined and shown in table 4.16. The CBR value ranges from 37% to 39% for the soaked and 50.7% to 85% for the unsoaked; hence can withstand some appreciable weight or loading.

Table 4.16: Table of Grain Size Distribution, OMC, MDD, CBR, LL, PL and PI

LOCATIONS	GRAIN SIZE DISTRIBUTION						OMC	MDD	CBR		LL	PL	PI
	V. FINE GRAVEL	V. COARSE SAND	COARSE SAND	MEDIUM SAND	FINE SAND	V. FINE SAND			SOAKED	UNSOAKED			
Afor Ukwu Gully Sample 1		1.20%	18.90%	47.70%	26.20%	6.10%	11.00%	1.91%		75.00%	28.50%	20.00%	8.50%
Afor Ukwu Gully Sample 2		2.20%	19.50%	52.80%	20.00%	5.60%	11.40%	1.92%		74.00%	22.80%	13.70%	9.10%
Ihioma Gully (Head)		0.80%	12.70%	70.30%	9.80%	6.50%	10.30%	1.91%		50.70%	29.10%	18.50%	10.60%
Ihioma Gully (Middle)	0.50%	1.80%	20.70%	44.80%	21.70%	10.50%	12.50%	1.90%		51.00%	31.70%	19.30%	12.40%
Njaba Gully (Okwudor Sec.) 1	0.50%	8.50%	32.20%	42.30%	13.20%	3.30%	10.60%	1.91%		79.00%	27.80%	20.30%	7.50%
Njaba Gully (Okwudor Sec.) 2	0.20%	8.20%	30.10%	43.80%	14.20%	3.50%	10.30%	1.93%		87.00%	26.80%	20.80%	6.00%
Ogberuru Orlu Gully							10.70%	1.98%	35.00%	51.00%	35.00%	25.00%	10.00%
Umueshi Gully							8.80%	1.99%	39.00%	53.00%	26.00%	17.30%	8.70%

CHAPTER FIVE

SUMMARY, CONCLUSION AND RECOMMENDATION

5.1 SUMMARY AND CONCLUSION: Since the primary objective of this study is to identify structures expressed as lineaments and classify them according to their spatial and directional attributes, it was necessary to process the Landsat -TM data in a manner that would both enhance trends and facilitate the computation of locations and depths. Drainage pattern, termination of drainage line on linear trends and straight stream segments were some of the basic hypothetical models used to map fractures. O'Leary et al. (1976) defines lineaments as a mappable, simple or composite linear feature of a surface whose parts are aligned in a rectilinear or slightly curvilinear relationship and which differ from the pattern of adjacent features and presumably reflects some subsurface phenomenon. The inferred structural trends from the Rose diagram (fig.23) are in the orientations: NE-SW, E-W and N-S. The NE-SW trend is the dominant orientation from the Rose diagram. According to Uzuakpunwa (1974), the NE-SW trending Abakaliki-Benue trough is thought to be the result of a pre-Albian rifting of the African shield prior to the opening of the South Atlantic. Linear structures running NE-SW observed from the study are suggested as the continental extension of the known pre Cretaceous oceanic fracture zones viz. Charcot and Chain fracture zones (Ananaba, 1991; Burke et al 1971; 1972) which run along the trough axis beneath the sedimentary cover. This present research is therefore in agreement with previous studies which suggested that Nigeria has a complex network of fractures and lineaments with dominant trends of NW-SE, NESW, N-S and E-W directions (Chukwu-Ike and Norman (1997); Ananaba and Ajakaiye (1987); Onyedim(2006); Udoh(1988). Furthermore, it is geologically plausible that the landward intersections of the transform fracture zones may have influenced the formation of the river patterns and basin formation. . The NE-SW trend and the other strikes confirm that Nigeria was subjected to Pan African orogeny.

The azimuths of the major axes of the anisotropy diagrams correlate significantly with the strikes of the geological formations. The coefficient of anisotropy obtained from the survey varies from 1.30 to 1.70, indicating that structural in-homogeneities exist. The evidence from available geophysical data indicate that the strike of the gully which is oriented in the NW-SE direction. This would suggest a juxtaposition of sediments of different degrees of saturation and resistance to shear and probably separated by a fractured region which may be a fault. The early cretaceous tectonic movement in the sedimentary basin of Southeastern Nigeria guided a major marine transgression across the continent and later determined the course of the Niger and Benue Rivers and probably had tremendous influence on gulling and erosion (Hospers, 1965). Consistent NW-SE orientation of maximum axes of electrical anisotropy and the form of the gully and its orientation which coincides with the regional geologic trend, narrow down wide range of other possible causes and have led to the speculation that the gully is structurally controlled and may indeed be running along the geologic contact between the Benin Formation and the Ogwashi/Asaba Formation. This conclusion however has been supported by remote sensing data used for this study.

The geotechnical property of soil plays a vital role in any engineering project such as buildings, roads, bridges or earthen structures like dams and embankment. These projects use soil as an engineering material in terms of its ability to carry the loads and support the structures safely. The analysis of soil properties provides sufficient data to the engineer towards ensuring an economical design for the type of soil to be used in terms of its stability, durability, strength and workability. The soil underlying the study area – Umueshi, Ihioma, Okwudor, Afor Ukwu, Urualla e.t.c., is probably the best from a foundation standpoint, but in some cases, the soils may be soft and wet, therefore, there could be fairly large settlements under excessive load. The settlement can be controlled by increasing its thickness. It shows moderately sorted soil particles which generally could be said to have some reasonable amount of shear strength, sequel to limited pore spaces. Furthermore, the soil is slightly

compressible and gives fair to good compaction with sheep-foot roller; this property makes it unsuitable for use as sub-base and base course in road construction. Undesirable compression or expansion (swelling due to increase in water content or shrinking due to loss of water) characteristics will not be experienced by distributing the load through a greater thickness of overlying material. The inability of the soil within the study area to contract or expand in the presence or absence of water makes it suitable for engineering purposes.

The results of the study also authenticates the fact that significant relationships exist between vegetation types, topography, geologic formations, soil characteristics (physical and chemical), and gully formation and development in the area. Therefore no one could reasonably deny the possible contributions of human activities to the development of gully erosion.

5.2 RECOMMENDATIONS AND CONTROL

Following the result of this study and the result from other researchers, I recommend the following control measures for gully erosion control in the study area.

1. Area with lineament which are yet to develop into gullies should be closely monitored, deep rooted trees planted, human activities reduced to the barest minimum and as well as properly planned drainages should be constructed to inhibit further development into gullies.
2. Human activity and agricultural practices should be controlled and their effects reduced to the barest minimum.
3. As a general rule of thumb, 70% groundcover is needed to protect soil in areas of high water flow this needs to be thicker, up to 100% cover. In areas above a gully where rain is likely to fall, a higher percentage of groundcover will help reduce run-off and prevent erosion.

4. Surface and subsurface flows and drainage should be controlled by directing water through concrete channels into lined artificial reservoirs or straight into the lakes or river plains.
5. The gully walls and bottom should be stabilized through engineered structures, grouting and bolting.
6. The complete removal of live stocks from the gully area and run-off area above the gully is preferred. If stock have uncontrolled access to these areas then careful stock management is required. Plants will regenerate more successfully and quickly if grazing pressure is removed, which will lead to faster stabilization of the gully.
7. Deep-rooted perennial grasses are recommended for planting in and on the sides of the gullies and ephemeral waterways that have the potential to become gullies.
8. Trees and larger shrubs should be planted further away from the gully to take up groundwater.
9. An Environmental Monitoring team or parastatal should be set up where not existing to monitor the environment, set up control measures and collect relevant information for future analysis.
10. Workshops and trainings on Erosion, Gullying and controls should be frequently organized for the residents within the area to educate them on the menace and its effect to human life and properties and possible ways to control it.

REFERENCES

- Agagu, O.K., 1979. Potential geo-pressured geothermal reservoirs in the Niger Delta Subsurface; Nig. Journ.Of Science, 13, 1& 2: 201-215.
- AASHTO, 2000.American Association of State Highway and Transportation Officials, Highway Safety Manual. p14.
- Ako, B.D., 1976. An integration of geophysical and geological data in dam site investigation; Journ.of Min and Geo., 13: 1- 6.
- Ako, B.D. and T.R. Ajayi, 1976. Detection of a fault by the Seismic refraction method; Journal of Min. and Geol., 1: 58-65.
- Asseez, L.O., 1979. A review of the sedimentary geology of the Niger Delta.In Geology of Nigeria.C.A.Kogbe, Ed., Elizabethan press, pp: 175-187.
- Amadi, A. N., Olasehinde, P.I., 2008. Assessment of Groundwater Potential of parts of Owerri, South eastern Nigeria. J. Sci. Edu. Technol. Vol.1 (2): 177-184.
- Amadi, A.N., Olasehinde, P.I, Yisa, J., 2010. Characterization of Groundwater chemistry in the coastal plain-sand aquifer of Owerri using factor analysis. Int. J. the Physical Sci, Vol. 5(8), pp. 1306 – 1314
- American Geological Institute, 1976. Dictionary of geological Terms, New York: Anchor Books.
- Aroka, K.R., 2009. Soil Mechanics and foundation Engineering.NaiSarak, Delhi: Standard Publisher Distributor.
- Avbovbo, A.A., 1978. Tertiary lithostratigraphy of Niger Delta: Ame. Ass. Pet. Geol.62: 297-306.
- Babalola O., 1988. Soil properties affecting infiltration, runoff and erodibility, In: Sagua, VO, Enabor EE, Ofomata GEK, Ologe KO, Oyebande L., Eds., Ecological Disaster in Nigeria: Soil Erosion. Federal Ministry of Science and Technology, Lagos, Nigeria. pp. 7 – 20

- Bhattacharya BB, Patra H.P., 1968. Direct methods in geoelectric sounding: Principle and interpretation: Elsevier Science Publ. Co. Inc. p.131
- Blanco, Humberto & Lal, Rattan (2010)."Soil and water conservation". Principles of Soil Conservation and Management.Springer.p. 2.
- Busby, J.P., 2000.The effectiveness of azimuthal apparent-resistivity measurements as a method for determining fracture strike orientations.Geophys.Prospec., 48 pg4: 677-695
- Carter, J., 1958. Erosion and sedimentation from Aerial Photographs. Journal of Tropical Geography, II, 31
- Carey, B., 2006. Gully erosion; FACTS Journal, Natural Resources and Water, L81, QNRM05374; pp.1-4.
- Casas, A. M., Cortés, A. L., Maestro, A., Soriano, M. A., Riaguas, A., and Bernal, J., 2000. LINDENS: A program for lineament length and density analysis. Comp. Geosc., 26, 1011-1022.
- Chukwu, Ike, I. M., 1978. Interpretation of marginal en-echelon lineaments in the mid Benue Trough, Nigeria: Nigeria Journal of Mining and Geology, 15(1), 14 -18.
- Coduto, D.P., 2007. Geotechnical Engineering: Principles and Practices. New Delhi: Prentice Hall of India Private Limited
- Cratchley, C.R. and G.P. Jones, 1965.An Interpretation of the Geology and Gravity anomalies of the Benue Valley, Nigeria.Geophys.Pap.Overseas geol. Surv. London, Paper NO.1.
- Deffontaines, B., and Chorowicz, J. 1991: Principles of drainage basin analysis from multisource data; application to the structural analysis of the Zaire Basin. Tectonophysics, 194 (3), 237-263.
- Deffontaines, B., Chotin, P., Ait, B. L., and Rozanov, M. 1992: Investigation of active faults in Morocco using morphometric methods and drainage pattern analysis. Geol. Rund., 81 Vol. 1, pp 199-210.

- Deroin, J.-P., and Deffontaines, B., 1995. Morphostructural analysis for linking streamflow, lithology, and structure: comparison with remote sensing data on the Cévennes, French Massif Central. *Z. Geomorph.*, 39 Vol.1 pp 97-116.
- Ehirim, C.N., and N.E. Ekeocha, 2009. Anisotropic Type Determination and Soil Structure Evaluation in Parts of the Gully Erosion Zones of SE Nigeria using Azimuthal-Offset Resistivity Sounding Technique and Erodibility Characterization; *Pacific Journal of Science and Technology*, 10 Vol. 2 pp 709-715.
- FAO., 1990. International Scheme for Conservation and Rehabilitation of African Lands. FAO, Rome.
- Fetter CW. 1994. Applied Hydrogeology. Third Edition. Englewood Cliffs, NJ: Prentice-Hall. 691
- Fubara, D.M.J., S.C. Teme, T. Mgbeke, A.E.T. Gobo and T.K.S. Abam, 1988. Master plan Design of flood and Erosion control measures in the Niger Delta. IFERT Technical Report No. 1.
- Greenfield, R.J., and C.H. Stoyer, 1976. Monitoring Groundwater contamination with geophysical methods. *Society of Mining Engineers AIME transactions*, 260: 20-23.
- Grove, A.T., 1956. Land Use and Soil Conservation in parts of Onitsha and Owerri Provinces. *Geological Survey of Nigeria, Bulletin No. 21*, pp79
- Grove, A.T., 1951. Soil erosion and population problems in Southeast Nigeria, *Georgia Journal*. pp117, 191-206.
- Goudie, Andrew 2000. The human impact on the soil. *The Human Impact on the Natural Environment*. MIT Press. p. 188
- Habberjam, G.M., 1975. Apparent resistivity anisotropy and strike measurement. *Geophys. Prosp.*, 23 Vol. pp 211-215.
- Hagrey, S., 1994. A. al Electric study of fracture anisotropy at Falkenberg, Germany; *Geophysics.*, 59: 881- 888.

- Hobbs, W. H., 1904. Lineaments of the Atlantic border region. *Geol. Soc. Am. Bull.*, 15, 483- 506.
- Holme, A.McR. Burnside, D.G. and Mitchell, A.A., 1987. The development of a system for monitoring trend in range condition in the arid shrub lands of Western Australia. *Australian Rangeland Journal* 9:14-20.
- Hospers, J., 1965. Gravity field and structure of the Niger Delta, Nigeria. In *Geology of Nigeria*, C.A.Kogbe, Ed.; Elizabethan Press, pp: 273-282.
- Howard, A. D., 1967. Drainage analysis in geologic interpretation: a summation. *Am. Ass. Petr. Geol. Bull.*, 51 Vol.11, 2246-2259.
- Hudec P.P., Simpson, F., Akpokodje, E.G., Umenweke, M.O., 2006. Termination of gully processes, Southeastern Nigeria. *Proceedings of the Eight Federal Interagency Sedimentation Conference, 8th FISC, April 2-6, 2006, Reno. NV. USA. Pp 671 679*
- Ibeneme, S. I., Idiong, I. A., Nwagbara, J. O., Selemo, A. O., Israel, H.O., 2014. Assessment of the Engineering Significance of Geo-Materials Derived from a Borrow Pit at Ugwu Orlu, South-East Nigeria.
- Igboekwe, M.U., Eke A.B., Adama, J.C., Ihekweaba, A.The Use of Vertical Electrical Sounding (VES) in the Evaluation of Erosion in Abia State University, Uturu and Environs.
- Jeje, L. K., 1988. Soil Characteristics, processes and extent in the lowland rainforest areas of southwestern Nigeria. In Enabor, E. E. et al., Eds. *Ecological Disasters: Soil Erosion* published by Federal Ministry of Science and Technology, Lagos, pp. 163-189
- Keller, G. V., and Frischknecht, F.C., 1966.*Electrical Methods in Geophysical Prospecting*, Pergamon Press.Inc.
- Koike, K., Nagano, S., and Kawaba, K., 1998. Construction and analysis of interpreted fracture planes through combination of satellite-image derived lineaments and digital elevation model. *Comp. Geosc.*, 24 pg. 6, 573-583

- Kogbe, G.A., 1976. The Cretaceous and Paleogene sediments of Southern Nigeria. In *Geology of Nigeria*, C. A. Kogbe, Ed., Elizabethan press. pp: 273-282.
- Kruseman, G.P. and N.A. de Ridder, 1994. *Analysis and Evaluation of Pumping Test Data*, 2nd ed., Publication 47, Intern. Inst. for Land Reclamation and Improvement, Wageningen, The Netherlands, 370
- Kunetz, G. 1966. Processing and interpretation of magnetotelluric soundings. *Geophysics* 37, 1000-1021.
- Lataste, J.F., D. Breysse, C. Sirieix, M. Frappa, J.P. Bournazel, 2002. Fissuration des ouvrages en béton armé auscultation par mesure de résistivité électrique. *Bull. Lab. Ponts et Chaussées.*, 239: 79-91.
- Leonard M.P.J., 1984. A Surface resistivity method for measuring hydrologic characteristics of jointed formations, U.S. Bur. mines Report of Investigations 8901
- Mammah, L.I., and A.S., Ekine, 1989. Electrical resistivity Anisotropy and tectonism in Basal Nsukka Formation., *Journ.Of Min. and Geol.*, 25: 121-129.
- McElfresh, S. B. Z., Harbart, W., Ku, C.-Y., and Lin, J.-S., 2002. Stress modeling of tectonic blocks at Cape Kamchatka, Russia using principal stress proxies from high resolution SAR: new evidence for the Komandorskiy Block. *Tectonophysics*, 354, 239-256
- Murat, R.C., 1972. Stratigraphy and paleogeography of Cretaceous and Lower Tertiary in Southern Nigeria in T.F.G. Dessauvage and A.J. Whiteman *Africa Geology*. Ibadan Univ. pp: 256-266.
- Nwajide, C.S., Hoque M., 1979. Gullying processes in Southeastern Nigeria. *The Nigerian Field* 44 Vol. 2; 64-74
- Nwankwo, N., and Ifeadi, C.N., 1988. *Case Studies on the Environment Impact of Oil Production and Marketing in Nigeria*. University of Lagos, Nigeria.

- Nyong, E.E., 1995. Cretaceous Sediments in the Calabar Flank. In Geological Excursion Guidebook. Published in commemoration of the 31st Annual Conference of the Nigerian Mining and Geosciences Society.
- O'Leary, D. W., Friedman, J. D., and Pohn, H. A., 1976. Lineament, linear, lineation: Some proposed new standards for old terms. *Geol. Soc. Am. Bull.*, 87, 1463-1469
- Ofomata, G. E. K., 1988. Soil erosion characteristics, processing and extent in the lowland rainforest area of southeastern Nigeria. In Sagua, V. O., Enabor, E. E., Ofomata, F. E. K., Ologe, K. O., & Oyebande Lekan, Eds. *Ecological Disaster in Nigeria: Soil Erosion* published by Federal Ministry of Science and Technology, Lagos, Nigeria, pp. 50-58.
- Ogbukagu, I.M., 1976. Soil erosion in the northern parts of Awka-Orlu uplands, Nigeria. *Journal of Min. and Geol.*, 13, pp 6-19.
- Olorumfemi, M.O., and M.A. Opadokun, 1989. Electrical anisotropy in Basement complex area of south western Nigeria and its effect on depth sounding interpretation results. *Journal of Min. and Geol.*, 25 Vol. 1&2, 87-95
- Onu, N.N., 1998. Gully erosion and neo-tectonism in Southeastern Nigeria: In *Geography and the Nigerian Environment*. I.E, Ukpong, Ed. pp: 222-229.
- Onu, N.N., and Opara, A.I., 2012. Analysis and Characterization of Njaba River Gully Erosion, Southeastern Nigeria: Deductions from Surface Geophysical Data
- Onyeagocha A. C., 1980. Petrography and depositional environment of the Benin Formation, Nigeria. *Journal of Mining Geology* 17: 147-151.
- Ramanujam, R., K.N. Murugan and A.A., Ravindram, 2006. Azimuthal square array resistivity studies to infer active fault zones in the areas of known seismicity, Kottayam District, Kerala – A case study; *J. Ind. Geophys. Union*, 10 Vol.3: 197-208.
- Reyment, R.A., 1965. Aspects of the geology of Nigeria, University of Ibadan Press, Ibadan Nigeria, pp: 145.

- Roderick, M., R. C. G. Smith, and G. Ludwick, 1996. Calibrating long term AVHRR derived NDVI imagery. *Remote Sensing of Environment* 58: 1-12.
- Rouse, J. W., R. H. Haas, J.A. Schell, and D. W. Deering, 1973. Monitoring vegetation systems in the Great Plains with ERTS, Third ERTS Symposium, NASA SP-351 I, 309-317
- Sauck WA, Zabik SM. 1992. Azimuthal resistivity techniques and the directional variations of hydraulic conductivity in glacial sediments, In Bell R.S., ed., *Symposium on the Application of Geophysics to Engineering and Environmental Problems: society of Engineering and Mining geophysicists*, Golden. CO, pp197-222.
- Short, K.C. and A.J. Stauble, 1967. Outline geology of Niger Delta. *AAPG Bull.*, 51: 761-771.
- Skjerna, L. and N.O. Jorgensen, 1994. Evaluation of local fracture systems by Azimuthal resistivity surveys: examples from Norway. *Appl. Hydrogeology*, 2: 19-25.
- Taylor, R.W. and A.H. Fleming, 1988. Characterizing joint systems by Azimuthal resistivity Surveys. *Groundwater*, 2: 464-474.
- Telford, W.M., L.P. Geldart, R.E. Sheriff and D.A. Keys, 1976. *Applied Geophysics*, Cambridge University Press. pp: 860.
- Watson, K.A. and R.D. Barker, 1999. Differentiating anisotropy and lateral effects using azimuthal resistivity offset Wenner soundings, *Geophysics.*, 64 Vol. 3 pp 739-745.
- Whiteman A., 1982. *Nigeria: Its Petroleum Geology, Resources and Potential*. London: Graham and Trotman Ltd.
- Wright, J.B., 1966. South Atlantic Continental Drift and the Benue Trough. *Tectonophysics*, 6: 301-310.
- Zohdy, A.A.R., 1965. The auxiliary point method of electrical sounding interpretation and its application to the Dar Zarrouk parameters. *Geophysics.*, 30: 644-660.

Zohdy, A.A.R., 1974. Application of Surface Geophysics to Groundwater investigation;
Techniques of water Resources investigation of the US Geological Survey., pp: 26 -30.

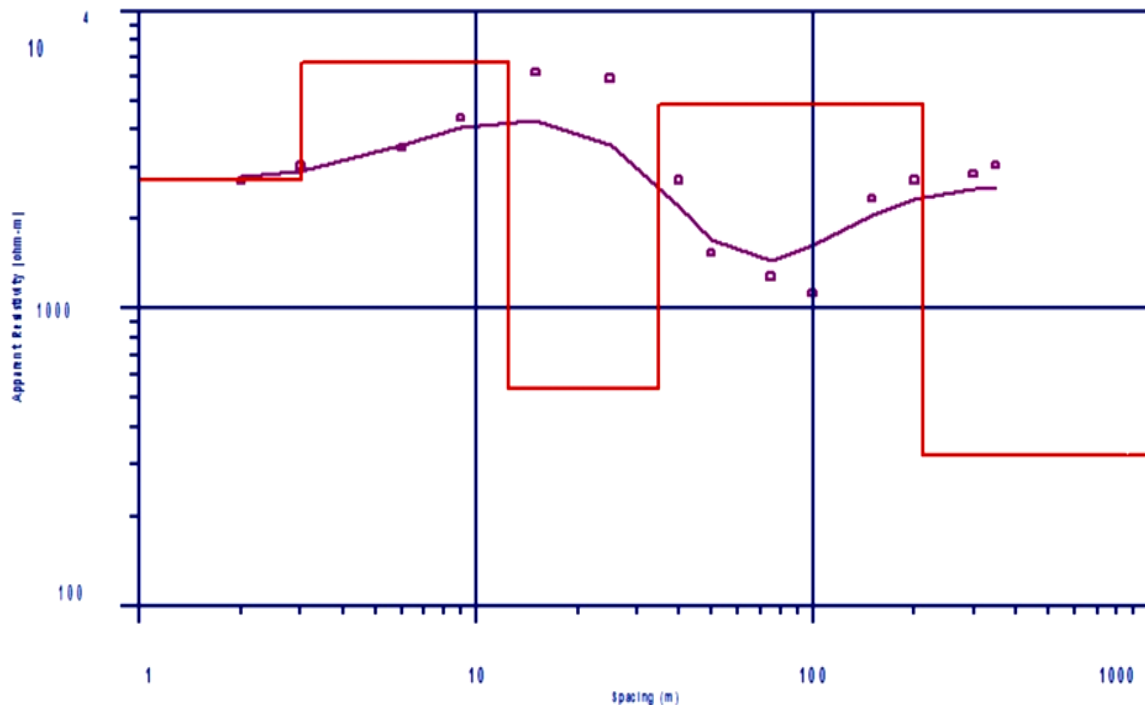
APPENDICES

VERTICAL ELECTRICAL SOUNDING(SHLUMBERGER ARRAY)

UMUAZZALA OGBERURU, IMO STATE

Point	AB/2	MN	Apparent Resistivity
1	2.00	1.00	2686.25
2	3.00	1.00	3026.00
3	6.00	1.00	3490.54
4	9.00	1.00	4382.65
5	15.00	4.00	6274.00
6	25.00	4.00	5948.59
7	40.00	4.00	2710.30
8	50.00	4.00	1541.41
9	75.00	4.00	1285.00
10	100.00	4.00	1130.40
11	150.00	20.00	2351.40
12	200.00	20.00	2703.30
13	300.00	20.00	2839.70
14	350.00	20.00	3048.40

#	Rho	Fix?	Thick	Depth	Elev
1	2708.7		3.0227	3.0227	191.98
2	6736.0		9.4655	12.488	182.51
3	536.21		22.240	34.728	160.27
4	4843.4		177.36	212.08	-17.085
5	320.54				



N05°49' 49.4"

E007°01' 43.4"

EL:195m

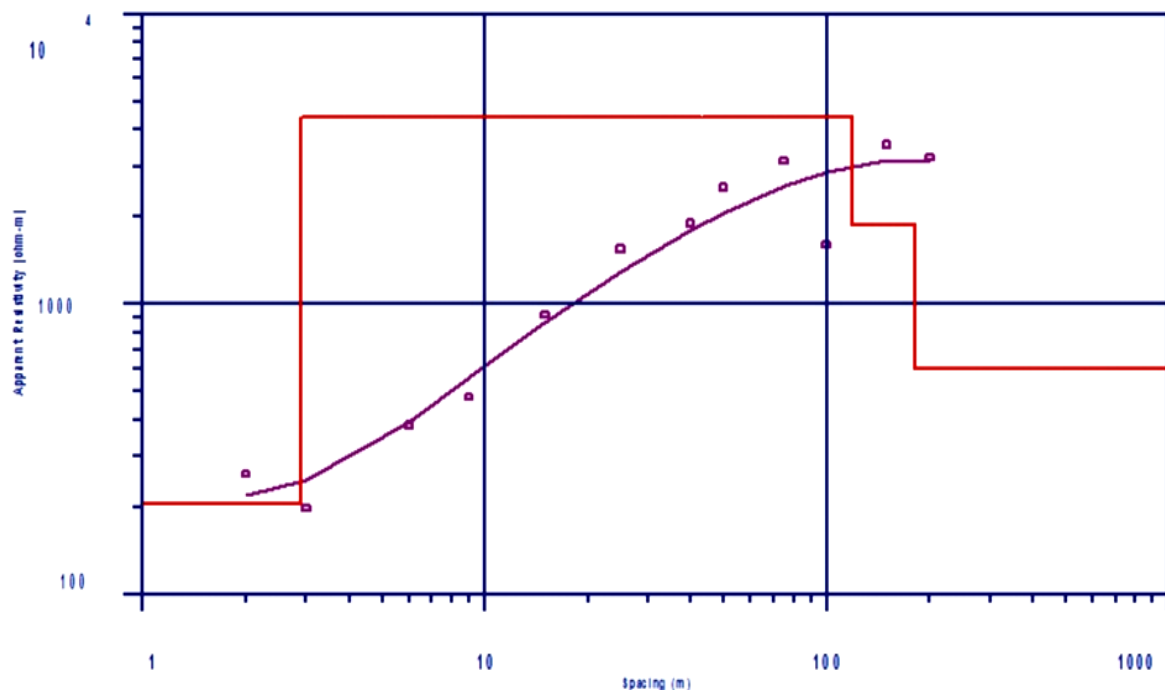
VERTICAL ELECTRICAL SOUNDING(SHLUMBERGER ARRAY)

OGBERURU, ORLU L.G.A IMO STATE

(VES 2)

Point	AB/2	MN	Apparent Resistivity
1	2.00	1.00	260.00
2	3.00	1.00	197.85
3	6.00	1.00	382.77
4	9.00	1.00	480.96
5	15.00	4.00	920.97
6	25.00	4.00	1548.78
7	40.00	4.00	1898.71
8	50.00	4.00	2537.11
9	75.00	4.00	3127.30
10	100.00	4.00	1603.90
11	150.00	20.00	3551.70
12	200.00	20.00	3216.50

#	Rho	Fix?	Thick	Depth	Elev
1	204.43		2.9033	2.9033	1209.1
2	4430.9		116.44	119.34	1092.7
3	1883.0		62.571	181.91	1030.1
4	601.70				



N05°49'55.2"

E007°00'55.4"

EL:121m

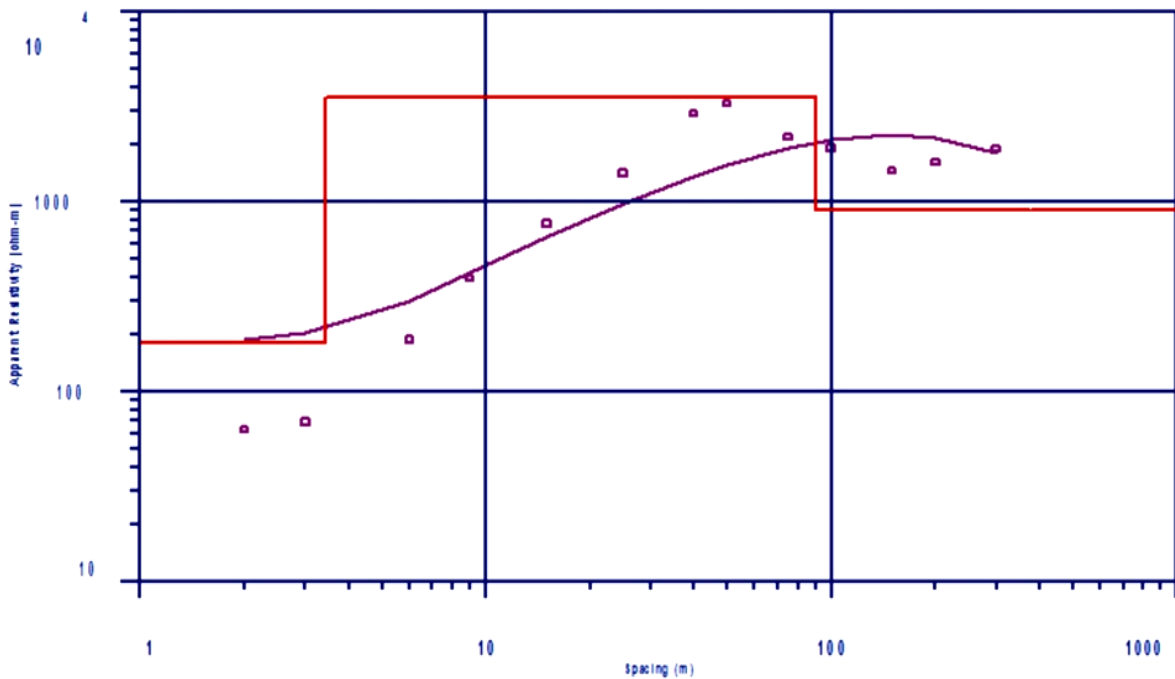
VERTICAL ELECTRICAL SOUNDING(SHLUMBERGER ARRAY)

UMUESHI IDEATO SOUTH L.G.A IMO STATE

(VES 1)

Point	AB/2	MN	Apparent Resistivity
1	2.00	1.00	62.71
2	3.00	1.00	69.25
3	6.00	1.00	187.70
4	9.00	1.00	394.51
5	15.00	4.00	767.64
6	25.00	4.00	1409.94
7	40.00	4.00	2895.34
8	50.00	4.00	3286.12
9	75.00	4.00	2191.40
10	100.00	4.00	1913.50
11	150.00	20.00	1457.30
12	200.00	20.00	1605.10
13	300.00	20.00	1893.00

#	Rho	Fix?	Thick	Depth	Elev
1	179.22		3.4263	3.4263	256.57
2	3498.7		87.232	90.658	169.34
3	897.07				



N05° 49' 44.4"

E007° 06' 37.7"

EL:260m

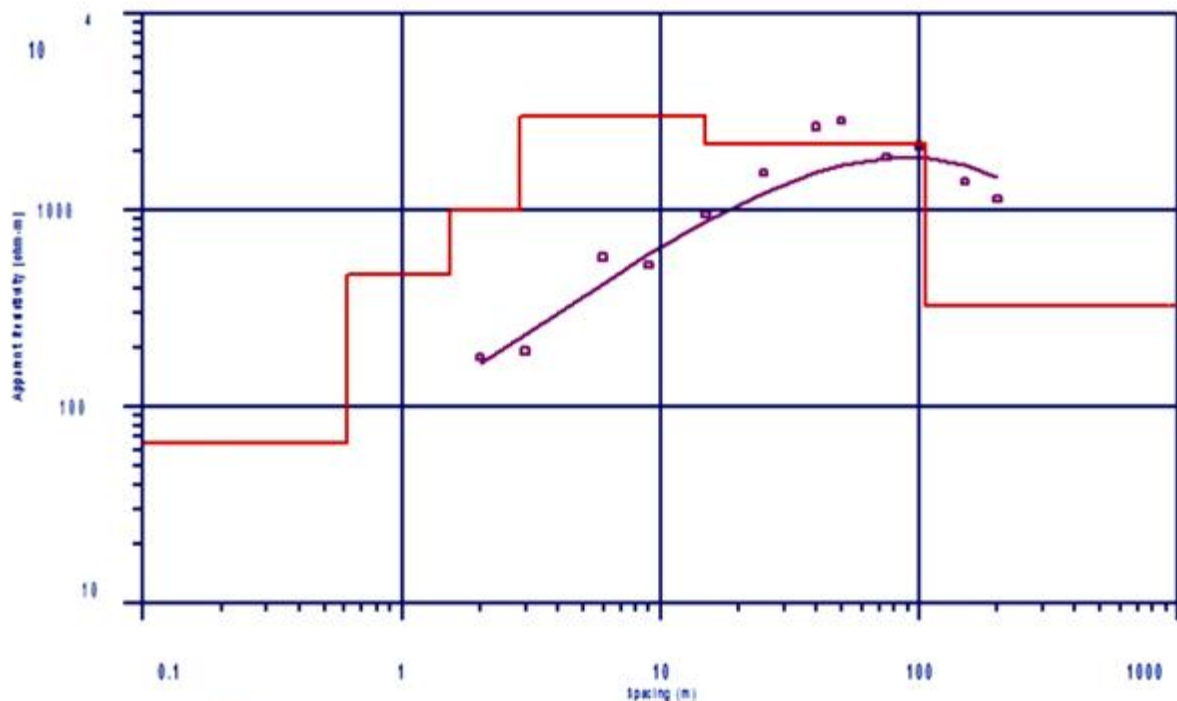
VERTICAL ELECTRICAL SOUNDING(SHLUMBERGER ARRAY)

UMUESHI IDEATO SOUTH L.G.A IMO STATE

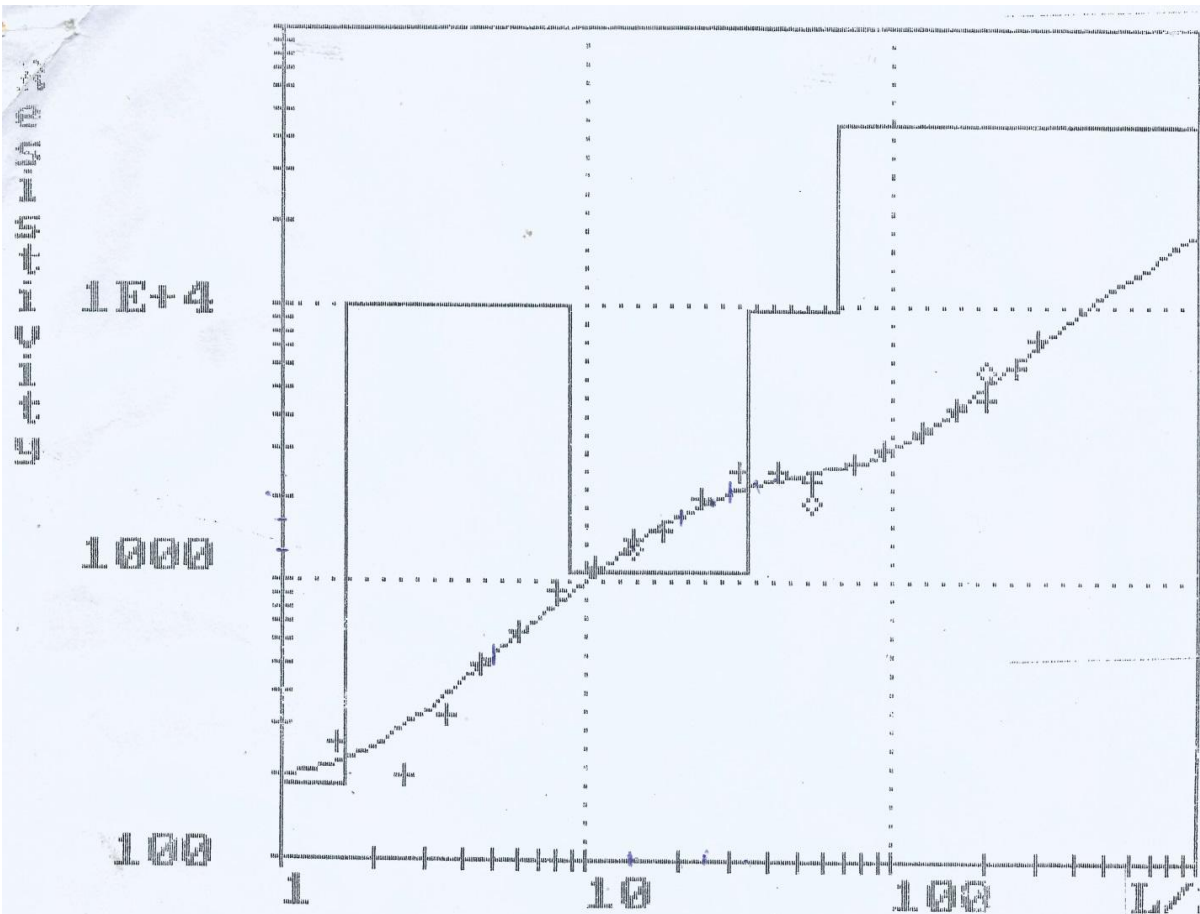
(VES 2)

Point	AB/2	MN	Apparent Resistivity
1	2.00	1.00	179.24
2	3.00	1.00	191.45
3	6.00	1.00	573.31
4	9.00	1.00	526.13
5	15.00	4.00	946.70
6	25.00	4.00	1552.99
7	40.00	4.00	2651.86
8	50.00	4.00	2847.51
9	75.00	4.00	1857.90
10	100.00	4.00	2120.40
11	150.00	20.00	1400.90
12	200.00	20.00	1134.90

#	Rho	Fix?	Thick	Depth	Elev
1	65.168		0.61059	0.61059	272.39
2	471.34		0.93316	1.5438	271.46
3	1000.1		1.2993	2.8430	270.16
4	2999.2		11.979	14.822	258.18
5	2167.0		90.745	105.57	167.43
6	325.43				



N05° 49' 50.9" E007° 06' 34.8" EL:273m

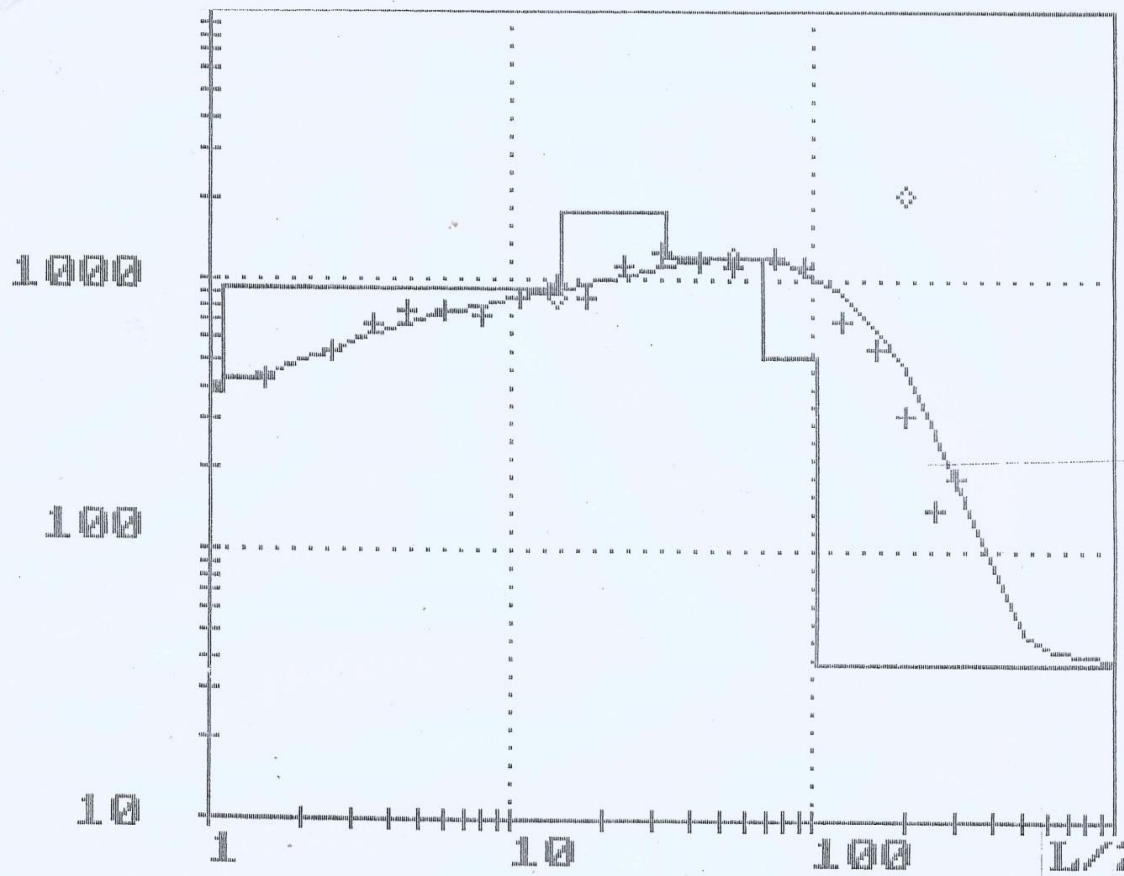


Data (File) name STUDENTS^o.PROJECTDate 13/07/2014
 Project name EROSION CONTROL Direction lay out
 NJABA RIVER - NJABA L.G H/QUATERS
 Code name VES II Remarks
 NJABA L.G.A. IMO STATE.
 Coordinates. . . . N05- 43-207', E07 00.695', H115m
 Schlumberger 0°Neill

L/2 (m)	Rho (Ohm.m)	L/2 (m)	Rho (Ohm.m)	L/2 (m)	Rho (Ohm.m)
1.5	255.2	14.0	1295.0	95.0	2962.1
2.5	194.6	18.0	1531.6	125.0	3506.7
3.5	329.9	24.0	2010.1	160.0	4330.3
4.5	500.3	32.0	2466.1	200.0	4655.7
6.0	660.1	42.0	2461.0	200.0	5693.2
8.0	916.2	55.0	2343.0	250.0	6109.8
10.5	1127.0	55.0	1889.0	300.0	7684.8
14.0	1408.0	75.0	2733.0		

Resistivity (Ohm.m)	Depth (m)
186.0	1.6
10000.0	8.7
1090.0	33.6
9500.0	65.0
44800.0	

RESISTIVITY

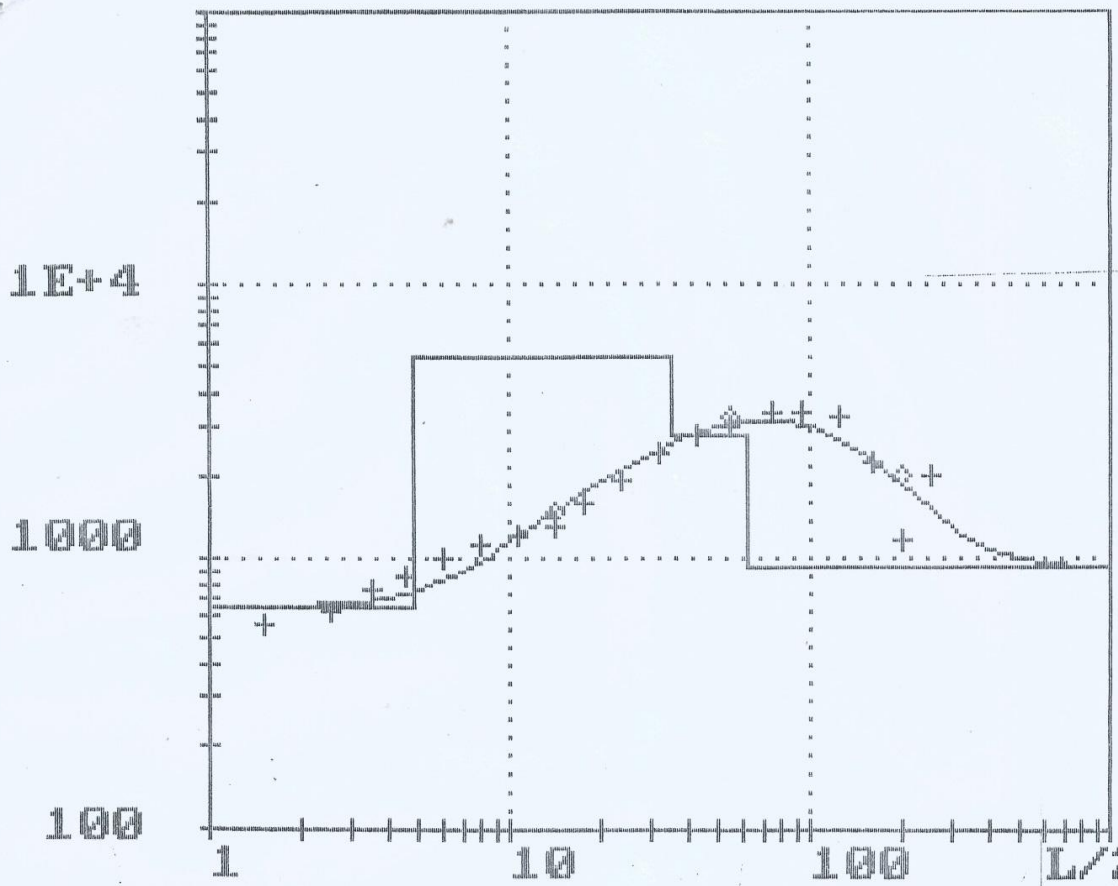


Data (File) name STUDENT PROJECT Date 12/07/2014
 Project name EROSION CONTROL Direction lay out
 EROSION SITE - ORLU/IHIALA ROAD
 Code name VES III Remarks
 MIOMA ORLU ORLU L.G.A. IMO STATE
 Coordinates N05 49.221°, E07 00.217° H102m
 Schlumberger 0°Neill

L/2 (m)	Rho (Ohm.m)	L/2 (m)	Rho (Ohm.m)	L/2 (m)	Rho (Ohm.m)
1.5	422.6	14.0	860.5	95.0	1113.9
2.5	542.2	18.0	858.3	125.0	711.7
3.5	671.8	24.0	1120.3	160.0	551.3
4.5	763.6	32.0	1260.3	200.0	312.1
6.0	763.6	42.0	1162.5	200.0	2087.7
8.0	737.8	55.0	1119.5	250.0	139.2
10.5	840.0	55.0	1201.4	300.0	181.0
14.0	953.3	75.0	1184.2		

Resistivity (Ohm.m)	Depth (m)
383.0	1.1
940.0	14.6
1810.0	33.0
1190.0	67.5
528.0	104.0
38.9	

RESISTIVITY LOG

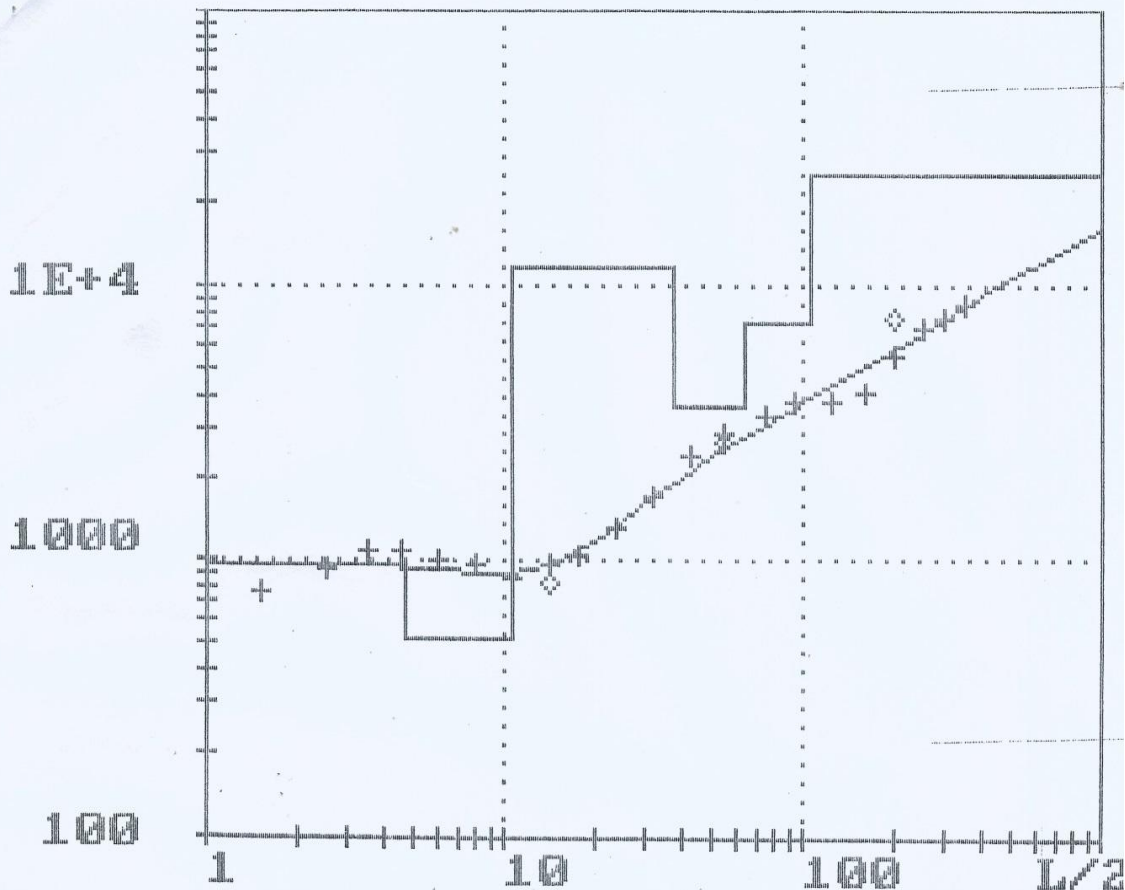


Data (File) name STUDENTS' PROJECT Date 11/07/2014
 Project name EROSION CONTROL Direction lay out
 OKWELLE/URUALLA ROAD - NWA-AFOR/NKWERRI
 Code name YES I Remarks
 IDEATO NORTH L.G.A IMO STATE
 Coordinates N05 47.372°, E07 07.705°, H152m
 Schlumberger 0'Neill

L/2 (m)	Rho (Ohm.m)	L/2 (m)	Rho (Ohm.m)	L/2 (m)	Rho (Ohm.m)
1.5	562.6	14.0	1479.2	95.0	3323.8
2.5	618.5	18.0	1573.6	125.0	3278.4
3.5	755.9	24.0	1907.6	160.0	2223.0
4.5	839.6	32.0	2369.4	200.0	1149.0
6.0	995.9	42.0	2821.0	200.0	1957.0
8.0	1104.0	55.0	3027.1	250.0	1965.0
10.5	1200.6	55.0	3274.6		
14.0	1296.4	75.0	3405.7		

Resistivity (Ohm.m)	Depth (m)
650.0	4.8
5460.0	34.5
2870.0	61.8
910.0	

RESISTIVITY

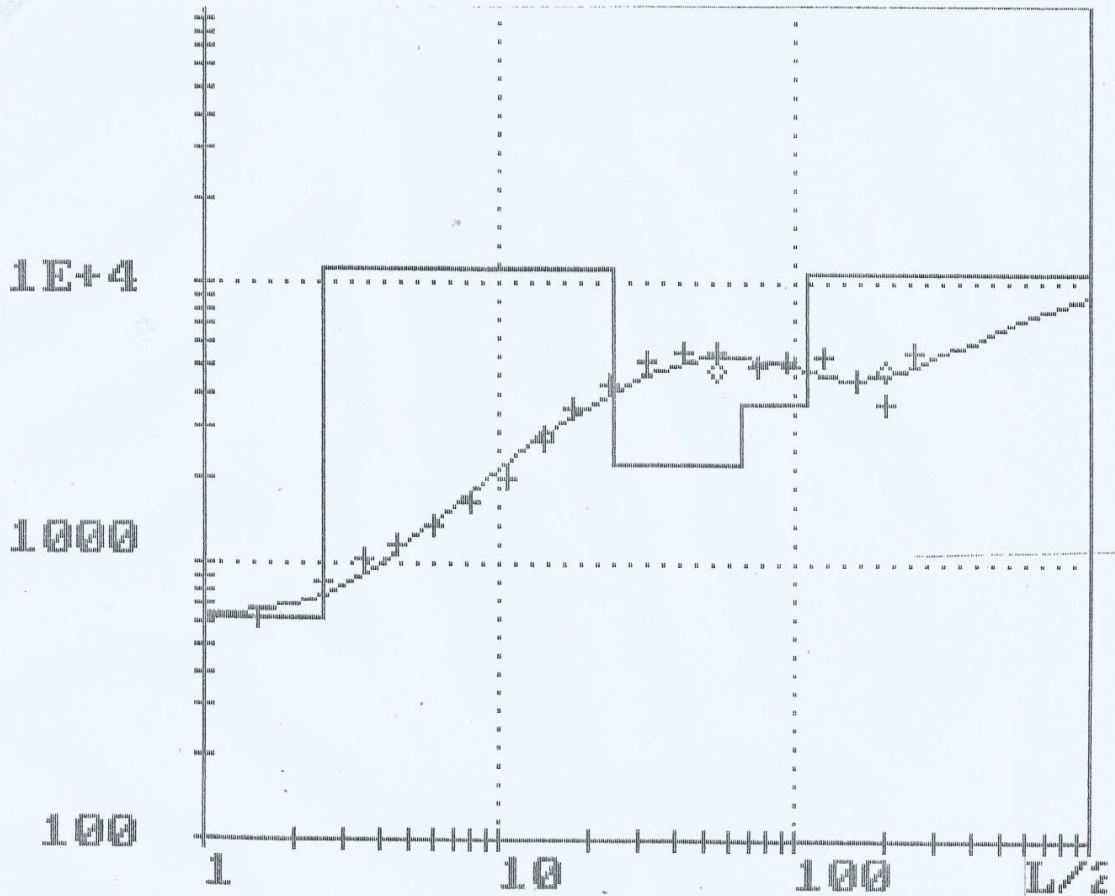


Data (File) name STUDENTS' PROJECT Date 11/07/2014
 Project name EROSION CONTROL Direction lay out AFOR UKWU - AFOR NTA
 Code name VES II Remarks
 IDEATO NORTH L.G.A IMO STATE
 Coordinates N05 47.283°, E07 07.878°, H155m
 Schlumberger O'Neill

L/2 (m)	Rho (Ohm.m)	L/2 (m)	Rho (Ohm.m)	L/2 (m)	Rho (Ohm.m)
1.5	744.8	14.0	808.6	95.0	3806.4
2.5	935.6	18.0	1037.1	125.0	3733.3
3.5	1065.2	24.0	1305.0	160.0	4071.1
4.5	1088.3	32.0	1688.4	200.0	5561.8
6.0	997.0	42.0	2389.4	200.0	7496.0
8.0	964.8	55.0	2931.1	250.0	6987.8
10.5	836.6	55.0	2682.5	300.0	7572.1
14.0	972.3	75.0	3356.4	350.0	8398.9

Resistivity (Ohm.m)	Depth (m)
970.0	4.7
521.0	10.6
11600.0	36.8
3710.0	64.9
7330.0	107.0
25500.0	

RESISTIVITY

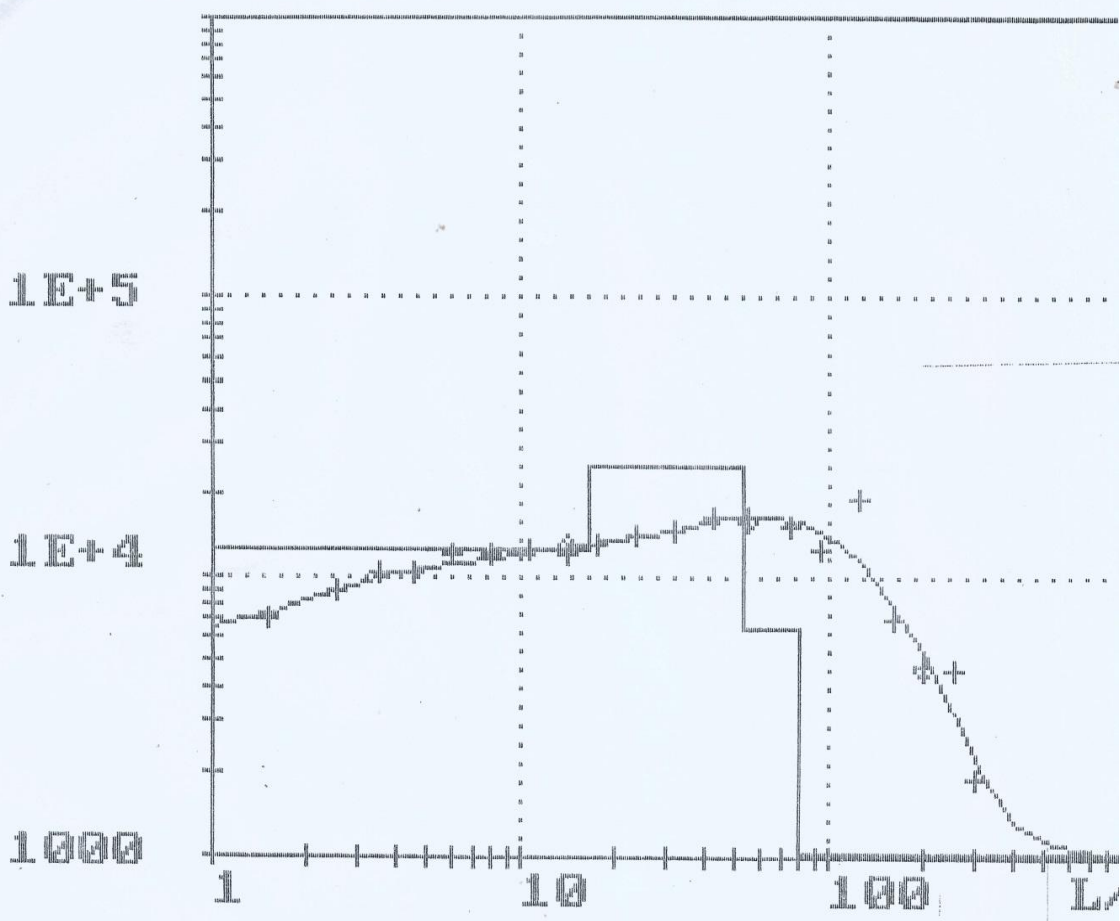


Data (File) name STUDENTS' PROJECT Date 11/07/2014
 Project name EROSION CONTROL Direction lay out
 OKWELLE/URUALA ROAD - TO THE EROSION SITE
 Code name YES III Remarks
 IDEATO NORTH L.G.A IMO STATE
 Coordinates NOS 47.099°, E07 07.740°, H137m
 Schlumberger O'Neill

L/2 (m)	Rho (Ohm.m)	L/2 (m)	Rho (Ohm.m)	L/2 (m)	Rho (Ohm.m)
1.5	619.3	14.0	2805.4	95.0	5181.9
2.5	838.2	18.0	3460.8	125.0	5276.5
3.5	1027.2	24.0	4230.2	160.0	4415.8
4.5	1158.0	32.0	5103.0	200.0	3718.7
6.0	1365.7	42.0	5496.5	200.0	4713.5
8.0	1639.8	55.0	5658.1	250.0	5670.8
10.5	2009.2		4786.7		
14.0	2673.4	75.0	4899.2		

Resistivity (Ohm.m)	Depth (m)
643.0	2.5
11200.0	24.8
2210.0	66.7
3700.0	110.0
11000.0	

RESISTIVITY

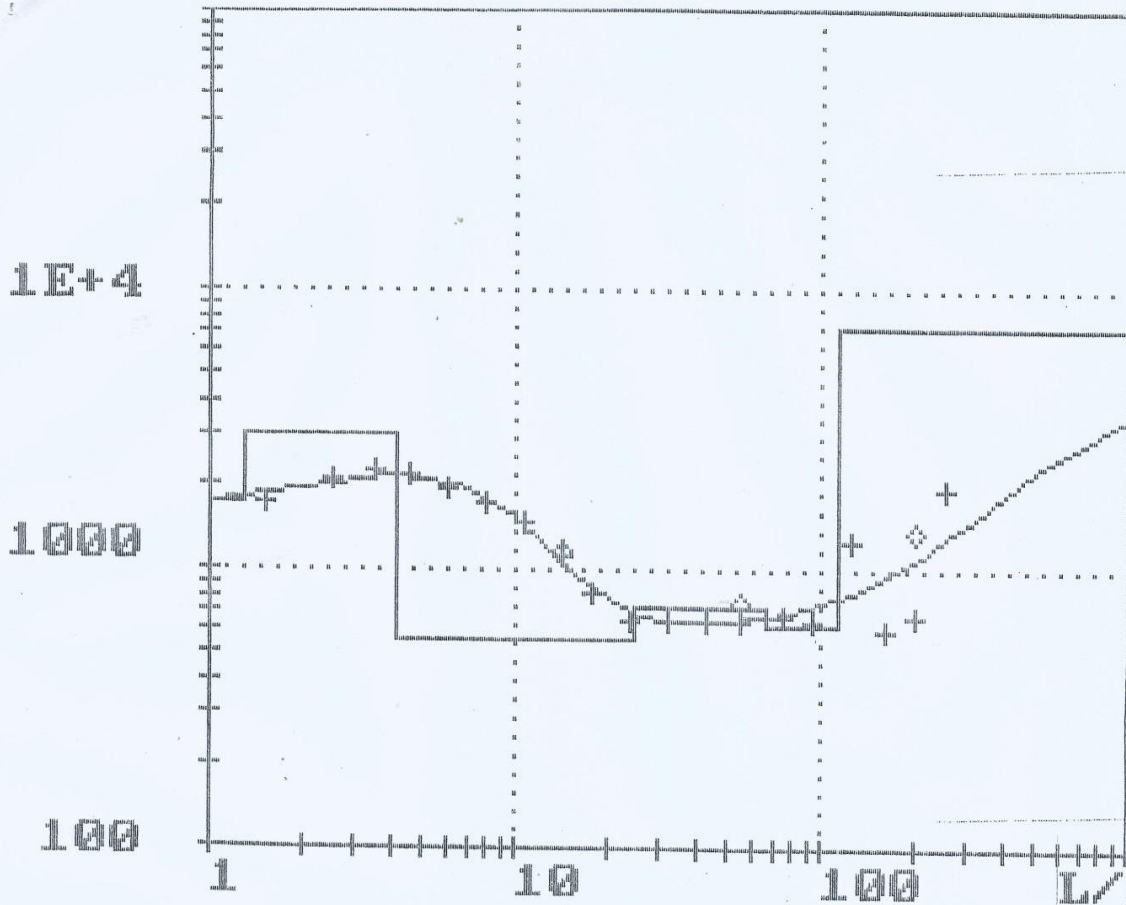


Data (File) name STUDENTS' PROJECTDate 13/07/2014
 -Project name EROSION CONTROL Direction lay out
 OWERRI/ORLU ROAD - OKWODOR EROSION SITE
 Code name YES I Remarks
 NJABA L.G.A. IMO STATE.
 Coordinates N05 43.160°, E07 00.914°, H107m
 Schlumberger O'Neill

L/2 (m)	Rho (Ohm.m)	L/2 (m)	Rho (Ohm.m)	L/2 (m)	Rho (Ohm.m)
1.5	7127.8	14.0	12787.5	95.0	12447.0
2.5	8917.0	18.0	13139.0	125.0	19099.2
3.5	10271.0	24.0	14023.8	160.0	6928.5
4.5	10117.1	32.0	14537.1	200.0	4794.0
6.0	11948.0	42.0	16168.0	200.0	4677.0
8.0	11856.0	55.0	16156.4	250.0	4657.2
10.5	12531.1	55.0	15580.6	300.0	1907.3
14.0	12213.9	75.0	14806.5		

Resistivity (Ohm.m)	Depth (m)
5970.0	0.9
12800.0	16.8
24900.0	53.6
6520.0	78.7
1020.0	

RESISTIVITY

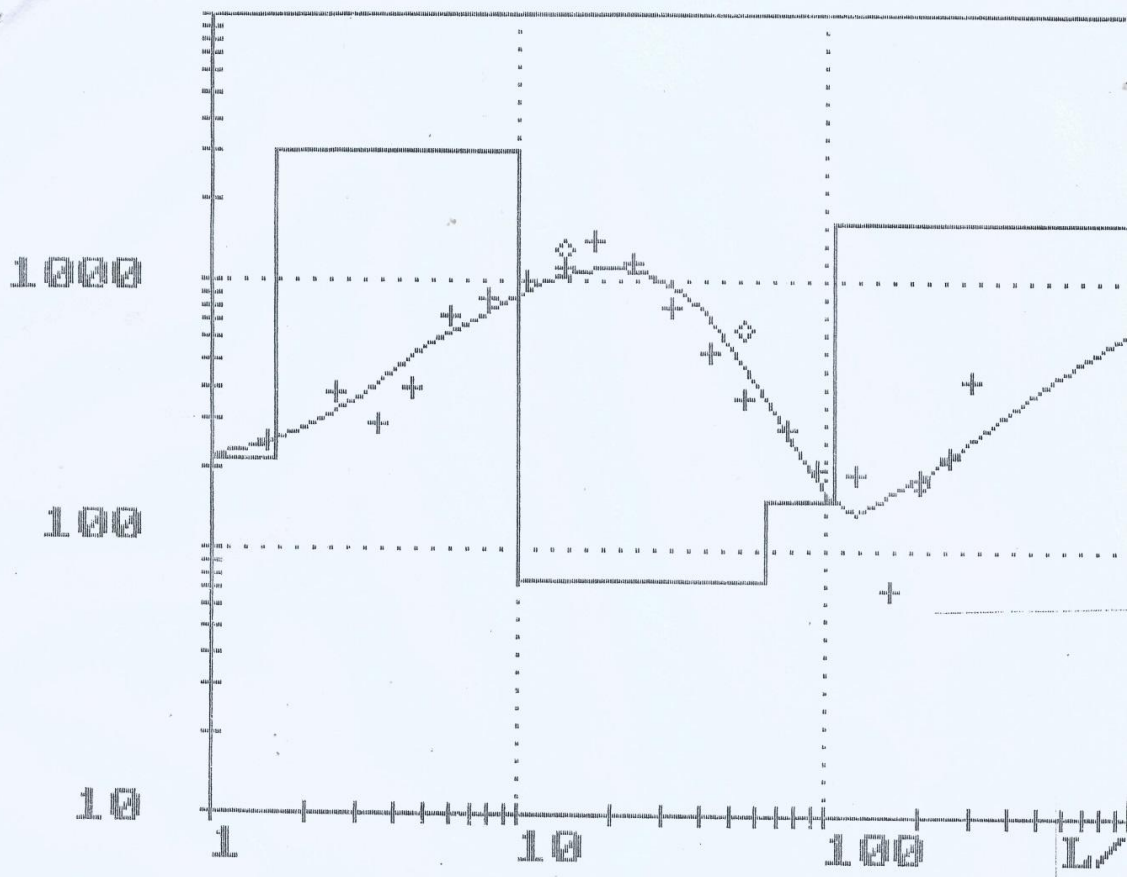


Data (File) name STUDENT PROJECT Date 12/07/2014
 Project name EROSION CONTROL Direction lay out
 ST PAUL'S CATH.CHURCH - UMUNGUMA IHEOMA
 Code name VES I Remarks
 IHIOMA ORLU ORLU L.G.A. IMO STATE
 Coordinates N05 49.398°, E07 00.950°, H110m
 Schlumberger 0°Neill

L/2 (m)	Rho (Ohm.m)	L/2 (m)	Rho (Ohm.m)	L/2 (m)	Rho (Ohm.m)
1.5	1718.2	14.0	1152.4	95.0	643.8
2.5	2042.3	18.0	824.3	125.0	1271.0
3.5	2199.4	24.0	656.3	160.0	609.1
4.5	2118.9	32.0	657.8	200.0	669.1
6.0	1922.6	42.0	651.6	200.0	1371.8
8.0	1729.0	55.0	646.7	250.0	1927.3
10.5	1445.5	55.0	761.1		
14.0	1127.9	75.0	666.0		

Resistivity (Ohm.m)	Depth (m)
1690.0	1.3
3100.0	4.1
560.0	24.3
748.0	65.5
621.0	113.0
7460.0	

RESISTIVITY LOG



Data (File) name STUDENT PROJECT Date 12/07/2014
 Project name EROSION CONTROL Direction lay out IKPA IHIOMA - IYI UZO
 Code name VES II Remarks
 IHIOMA ORLU ORLU L.G.A. IMO STATE
 Coordinates N05 49.516', E07 00.514', H94m
 Schlumberger O'Neill

L/2 (m)	Rho (Ohm.m)	L/2 (m)	Rho (Ohm.m)	L/2 (m)	Rho (Ohm.m)
1.5	252.0	14.0	1312.6	95.0	199.8
2.5	374.2	18.0	1418.2	125.0	191.0
3.5	295.2	24.0	1161.5	160.0	71.6
4.5	401.6	32.0	777.2	200.0	185.5
6.0	729.5	42.0	540.1	200.0	180.2
8.0	843.2	55.0	367.2	250.0	221.4
10.5	983.4	55.0	661.9	300.0	428.9
14.0	1096.5	75.0	280.1		

Resistivity (Ohm.m)	Depth (m)
213.0	1.6
3040.0	9.9
76.2	64.2
152.0	106.0
1660.0	